eman ta zabal zazu

Universidad del País Vasco

Euskal Herriko Unibertsitatea

FACULTY OF ENGINEERING BILBAO

UNIVERSITY OF THE BASQUE COUNTRY

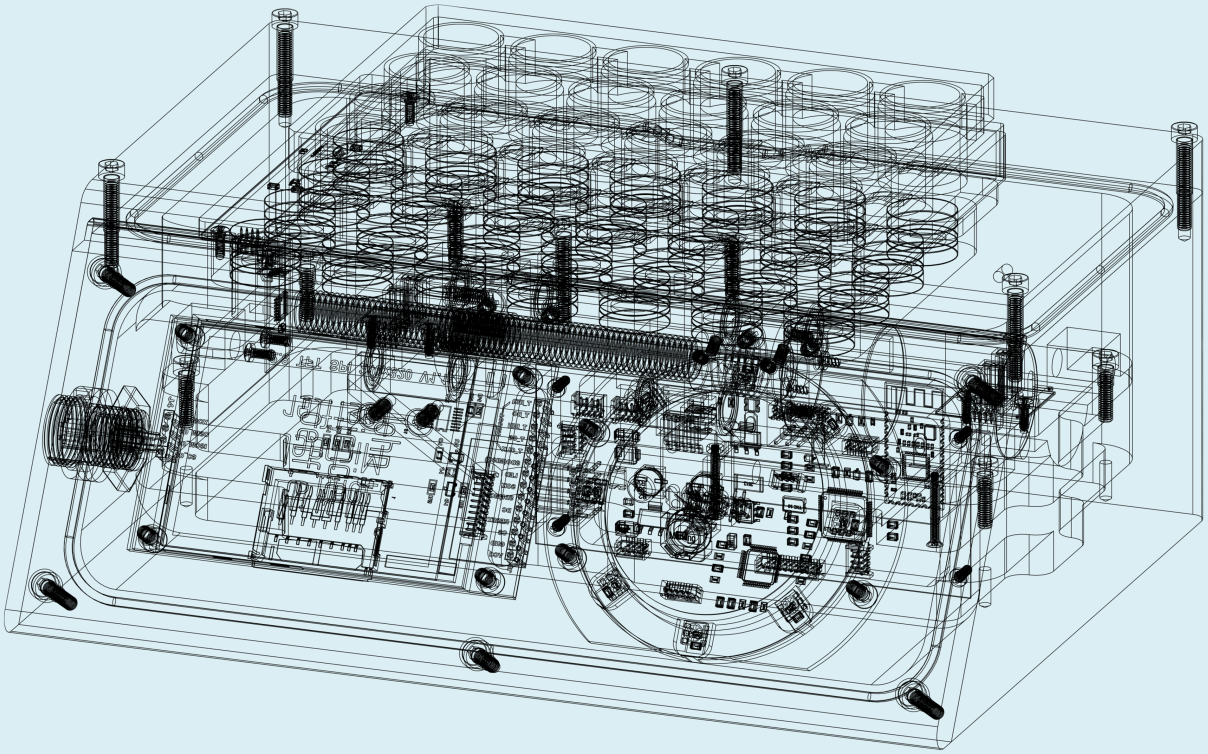

Design, Construction and Validation of a New Generation of Bioreactors for Tissue Engineering Applications

Nélson José Fernandes Castro

Department of Graphic Design and Engineering Projects

2020

eman ta zabal zazu

Universidad del País Vasco
Euskal Herriko Unibertsitatea

FACULTY OF ENGINEERING BILBAO
UNIVERSITY OF THE BASQUE COUNTRY

Design, Construction and Validation of a New Generation of Bioreactors for Tissue Engineering Applications

Nélson José Fernandes Castro

2020

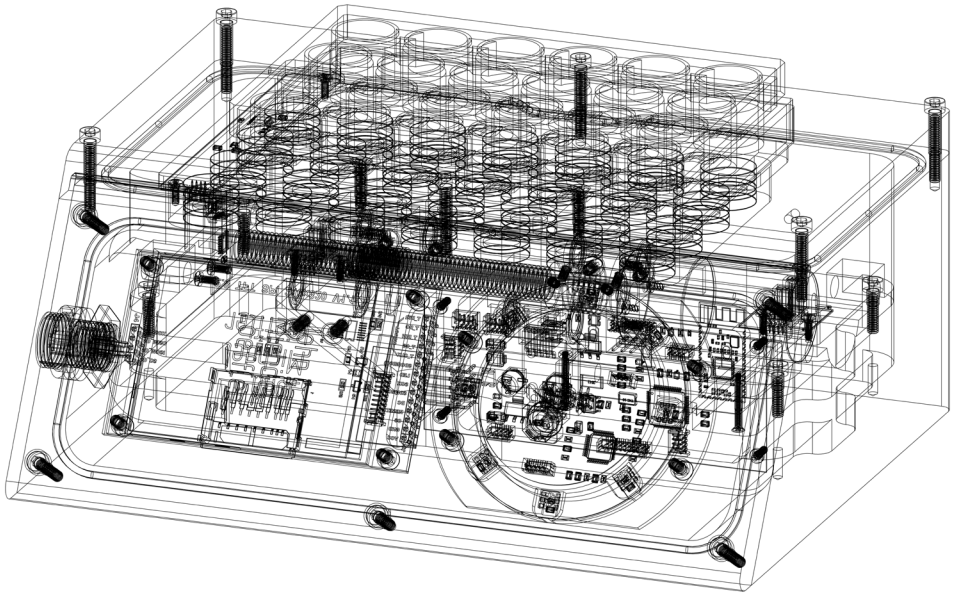

Ph.D. Thesis in the Department of Graphic Design and Engineering Projects

Directed by:

Doctor Rikardo Minguez Gabiña and

Doctor Senentxu Lanceros-Mendez

(c)2020 NELSON JOSE FERNANDES DE CASTRO

Acknowledgements

This project was a journey, which took a lot of effort from the people that supported me technically and personally. By no means, it was an easy task in terms of personal cost, taking me away for a while from home, from my family and my future wife Marina, which held everything together, for me to pursue my goals in order to develop myself both technically and personally opening new horizons to realize how much I am yet to learn. Therefore, she is the very first person I thank for the dedication, love and support she always provided every time I needed, as well as my family and oldest friends for the care, support and encouragement, which took me every step of the way until where I am today and shaped who I am. Furthermore, I take this opportunity to thank both my thesis directors, Rikardo Minguez Gabiña head of the Department of Graphic Design and Engineering Projects at the University of the Basque Country UPV/EHU and Senentxu Lanceros-Méndez the Basque Center for Materials, Applications and Nanostructures director, for all the time and patience I took from them in order to make this thesis project possible and putting me together with the right people to collaborate with and learn from throughout this time. Therefore, I want to thank the Fundación BCMaterials administration for admitting me as an employee in their institution and giving me the opportunity to work and collaborate with their research teams, while providing all of the financial support I needed, which was fundamental to finish this project. I also want to thank all of the people in my research team, such as Alberto, Liliana, Clara, Bruno, Erlantz, Cristian, Ander, Mikel, Asma, Niko among many others that helped me fit in, and collaborated with me that let me grow immensely technically with materials development and research. In addition, all the people from BCMaterials from all the other research lines, especially to Rajasekhar, which helped me in many occasions with his wit and competence, becoming a great colleague and friend both in and outside the work environment, and I wish him the best of luck on his new life phase. Furthermore, I want to thank the electroactive smart materials group in the University of Minho, Braga for all the companionship during my stays there, technical support and collaborations with biological department that made all of this possible, namely, Clarisse, Vitor, Sylvie and Margarida, and all the ones that visited BCMaterials for work cooperation and after work hangouts among Bilbao and outskirts and all the other group members that contributed directly and indirectly to make all of this time easier and enjoyable.

"It is paradoxical, yet true, to say, that the more we know, the more ignorant we become in the absolute sense, for it is only through enlightenment that we become conscious of our limitations. Precisely one of the most gratifying results of intellectual evolution is the continuous opening up of new and greater prospects."

Nikola Tesla

Summary

Health problems related with population aging take an increasingly significant role in the current society and putting pressure in healthcare cost with infrastructures and medical staff. Thereby, cost effective solutions are required in order to aid especially elder people that has lost their regeneration rate throughout the years to recover from health issues such as bone fractures or micro-fractures, myocardium infarction, muscular and joints injuries due to repetitive movements, among others. This type of health problems are common and take, especially in old age, a long time to heal, requiring at the same time longer monitoring by medical staff. Thereby, *in-vitro* cultures of regenerated living tissue may pose a new viable method for faster recovery through healthy tissue implants. Thus, in order to build a tissue *in-vitro*, a tissue culture is required, and those tissue implants can deliver improved benefits by being enhanced with higher cellular proliferation and differentiation, resulting in an improved tissue structure with higher chances of a successful therapy. Thereby, it requires devices that can better mimic the cellular microenvironments, which are key components to enable this medical segment. Therefore, a biomimetic approach provides an enriched method to keep on exploring how cellular sites respond to specific types of stimuli and morphologies of scaffold materials. Resuming, tissue engineering is composed mainly by cells, scaffolds and stimuli, whereas scaffolds provide the structure for cellular growth and orientation, being the most important alongside the medium, which provide nutrients and oxygenation enabling a static culture, where cells can proliferate and differentiate, providing that the setup is at a suitable temperature as in living being. However, those variables alone do not suitably mimic the natural cellular environment inside a living being, thus cells will not have the same growth behavior as they would have in a body subjected to mechanical stress from walking, breathing, and even the piezoelectricity and mechanical stress produced in bones and muscles during our daily lives. Thereby, bioreactors that provide actuation combined with magnetoactive or electroactive biocompatible scaffolds represent a future path of bioreactor systems in order to achieve most of those variables, which are required for a proper tissue engineering culture. **In the context of the mentioned facts, a modular bioreactor system was projected, designed and built, harboring biocompatible materials and using magnetic force as direct and indirect stimuli.** The system was designed to harbor different mechanical modules for magnetic stimuli application and electro-stretching of polymeric scaffolds using permanent magnets displacement as force field source for direct and indirect stimuli application. Employing a permanent magnet holding structure, mechanically connected through a ball-screw assembly and moved by a motor, the setup enables

magnetically actuated mechanical stimuli to the scaffolds. The system is actuated by the motor on the permanent magnets support, which is being controlled through pulse width modulation signals applied in an H-bridge adapter connected to a microcontroller, simultaneously, enabling user-interface and system communication with peripherals and remote terminals through wireless components. Therefore, the electromechanical components were designed and adapted through computer-assisted design software, enabling easier prototyping and, inclusively, three-dimensional printing of system components. The developed device is able to provide alternated magnetic field stimuli up to 35 mT, at a frequency depending on magnet displacement distance, up to 25 mm, with varying speed. This configuration is aimed to be used with magnetoelectric scaffolds containing cells, which can take advantage of piezoelectricity and magnetostrictive vibration, as well as any other magneto-active scaffolds that can make use of alternated magnetic field and convert it in cellular stimuli. This magnetic module configuration is employed to perform a dynamical cell culture and was evaluated with mouse pre-osteoblasts cells supported in three-dimensional porous magnetoelectric scaffolds composed by polyvinylidene fluoride and cobalt ferrite nanoparticles, increasing significantly the cellular proliferation, and even more than doubling in the 80 μm size porous scaffolds case, by comparison with static cultures. In addition, for electro-stretching modular configuration, the system is able to provide electrical stimuli up to 20 mA, with resolution steps of 300 nA, and a scaffold stretching distance up to 12 mm with varying speed, applying a z-axis force of 9.5 N. The electro-stretching stimuli can be used with polymeric elastic or fibrous film scaffolds with cells such as muscle and cartilage, which are body components that continuously receive those type of stimuli. The scaffold holding clamps were analyzed and concluded to be non-cytotoxic, supporting the applicability for tissue engineering. Finally, as future developments, the system is being designed to be adapted with peripheral devices such as a peristaltic pump, in order to be used as a magneto-perfusion stimuli system, increasing the range of possibilities and tissue engineering applications where it can be employed in.

Table of Contents

Table of Figures

List of Acronyms

AC	*Alternated Current*
ADC	*Analog-to-Digital Converter*
ASC	*Adipose Stem Cells*
CFO	*Cobalt Ferrite Nanoparticles*
CPU	*Central Processing Unit*
DAC	*Digital-to-Analog Converter*
DC	*Drowning Current*
DMEM	*Dulbecco® Modified Eagles Minimal Essential Medium*
DMF	*N, N-Dimethylformamide*
DMSO	*Dimethyl Sulfoxide*
ECM	*Extra Cellular Matrix*
EEPROM	*Electrical Erasable Programmable Read-Only Memory*
FPU	*Floating Point Unit*
LCD	*Liquid Crystal Display*
LED	*Light Emitting Diode*
ME	*Magnetoelectric Effect*
MSC	*Mesenchymal Stem Cells*
MTS	*(3-(4, 5-Dimethylthiazol-2-yl)-5-(3-carboxymethoxyphenyl-2-(4-sulfophenyl)-2H-tetrazolium)*
MTT	*(3-(4, 5-Dimethylthiazol-2-yl)-2, 5-diphenyltetrazolium bromide)*
PBS	*Phosphate Buffered Saline*
PCB	*Printed Circuit Board*
PDMS	*Polydimethylsiloxane*
PGA	*Polyglycolic Acid*
PLA	*Polylactic Acid*
PLGA	*Poly Lactic-Glycolic Acid*
PLLA	*Poly-L-Lactide Acid*
PVDF	*Polyvinylidene Fluoride*
PVDF-TrFE	*Poly(Vinylidenefluoride-co-Trifluoroethylene)*
PWM	*Pulse Width Modulation*
RGB	*Red Green Blue*
SEBS	*Styrene-Ethylene-Butylene-Styrene*
SEM	*Scanning Electron Microscopy*
SPI	*Serial Peripheral Interface*
TE	*Tissue Engineering*
USART	*Universal Synchronous/Asynchronous Receive/Transmit*
UV	*Ultraviolet*

1 Introduction

Tissue engineering (TE) is a scientific field, which is presenting an exponential development through the last years encapsulating several scientific fields such as biology, physics, medicine and engineering [1]. It was founded in 1988, in a meeting issued by the National Science Foundation, as a field that employs life sciences and engineering with the purpose of developing biologic or synthetic supports in order to restore, keep or enhance tissue function or damaged organs [2]. For the culture of viable functional tissues, there are two main strategies. One consists in the development of a stimuli-able structure, which supports and results in positive cellular growth after its implementation in the organism while the other relies on *in-vitro* solutions for tissue generation, using an appropriate cellular support structure before being deployed into the organism [3]. The main therapeutic targets of TE are spread over several biological systems in the human body. A human being requires that every system and involving organs to function properly in order to have its daily vital functions being accomplished suitably for a normal life. When building a new tissue culture, three tools are typically needed: cells, scaffolds and stimuli. The cells are the main base for tissue culture as they contain the pre-programmed information that allows the tissue regeneration. This process must be staged in a support (scaffold), where the cell culture can be made possible by reproducing the necessary environment to receive biochemical stimuli (growth factors) and biophysical stimuli using bioreactors [4]. TE field is being employing bioreactors as important tools for several tasks such as: enable simulating in-vitro an in-vivo state environment in order to understand normal cell/molecular physiology; develop cells for medical purposes for instance gene therapies or pathological state simulations for disease studies and progress parameters; and to test new potential treatments to new therapeutic ambitions in a more realistic setup by comparison with conventional static in-vitro cultures. However, bioreactors are used not only for medical purposes, they are employed in fields such as fermentation, water treatments, food processing and pharmaceutical products [5]. The main reasons for their use are their working principles based in biologic and biochemical processes, aiming for a strict monitored and controlled environment.

1.1 General Context

Bioreactors are important tools in nowadays TE strategies taking a key role in the recovery, rebuild of organs, among other body components. Thereby, this work aims to project, design and develop a modular bioreactor aspect, mechanics and operating concepts, which will assist TE researchers with tissue types such as bone and muscle, in the context of a doctoral thesis in project engineering, comprehending system design according to TE applications requirements. Furthermore, custom electronics development and construction is one of the main components, as the system requires control, timing and user interface, resulting in a bio-mechatronics project encapsulating several fields of knowledge such as even materials engineering for smart cellular support construction (smart scaffolds). Thus, it involves several institutions, which took different roles in the support of this project which were: Basque Center for Materials (BCMaterials) providing the workplace, funding and smart composite materials for scaffold development; Graphic Design and Engineering Projects department in the faculty of engineering (UPV/EHU) in Bilbao providing support with design and fabrication; and finally, regarding biologic field tests and feedback, as well as electronics support and materials provided by Minho University research group, Electroactive Smart Materials. This group of institutions and their respective expertise support was key to make this complex and ambitious project possible.

1.2 Motivation

Longer lifespans has given us the opportunity to make and take more of life for ourselves, but in the current days and age, societies are noticing and awakening to a new dawn of problems that will require clever and sustainable solutions in many areas of human societies. One of them can be traced to medical issues related to population aging, which are already representing significant societal costs and at the current rate will represent a bigger number in the coming years. Regeneration rate of tissues, organs and many other body parts after a point in age, start to decay and increasing the regeneration difficulty at advanced ages. Among many problems that may arise, bone related diseases and fractures

are directly related with population aging, and the rate of recovery is slow, requiring several months of physiotherapy in order to provide the required mechanical stimuli for proper bone regeneration. Furthermore, myocardial infarction affects a large number of people worldwide, and it has a very peculiar issue related with the infarcted myocardium inability to self-repair becoming a formidable challenge to achieve a successful therapy. Those, among others, are medical issues aiming to tackle in research with the development of this project, among other possibilities related to the type of stimuli to be enabled by this system as it can be checked in the following chapters and respective referenced literature.

1.3 Objectives

The main objective relies in the design, development, construction and validation of a modular bioreactor system, which can be adapted for bone TE employing alternated magnetic stimuli to magnetoelectric scaffolds and for skeleton muscle TE by converting the system to apply stretching force and electrical impulses. Both cultures require a user-friendly interface, which enables controlled stimuli while providing control over temperature, culture active, repose and total time. Bone TE requires a modular magnetic bioreactor with an interchangeable magnets table, which needs to be designed to use with 24 and 48-multiwell standard plates that can be easily operated and calibrated by the user. Skeleton muscle TE requires a range of frequencies, amplitudes and waveforms of controlled currents and stretch force, where researchers can use this tool to find the best parameters for cellular growth, giving further features to develop new TE strategies for in-vitro cell cultures. The expected results are meant to be used for cellular studies with diseases, therapies and cellular response *in-vitro* simulations. According to literature related with tissue engineering observing that cells are susceptible to be "persuaded" to differentiate into bone, muscle, cartilage cells among others while, simultaneously, proliferate according to the type of scaffold and stimuli applied to a cellular culture, a device and respective cellular supports, which provide the environment and bridges cellular stimuli, brings high chances of success. Previous studies, with intended similar cells and materials provide results that supports this project to be developed and implemented for further development on those past results.

Therefore, it is expected to develop this modular system to be operational for magnetic, magnetoelectric, electric and stretching stimuli types, interchangeably or simultaneously according to culture requirements. The magnetic field can be generated by permanent and electro-magnets, as it will be discussed in the next chapters, their respective tradeoffs intersected with the aimed application. This system, simultaneously, is being designed with the possibility to be integrated with further peripherals through firmware communication. This project is meant to be a layer of a research field composed by many types of knowledge, and is supposed to be employed as a biomedical tool for diseases, therapies and cellular response *in-vitro* simulations.

2 State of The Art

Bioreactors have multiple configurations according to tissue target type and geometry, production quantity, processing time and operating costs. The most varied types of bioreactors comes from research for custom specific experiments, since the simplest bioreactor, such as a basic spinner flask, to the most complex one harboring two or three types of simultaneous cellular stimuli by assembling together many synchronized mechanisms. These devices are wonders of many sciences put together with a common goal, which keep on evolving since the very beginning of TE field. Beyond laboratory custom devices for small proof of concept experiments, and scalability studies, an industry has been established due to the window of opportunity related to these devices capable of harboring human tissues for medical therapy and studies resulting in high demand and an increased market growth for both devices and consumables. Thereby, the several TE market segments fuels the investment for both startup companies and public research projects to keep on the development and competitiveness of this engineering field for the common good of societies. Lastly, the most common bioreactor principles are employed in both segments of bioreactor construction and development and a considerable amount of knowledge has been obtained throughout the several technologies achieved so far, resulting in many creative solutions with both advantages and setbacks according to culture type, size and operating costs.

2.1 Tissue Engineering

Fundamental biological studies and therapeutic applications rely in TE techniques, which aim to mimic physicochemical and bioactive characteristics of natural cellular matrices [6, 7], in order to achieve the replacement and/or regeneration of damaged tissues or organs [8, 9]. When building a new tissue culture, three tools are fundamental: cells, scaffolds and stimuli. The cells are the main base for tissue culture as they contain the pre-programmed information that allows the tissue regeneration. This process must be staged in a scaffold, which acts as the cell culture support, where the necessary environment is present for biochemical stimuli (growth factors) and biophysical stimuli using a bioreactor [4]. Biomaterials can be tailored, allowing to be passively tolerated by the organism whereas providing the appropriate environment to assist specific cell responses and tissue structures [10]. It is possible to find in the literature implementations of novel scaffold supports in order to restore native functionalities of tissues like muscle, nerve and bone [6, 11].

2.1.1 Cells

Tissue-specific functions are provided by cellular building blocks cooperation, representing complex organisms. These groups of cell and molecules, wrapped in an extracellular matrix, form a biological system with a specific role creating a convoluted microenvironment [12, 13]. *In-vitro* cultures aim to mimic the biological conditions, although the complexity of these microenvironments makes it challenging. Cell-culture studies performed in vitro are mostly based on two-dimensional platforms for cellular growth, interacting with naturally absorbed proteins in the surface. However, this method presents limitations such as cellular interactions when compared to 3D scaffolds, diminished control over cell-adhesion interactions and signaling, as well as, commonly used materials stiffness [14]. Therefore, *in-vitro* culture models are constantly under development and seeking new approaches to control the cellular behavior, thus mimicking the cellular microenvironment in order to prompt specific cellular functions.

2.1.2 Scaffolds

Several TE culture types such as bone, cartilage, muscle and neural regeneration, skin growth, cardiovascular and wound healing have been using multifunctional biomaterials based on smart materials. Furthermore, depending on culture type, the biomaterial requirements may differ, as the microenvironment in each tissue or organ can be significantly distinct in terms of morphology and stimuli to which is subjected on in vivo conditions and shaping the tissues. In the case of bone, the microenvironment is defined as a complex structural and biological system, mainly divided by the organic phase (collagen based), the mineral phase (crystalline hydroxyapatite based) and porosity [15]. Furthermore, bones are composed by 80% of cortical bone[1] and 20% of trabecular bone[2] in a human adult, where these ratios depend on the bones and skeletal sites [16]. Bones also harbor another key characteristic, being their piezoelectric nature, and it has been demonstrated that the bone growth and remodeling rely in electromechanical processes: thereby, mechanical stress on bones induces electrical signals, which encourages bone growth and remodeling [17]. In the skeletal muscle case, it is a very adaptable tissue composed by stretched parallel bundles of multinucleated contractile muscle cells known as myofibers [18]. In addition, the skeletal muscle cells grow endogenous[3] electrical fields in the form of membrane potentials, due to the undergoing mechanical stretch and compression on the 3D tissue constructs embedded with these cells [19, 20]. Opposing, endothelial cells[4] in a two dimensional interface within fluid contact, are also exposed to stretch and compression transmitted from shear stress generated by pulsatile blood flow [21]. Moving to neural tissue, which is the main component of the nervous system and can be divided into neurons and neuroglia [22]. In addition, neural tissues are complex 3D environments harboring large range morphologies and size scales [23]. Neural growth electric fields have been measured, turning bioelectrical control mechanism each more relevant for the regeneration and development of nerve fibers [24]. Thereby, in order to reach improved and more efficient TE approaches, platforms strategies must be taken into consideration the mechanobiological niche of each tissue type.

[1] Dense outer surface of bone that forms a protective layer around the internal cavity.
[2] End of long bones, very porous and containing red bone marrow, where blood cells are made, weaker and easier to fracture than cortical bone, which makes up the shafts of long bones.
[3] Endogenous substances and processes are those that originate from within a system such as an organism, tissue, or cell.
[4] Cells that line the interior surface of blood vessels and lymphatic vessels, forming an interface between circulating blood or lymph in the lumen and the rest of the vessel wall.

2.1.3 Bioreactors

Due to limited understanding of specific physicochemical culture parameters regulatory role on tissue development, the need for bioreactor systems with reproducible and controlled variations of a specific environment in an *in-vitro* culture has become key in this multidisciplinary engineering field. These systems provide the required technology to expose cell function vital mechanisms while enabling a potential improvement in engineered tissues quality, by increasing mass transport inside three-dimensional structures while reducing the contamination chances [25]. According to bioreactor type, static or dynamic cultures or both are allowed, where static relies mainly in providing a setup support for cells seeded in scaffolds with medium, whereas dynamic culture provide adds extra stimuli, which enhances cell proliferation and differentiation. Stimuli types employ an important role depending on which type of cells are used in a TE culture, so several bioreactor setups (commercial and custom build) according to production capacity (from mass production to laboratory scale) can be found in the literature [26-28]. In addition, using these setups enable learning of standard control culture parameters about several tissues types, allowing respective standardization for future automated production processes, which may be designed in order to reduce production costs, and widespread the medical deployment of engineered tissues increasing application development and reach a next phase of further research, such as organ 3D printing.

2.2 Current Applications and Research

Regarding the research targets of this thesis are bone and muscle TE, this engineering field research range is vast as there is many types of tissues under research as previously mentioned. Thus, in the scope of this document, a brief state of the art is presented on the field regarding how and how much progress has been achieved in the last years, as this information provides clues how to move forward and improve.

2.2.1 Bone Tissue Engineering

Bone TE will take a preponderant role with cost reduction of societies expenses with healthcare [29, 30]. Therefore, new materials for bone TE are under intense investigation in order to formulate new bone TE strategies through passive cell supports [31-33], although most don't consider the bone natural piezoelectricity present in its tissue [34]. Performance of bone tissue along with its development and functional time is strongly influenced by the voltage variation generated by mechanical stress to which the bone is subjected. In another approach, magnetoelectric (ME) scaffolds were used in order to provide a cellular support for cell seeding while taking advantage of the scaffolds construction materials in order to enable electromechanic stimuli generated by a remote magnetic field [35, 36]. These composites are composed by a magnetostrictive and piezoelectric layers working synergistically to produce the ME effect [37]. The ME effect can be described as a transduction from magnetic field to an electrical field, the vibration of the magnetostrictive phase generated by an alternated magnetic field results in an electrical charge at the piezoelectric phase terminals at room temperature [38, 39]. Thus, it is possible to vibrate the scaffold while generating a charge in a ME scaffold inducing the stimuli at the neighboring cells [40]. The flexibility, versatility and biocompatibility of these materials [11, 41] can be taken advantage for *in-vitro* dynamic cultures through the support of a remote magnetic field, while avoiding the need for patient movement [40]. Several studies applying magnetic stimuli through the assistance of magnetic fields and magneto sensitive particles in order to control cellular function and positioning to create cellular clusters, enabling more complex tissue structures than conventional strategies based on static scaffolds [42]. As a recent example, the use of superparamagnetic iron oxide nanoparticles proved to be a promising bioactive additive for scaffold fabrication as it has been reported in [43], where their new scaffold enhanced the performance of human dental pulp stem cells yielding higher count of phosphatase activities[5], higher osteogenic marker genes expression[6] and improved cell-synthesized bone minerals. In other study, C2C12 cells were marked with magnetite cationic liposome, mixed in a collagen solution, and seeded in a cell culture space of a hollow-fiber bioreactor [44]. The results demonstrated that high cell-dense and viable tissue constructs containing myotubes were successfully obtained. Magnetic stimuli through permanent magnets by displacing the magnets

[5] Phosphatase are enzymes, which are essential to many biological functions, because phosphorylation and dephosphorylation (by phosphatases) serve diverse roles in cellular regulation and signaling.
[6] Differentiation of MSCs into mature osteoblasts during the expansion in vitro.

or the culture plate was proposed in [45] where the authors apply a remote variable magnetic field by displacing the culture chamber or permanent magnets horizontally or vertically. Rotation of permanent magnets was also employed in order to induce cellular growth proving that the varying magnetic field between 7 and 10 Hz increased the growth of neurite[7] on chromaffin cells[8] [46]. These devices can give a contribution in order to overcome the issues related to the traditional cell culture conditions, improving the cellular distribution and accelerating the cellular growth [47]. Besides biocompatibility and sterility, the design of mechanical bioreactors, requires accurate control of the stimulus, which is being applied in order to get accurate data and allow replicating results for the same culture parameters.

2.2.2 Muscle Tissue Engineering

This engineering field is being used to overcome several difficulties in medical treatments like the myocardial infarction, which can be described as the myocardium inability to self-repair posing an extreme challenge to provide a successful therapy for almost one million people affected every year by myocardial infarction in the United States alone. In order to formulate potential cell-based therapies, it is possible to find in the literature the use of skeletal myoblasts and bone marrow-derived stem cells [48]. These types of cells can be used for genetic manipulation and autologous[9] isolation before implantation, although ventricular arrhythmia can be provoked by skeletal myoblasts injected at the myocardial infarcted sites [49, 50]. The application of pre-developed and matured skeletal muscle cell sheets has been suggested to better comply with myocardium requirements rather than single myoblasts injection [51, 52]. The need for more efficient techniques to achieve matured skeletal muscle cells encourages this study and system design. Cell-to-cell and cell to matrix interactions influence the development of skeletal myotubes matured from singled myoblasts[10], resulting in a complex process.

[7] A neurite or neuronal process refers to any projection from the cell body of a neuron.
[8] Chromaffin cells are found mostly in the medulla of the adrenal glands in mammals, serving as a response to stress, monitoring carbon dioxide and oxygen concentrations in the body, maintenance of respiration and the regulation of blood pressure.
[9] Derived from the same individual.
[10] Myocytes are long, tubular cells that develop from myoblasts to form muscles in a process known as myogenesis.

Cytoskeletal[11] stress is initiated in the underlying extracellular matrix dictating the differentiation of myoblasts, resulting in a reorganization of the actin cytoskeleton [53-55]. Matured skeletal fibers can be characterized by the capability to undertake several types of stimulation like stretching repetitively. In previous experiments, hydrogel[12] cultures were employed, such as matrigel or fibrin gel scaffolds, where skeletal myotubes demonstrate the production of tetanus forces up to 1 mN with a defined sarcomeric[13] structure [56-58]. Whereas, skeletal myoblasts elongate and align on nanofiber surfaces, with a tetanus force up to 500 μN [59-61]. Among mechanical stimuli, it is possible to find in the literature several cases of custom made setups in order to provide the mechanical stimuli (stretching and compression) to bioengineering of cell cultures. Thus, stretching stimuli is applied in cells such as heart muscles [62], cyclic mechanical stretching influence on skeletal muscle differentiation in C2C12 cells [63, 64] and tendon constructs study of ultimate tensile stress and elastic modulus [65]. As for compression has been used to examine the effects of cyclic compressive loading on human bone mesenchymal stromal cells [66], engineered cartilage constructs [67, 68] and chondrogenic[14] differentiation of rabbit bone-marrow mesenchymal stem cells [69]. Electrical stimulation also plays an important role, which may influence in growing aligned and orientated tissues, initiating new possibilities that can culminate in 3D printing of tissue and organ engineering [70]. This type of stimuli can be used within a large range of ways, as in current or voltage mode, continuous or alternated which can be used also in different frequencies, amplitudes and wave geometries [71]. These electrical impulses can be generated by embedded systems focused on specific cell stimulation profiles. A report of an experiment with embryoid bodies derived from human embryonic stem cells which went through a stimulus of 1 V/mm, 5 ms pulses, at 1 Hz resulting in a significant growth in intracellular generation of reactive oxygen species [72]. Another report using 6.6 V/cm, 2 ms pulses, at the same frequency in derived cardio-myocytes from human embryonic stem cells stated an upregulation of cardiac-specific genes and the yield of differentiation promoted ventricular-like phenotypes and improved calcium handling [73]. Thereby, custom setups were built to employ the use of both types of stimuli, simultaneously and concurrently, in order to evaluate how both stimuli would influence in cell proliferation and

[11] The cytoskeleton is a network of microfilaments, intermediate filaments, and microtubules giving shape to cells lacking a cell wall, allowing for cell movement, enabling movement of organelles within the cell, endocytosis, and cell division.
[12] A hydrogel is a network of polymer chains that are hydrophilic, sometimes found as a colloidal gel in which water is the dispersion medium.
[13] A sarcomere is the basic unit of striated muscle tissue.
[14] Chondrification (also known as chondrogenesis) is the process by which cartilage is formed from condensed mesenchyme tissue, which differentiates into chondrocytes and begins secreting the molecules that form the extracellular matrix.

differentiation. Thus, through electromechanical stimulation, maturation of myotubes on aligned electrospun fibers were subjected to 1.1 mN tetanus forces and 10 ms pulses of 20 V at 1Hz, reaching cell elongation, focal adhesion[15] reorganization and myotubes with enhanced process of myogenesis and differentiation [74]. Cyclic stretching ranging from 0.5 to 20% elongation at 1 to 2 Hz and square pulse waves of 6 to 8 V of 10 ms pulses at 1 to 10 Hz, mimicking the physiological physical stimuli were also applied to cardiac tissue through a custom bioreactor [75]. More recently, a tissue engineered construct with cardiac adipose tissue-derived progenitor cells, went through 2 ms pulses of 50 mV/cm at 1 Hz and 10% stretching during 7 days on an in-vivo environment [76]. The authors concluded that the electromechanical stimuli, in an in-vivo environment, after a myocardium infarction, maintain their cardio-myogenic potential, migrate the murine myocardium and scar, while improving cardiac function and increasing vessel density [76]. Although this type of research of electro-stretching stimuli on cellular supports keeps on increasing in the scientific community, there is not a definitive solution for multi-purpose stimuli, only laboratory custom setups.

2.3 Bioreactors – Main Types

Bioreactors represent a useful tool for engineering physiologically functional 3D tissues in vitro by resembling the microenvironmental niche conditions. These devices possess multiple configurations according to the tissue target type, the geometry of the scaffolds, production quantity, processing time and operating costs. Most of bioreactors are developed in the framework of scientific experiments according to their specific needs. From the simple bioreactor such as the basic spinner flask, to the most complex one with two or three types of simultaneous cellular stimuli by assembling together different synchronized mechanisms, these devices have been valuable for the advances in regenerative medicine. Thus, in the following section, the main types of bioreactors will be described according to their application objectives, operating methods and main therapeutic targets. Furthermore,

[15] Focal adhesions are large macromolecular assemblies through which mechanical force and regulatory signals are transmitted between the ECM and an interacting cell.

at the end of this chapter, in Table 2.2 it is summarized the technologies being employed and what type of scaffolds, cells and stimuli are related in literature.

2.3.1 Stirred Bioreactors

Cylinder containers provide the usual base construction of stirred bioreactors such as the ones in Figure 2.1, where scaffolds and cells are coupled with a mechanism inside the liquid medium, which create medium motion in order to distribute evenly the nutrients, heat and shear stress stimuli among all scaffolds.

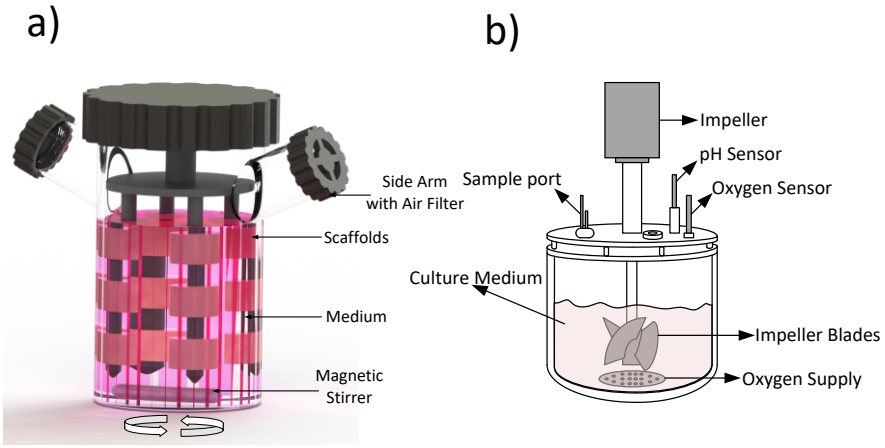

Figure 2.1 – a) Spinner Flask bioreactor schematic demonstrating how the shear stress is applied in a medium convection method to the cell constructs attached in needles (adapted from [77]) and b) Schematic of main components for cell cultivation in a stirred tank bioreactor (based on [78]).

2.3.1.1 Spinner Flask Bioreactor

Starting by the most basic shape of bioreactor, the spinner flask is one of the most simple and most used ones, which is optimum for static condition cultures and are being mainly used for cartilage and bone tissue cultures [26, 27]. One of the main advantages of this type of bioreactor is its capacity for allowing a perfect mixed environment inside the balloon, reducing the stagnated layer of cells, thus avoiding an uneven environment. Scaffolds are suspended in needles and then placed in the middle of the flask while the environment is agitated with a magnetic stirrer, inducing the nutrient mix with the scaffold (Figure 2.1a). Some experiments can be found in literature using this functional basic type of bioreactor: for bone tissue enhancing osteoblastic markers within coralline hydroxyapatite scaffolds for

human mesenchymal stem cells (MSCs) reaching significant higher cells count for 500 μm pore scaffolds [79]; for cartilage constructs using poly lactic-glycolic acid (PLGA) scaffolds for rabbit MSCs ensuing in tubular tracheal grafts formation [66] and fibrin gels as scaffolds for human adipose stem cells (ASCs) resulting in chrondrogenic differentiation [80]. Spinner flasks have mainly two variation culture setups, first as in batch culture, a closed type of culture mode that disables the addiction of fresh medium and waste removal, limiting production but providing a solid method to avoid contamination, whereas the second setup continuous culture enables waste removal, but puts the system susceptible to potential contaminations [26]. However, spinner flasks may not always be the most appropriate tool because of the constant mixture flow has the tendency to cause a turbulent flow inside the capsule adding a high risk of tissue deformation, resulting in an external fibrous capsule in the tissue. The spinner flask bioreactor is designed for small-scale production, having a low efficiency in the cell culture results, because of low homogeneity of cell distribution in the scaffold, prevailing in the peripheries of construction [81, 82].

2.3.1.2 Stirred Tank Bioreactor

Due to their high productivity, stirred tank bioreactors are one of the most important ones for industrial production. These systems can be used to produce red blood cells in an attempt to reduce the hospital's dependency in blood donations and thus keep a sufficient stock. Production of red blood cells are already under research with cord blood derived CD34+ cells [83]. It has similarities with the spinner flask version, consisting in a cylindrical recipient with a central shaft coupled to a motor, which supports one or more stirrers. The stirrers are necessary in order to accomplish a large range of functions such as control of the proper thrust, provide the mass from stirred particles and heat transfers, mixing and homogenize the cell culture. Their working principle relies in a motor coupled to stirrer blades, which when activated mix the culture environment while being pumped to the bioreactor tank (Figure 2.1b). This tank is coated by a thermic mesh in order to avoid temperature variations within. The whole system is covered by sensors in order to evaluate and monitor the culture process by controlling the variables on the tissues [84]. Studies using stirrer-based bioreactors as cell microcarriers for MSCs have been shown to induce cell expansion and differentiation, and have used to monitor proliferation, metabolic status and phenotype expression during suspension cultures [85]. The conventional stirrers used in fermentation are typically classified as axial or radial flow stirrers. Inside the radial flow stirrers, there are two types of turbines, one of six plane blades (Rushton disc) and other of six curved blades. The stirrers of axial flow are helixes, composed usually by three rounded blades,

and a turbine with four flat blades with a 45 degrees inclination in each. An example of use of this bioreactor for non-medical purposes, was for extraction of proteins with proteolytic activity from jacaratia mexicana fruits reaching a cell growth of 44%, employing with Rushton turbine impellers, stirring at 300 to 400 RPM [86]. In these devices is possible to find stirrers with two or three turbines in the axis, reaching a higher uniformity mixture [87].

2.3.2 Non-Stirred Bioreactors

The following bioreactors produce medium motion and shear stress on the scaffolds with different types of mechanisms instead of impellers such as turbines or magnetic stirrers (Figure 2.2).

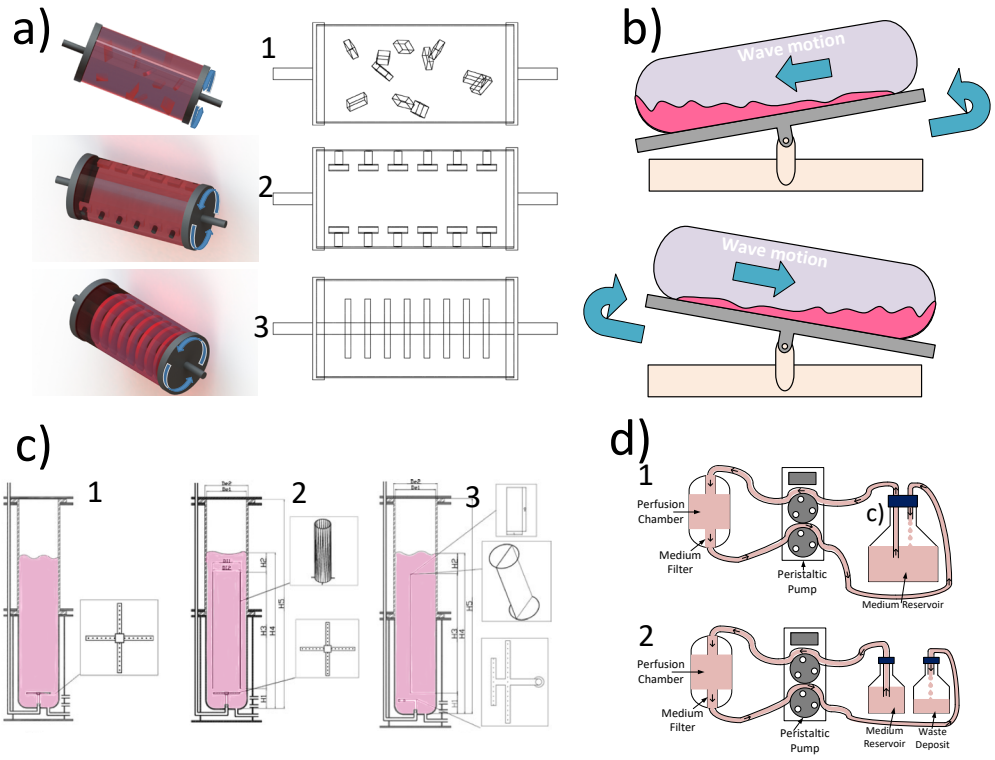

Figure 2.2 – a) Wall vessel bioreactor drawing models where arrows point out the rotation direction; (1) Free-fall variation; (2) Scaffolds attached to outer vessel wall; and (3) - Rotating bed bioreactor variation (adapted from [77]); b) Wave bioreactor working principle (adapted from [88]); c) Main pneumatic bioreactor possibilities as (1) bubble column, (2) concentric tube airlift and (3) split cylinder airlift (adapted from [89]); and d) (1) Perfusion bioreactor setup flow chart for closed loop and (2) perfusion bioreactor setup flow chart for single pass method (adapted from [77]).

These mechanisms bring other features, from bioreactors able to produce an interior micro gravity to cancel outside gravitational forces in order to prevent them from damaging the ongoing cell culture, to oxygen production in the medium from waves, and to clear waste from a constant stream of medium. Providing important benefits for other conditions, which the stirred bioreactors cannot.

2.3.2.1 Rotating Wall Vessel Bioreactor

The rotating wall bioreactor was initially developed by NASA (National Aeronautics and Space Administration) in order to protect the cell culture experiments from the forces to which they were subjected in the takeoffs and landings of spaceships [90]. However, later on, the device proved to be useful for TE as well, being employed to cartilage, bone and skin tissue cultures [27]. It consists in a cylindrical chamber where the wall is able to rotate in a constant angular speed. The cylinder wall is rotated at such speed, that it is capable to achieve balance between gravitational forces, hydrodynamic dragging force and centrifugal force, originating a micro gravitational environment, which is felt in the scaffold (Figure 2.2a). This balance of forces enables the scaffold to remain suspended in the cellular environment, taking full advantage of the mass transfer and reducing the shear stress [91]. Throughout the cell culture, the tissue mass and cells increase inside the bioreactor, raising the need to increase the rotation speed in order to keep balancing the forces and assure to maintain the scaffold in the micro gravity environment. Experiments using this bioreactor can be found in literature for tissues such as cartilage constructs TE, describing the use of alginate hydrogel as a scaffold, seeded with human cartilage progenitor cells resulting in elastic cartilage like tissue [92]. Scaffolds composed of collagen, hydroxyapatite and chondroitinsulfate seeded with bovine and human articular chondrocytes getting enhanced type II collagen production [93]. Furthermore, with other types of tissue such as bone constructs, experiments can be found using PLGA as scaffolds seeded with rat calvarial osteoblast cells, where the bioreactor enables cell phenotypic expression enhancement and matrix synthesis mineralization [94]. Although the system presents reduced diffusion limitations of nutrients and waste products, the cellular growth is not always uniform due to rotation, some capsule scaffolds jump into the walls causing cellular damage to the culture (Figure 2.2a(1)). In order to overcome that, it is possible to find in literature some derivative models such as in Figure 2.2a(2) and Figure 2.2a(3), however mineralization effects and culturing benefits due to the rotation are still limited to the scaffolds outside edges [77]. Comparing static cultures and the spinner flask assisted cultures, the rotating wall vessel bioreactor presents much better results in cellular proliferation and differentiation [77].

2.3.2.2 Wave Bioreactor

The wave bioreactor is a system composed by two main parts, the stirring platform and a cell bag that receives the cellular mixture. The particularity of this bioreactor is the way its stimuli is applied by the employment of waves generated by the platform to which the cell bag is attached. It is possible to control the wave motion intensity through the stirring of the motor and platform inclination [95]. These waves provide the necessary mixture and oxygen transfer to the culture, resulting in a perfect cellular growth environment, which can support more than 10 million cells per milliliter. With the angular motion of the platform, the cellular mixture keeps generating waves, stimulating the culture continuously (Figure 2.2b). The combination of this type of bioreactor with Cytodex microcarriers has been reported, aiming to optimize the expansion of adherence cells for stem cell therapy [96]. In the case of therapeutic MSCs through the combination of single placenta, a wave bioreactor and microcarriers has been estimated to produce up to 7000 doses [97]. One of the greatest advantages of this bioreactor is the fact that there is no need of cleaning or sterilizing process of the bioreactor for each culture, due the use of disposable cell bags, providing higher protection against contaminations and simplicity of use, also reducing the costs and time to start a production process. This only works because the culture bag is manufactured with inert biocompatible material for a single use. Another great advantage of this type of system is the capacity of production it offers such as quantities up to 500 litters, being able, as well, to produce small quantities of 100 ml [88]. They are able to keep the oxygen concentrations in the small cultures, becoming comparable to the stirring tank bioreactor by its production capacities. These devices can be divided by production quantities, considering between 0.1 to 5 litters for small quantities or 1 to 25 litters for lab production scale. For higher quantities, industrial scale, there are devices with production capacities from 10 to 100 litters and 100 to 500 litters, enabling up to 5 trillion cells in a single culture [88]. However, the main disadvantage of this devices, are the costs of the disposable cell bags, as the large-scale production gets too costly. Another disadvantage is the fact that each cell bag is limited to a single culture, justifying the use of this bioreactor only for high scale production in order to get the most out of each bag.

2.3.2.3 Pneumatic Bioreactor

This type of bioreactor employs gas injection in order to stirrer and balance the cellular culture particles. They can be used for the creation of several products, like hydrogenated fat (margarine), carbonates and bicarbonates, gluconates (calcium, magnesium, sodium, and zinc), lipideous (biodiesel), biologic yeast, unicellular protein, vaccines, fuels, etc. This device operates with several

processes as well, since lipideous hydrogenation, alkalis carbonation, glucose oxidation, seaweed and cyanobacterial cultures, yeasts cultures, cell culture, extractive fermentation, among others [98]. The pneumatic bioreactors can be divided mainly in three types: bubble column, the concentric airlift and split airlift (Figure 2.2c). These devices are mainly composed by a cylindrical tank, having in its base a sprinkler from where the bubble form gases and are injected in the liquid [89]. Thereby, the incorporation of the gas in the liquid phase and the uniformity of the reaction environment are obtained exclusively by the injected gas, which drains upwards due its lower density, dragging with itself the liquid and promoting a random motion of the environment that further stimulates the gas-liquid mixture. In this type of devices, the rising and decreasing zone of the liquid-gas is in the same compartment, being separated in a way to drain the liquid-gas dispersion. The main difference between the bubble column and airlift based bioreactors are the draining method. While in the bubble column bioreactor the draining process results from a random motion in the liquid phase, in the airlift version, a liquid cyclic drain is obtained [89]. A report can be found in the literature where the performance of the three variations of these pneumatic bioreactors was studied, and it was concluded that the concentric tube airlift presented the higher average shear stress generation among them [98].

2.3.2.4 Perfusion Bioreactor

Perfusion bioreactors are ones that better simulate *in-vivo* environment by providing a flow of medium to a cell culture, providing oxygen and nutrients through the cell-seeded scaffolds [28, 99]. Perfusion systems usually show better results than the other systems, thus most micro bioreactors are based on these systems [100]. These devices are mostly used in the construction of bone [101] and cartilage tissues [102, 103], TE approaches, which take advantage of the flow generated shear stress. These are reported to provide better outcomes when compared with stirred flask or rotating vessel bioreactors due to higher uniformity in the mixed medium, which allows a better environment and physical stimulation on larger constructs [25, 27]. These devices are very versatile enabling several configuration types such as closed loop (Figure 2.2d(1)), where medium recirculates providing naturally produced growth factors, and single pass, which supplies always fresh medium removing any waste accumulation (Figure 2.2d(2)) [26]. However, the medium flow must be optimized in order to avoid damaging the cell culture. High flow rates may induce high shear stress while low flow rates may induce lack of nutrients and low oxygen supply. In fact, the rate of medium perfusion has a significant effect on tissue characteristics as was verified in [101] where bone marrow-derived human MSCs were seeded in a scaffold composed by a fully decellularized bovine trabecular bone. Low flow rates have

been reported to result in higher cell viability as it has been used in [103] (0.075 to 0.2 ml/min) with cartilage constructs composed by human chondrocytes seeded in PGA scaffolds, but in the case of bone TE it does not accomplish a suitable distribution of nutrients, oxygen and waste removal [25]. On the other hand, very high flow rates might hinder cell attachment as well as the formation and deposition of the extra cellular matrix making the perfusion system useless. Therefore, it has been suggested that the use of a dynamic non-continuous flow could be a solution that allows detached cells to reseed again into the scaffolds [25]. The type of scaffold used for the tissue construction will also influence the mass transfer according to thickness and pore sizes [28], requiring interconnected pores with 70 to 99% porosity for easier direct perfusion [25].

2.3.3 Mechanical-Based and Multi-Stimuli Bioreactors

Several types of stimuli are felt by tissues in the human body as a result of the daily activities that result in cues such as vibration, forces, impacts and compressions on joints, muscles and bones, as well as electrical signals that expand from brain to every part of our body. In order to resemble those conditions and thus create a biomimetic microenvironment for TE, several equipments have been designed. Single stimuli devices have been developed namely: for compression of cartilage constructs [68], stretching of muscular based fibers [104] and electrical stimuli for human embryonic cells [72] showing better results than the ones performed in static conditions. However, the multi-stimuli devices, joining both mechanical and electrical stimuli are able to better mimic the conditions occurring in-vivo, reaching a better biomimetic microenvironment such as the ones in Figure 2.3.

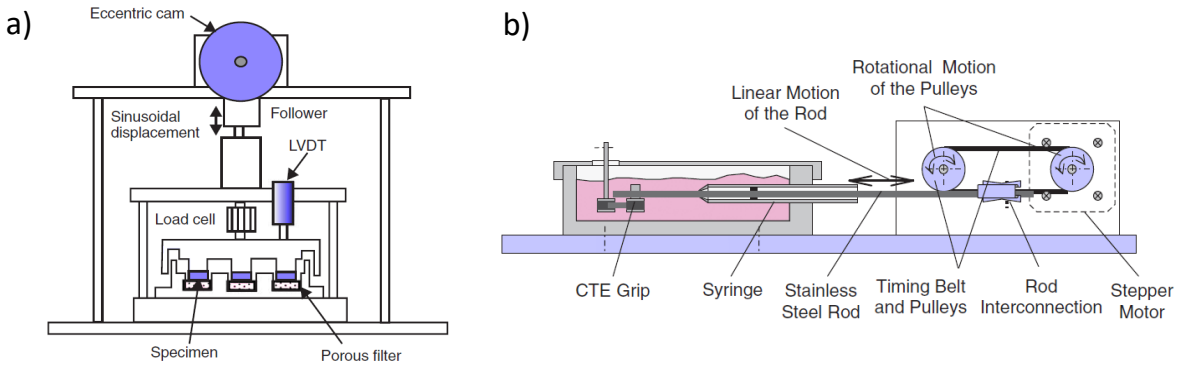

Figure 2.3 – a) Mechanical schematic of a cyclical compression bioreactor for bone marrow derived mesenchymal stem cells (adapted from [105]) and b) Design of electromechanical bioreactor actuation and motion-transform unit for culture of cardiomyocites [106].

2.3.3.1 Compression-Based Stimuli Bioreactors

Mechanical compression bioreactors are commonly used in TE, inducing the well-known mechanic-transduction phenomenon on cells. The most used one is the one providing dynamic stimulation to cells such as cartilage, offering better results by comparison with other types of stimuli for these types of tissues [68, 107]. These devices are usually composed by a system of linear vertical movement with the aid of a motor, and control system, which manages different amplitudes and frequencies of motor oscillations as exemplified by Figure 2.3a. The applied loads and movements frequency in a petri box or culture plate can be defined by digital control through local control or a computer. The load is uniformly distributed to each scaffold through cylinder pins, although the height of each scaffold must be the similar in order to apply the load evenly throughout all the cells, in order to avoid an unbalanced culture [105]. However, some systems were developed to provide dynamic shearing motions by oscillating along the X-axis as well, in order to spread shear stress throughout the culture wells [67]. For that, a biaxial loading bioreactor was developed in order to stimulate cartilage tissue constructs in two directions. The authors employed an experiment of 10% of the sample thickness compression at 1 Hz on the Z-axis, and 0.5 Hz in the X-axis generating shear stress for a period of 3 hours per day, reaching increased proteoglycan, collagen deposition and samples thickness. Although, the authors did not find a significant influence in the mechanical properties as they expected, whereas using a uniaxial compression increased both proteoglycan deposition and Young Modulus [67]. Mixed type of stimuli rather than just mechanic was also developed through customized bioreactors using mechanical compression and perfusion in order to study the influence of both in human bone mesenchymal stromal cells contributing to equilibrium modulus enhancement and procollagen type I N-terminal propeptide synthesis [66].

2.3.3.2 Stretching-Based Stimuli Bioreactors

Stretching bioreactors use an operation principle close to the mechanical compression bioreactors, whereas the motion relies mainly as well on motor displacement or magnetic displacement. This type of stimuli is being used stimulate heart muscle [62], smooth muscle bone tissues [63] and tendons [65] through cyclic stretching forces. Due to greater response in cell proliferation and differentiation using the above-mentioned type of cellular constructs and bioreactors, the interest in applying electrical stimuli as well has also been a focus of study. Thus, some devices have been develop in order to tackle these stimulation needs in TE cultures. Some examples can be found of electromechanic bioreactors such as the one presented in [106], capable of providing the tissues electrical and mechanical stimuli, employed to cardiomyocites cell culture. This device is composed by three main units: control unit, culture chamber, transform unit and actuator of the applying forces. The culture chamber is equipped with electrodes, which provide the electrical stimuli to the tissues, with voltage amplitudes comprehended between 5 to 20 V, generated with 50 Hz frequency [106]. This unit is composed by a step-motor, which is coupled to a toothed wheel connected to another with a timing belt (Figure 2.3b). This mechanism is used to connect the stainless steel rod to the motor motion, making the culture mixture inside the syringe, which is united to the rod, to react with the electrodes in the culture chamber [106]. However, this bioreactor is limited to the quantity and culture type inserted in the syringe. In addition, for cardiac patches, other even more complex electro-stretching mechanism was developed in [75] able to apply cyclic strain from 0.5 to 20% at 1 to 2 Hz with square wave pulses from 6 to 8V at 1 to 10 Hz, also including a medium recirculation system. The authors employed a validation experiment by submitting the cardiac patches through mechanical stimulation (strain 5%, frequency 1 Hz) for 24 hours, evaluating the stimuli influence by comparison with static conditions [75]. In [76] the authors developed an electro-stretching bioreactor for cardiac adipose tissue-derived progenitor cells stimulation, where the stretching force was generated through permanent magnets force by keeping a static end of the scaffold held by disposable PDMS supports coating neodymium magnets, where the first end was fixed and the second end was pulled by a linear movement produced by a motor. Thus, applying 50 mV/cm square waves at 1 Hz through platinum wires and 10% stretching for a period of 7 days, resulted in improved cardiac function after myocardial infarction and increased vessel density while migrating to the murine myocardium and scar, maintaining their cardio myogenic potential as an *in-vivo* environment [76]. In an earlier stage complex custom setups for stretching and electro stimuli of mouse skeletal myoblasts were employed through tubular setups, which synchronize

the electromechanical stimulation to aligned electrospun fibrous scaffolds wrapped around the silicone tubes with regulated 10 PSI pressure producing up to 10.6% strain [74]. The electrical stimuli were applied through wrapped electrodes around tubes endings using 10 ms square waves of 20 V, controlled by a computer running a Labview application to synchronize both types of stimuli, inducing cell elongation, focal adhesion reorganization, and stretch-activated ion channel upregulation, similar to effects previously observed during application of constant uniaxial stretch. The electrical stimulation applied post-myotube formation also enhanced the myogenesis process [74]. In terms of technology development and achievement, these customs devices and multi-device assemblies already allowed important advancements in the understanding of the effects of physical stimulation on cellular constructs, although still lacks more research and some quantification on ECM production according to stimuli intensity.

2.3.4 Magnetic Bioreactor

The magnetic stimuli bioreactor operating principle consists in applying a remote stimuli in a culture place without any mechanical attachment and reducing the changes of contamination while providing an actuation in the experiment. If the method is applied *in-vitro*, the magnetic field can be generated outside of the tissue culture recipient, or in the case of being applied *in-vivo*, can be generated outside the organism [45]. The magnetic signal can be supplied through a permanent magnet or electromagnet. The permanent magnets can be used in order to create an alternated magnetic field by changing their position relatively to the cells that are on the culture. Thereby, the motion of the permanent magnets platform can be perpendicular to the culture chamber or longitudinal. In the electromagnets case, the position variation platform is unnecessary, as they can be controlled by current amplitude and frequency and their static presence is enough [45]. In Figure 2.4 the main system configurations of this bioreactor are displayed (vertical and horizontal displacement), where a culture chamber can be seen (1) the scaffolds are introduced with longitudinal space between them (4), and the permanent magnets (2) are connected to the moving platform (3), which is connected to a computer-controlled terminal. The permanent magnets are applied externally to the culture chamber, and with the same spacing as each scaffold will have a magnet related to it. In this patented example

[45], the nutrients are supplied by perfusion of medium flow to the bioreactor by the entrance in the culture chamber (5) and are directed until the exit (6).

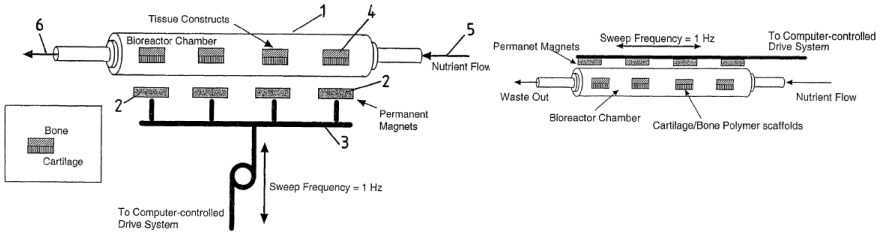

Figure 2.4 - Patented design of possible magnetic stimuli configurations through vertical and horizontal permanent magnets displacement [45].

Furthermore, the permanent magnets can be replaced by electromagnets, removing the need of moving parts in the system. This mechanism keeps the culture chamber fixed, making the permanent magnets platform oscillate, resulting in an alternated magnetic field applied to the culture. The usually applied oscillating frequencies vary between 0.1 to 10 Hz, even though other frequencies outside this range are possible to apply by the system. The magnet field oscillation stimulates each compression/relation cycle applied to the scaffolds, producing a motion in the nanoparticles relatively to the magnets, compressing the cells and the scaffold. With this compression, a mechanical load is simulated without direct contact. The load amplitude can be easily changed, through magnets position or changing the physical properties which compose the scaffold. The scaffold can be composed by materials that react to alternate magnetic fields and provide further stimuli as it has been observed with magnetoelectric composites based on Terfenol-D and PVDF-TrFe, where it was possible to achieve an enhancement of up to 25% in cell proliferation with pre-osteoblast cells[108]. However, this type of bioreactor is limited to the culture nature, meaning it only allows the use of one type of nutrients for each culture, in spite of the usual need of different cells for TE experiments in single cultures.

2.4 Commercial Bioreactors

Regarding the market of bioreactors worldwide, many companies can be found to take commercial advantage of these devices beyond this engineering field by building several models of bioreactors for many types of tissue cultures and any other biochemical engineering purposes such as fermentation, fuel and wastewater treatment, among others. Currently, bioreactors market growth include hybrid technologies employment and increased rate of adoption of single-use technologies. However, the increased attractiveness of contamination-free single-use bioreactors among the biopharmaceutical companies and substantial advances in the biologics market has brought some challenges regarding regulations on these devices and issues related to the use of disposable bags, which are extractable and leachable [109]. In Table 2.1 many bioreactor manufacturers are disclosed according to country and manufactured bioreactor types, resulting in a gross majority to build bioreactors aimed for laboratories (41) and bigger stainless steel based apparatus (43) for higher production scales. As previous stated the single-use bioreactors are currently a growing market and it is possible to find in Table 2.1 around 15 manufacturers producing such type of bioreactors with prospects for increasing, while photobioreactors are the scarcest device to find a manufacturer with only 10 manufacturers in this list.

Table 2.1 - Bioreactor manufacturers around the globe according to country and bioreactors type (L - Laboratory Bioreactors; SS - Stainless Steel Bioreactors; Ph - Photobioreactors and SUB - Single Use Bioreactors) [110, 111].

Company Name	***Country***	***Bioreactor Types***
Aglaris Ltd	Spain	L
Amering Technologies	India	L SS
Andel Equipment	India	L SS
Applikon	Netherlands	L SS SUB
Aroko Bio Engineering Co.	Iran	SS
Bioforce	Malaysia	L SS
BBI - Biotech	Germany	L SS Ph
Bailun Biotecnology	China	L SS
Belach Bioteknik	Sweden	L SS
Bellco Glass	USA	L
Bio-Age	India	L SS
Bioengineering	Switzerland	L SS Ph

Bilfinger	Germany	SS
Bionet	Spain	L SS
Biotehniskais Centrs	Latvia	L SS Ph
Biotron	USA	L SS Ph
Biozeen	India	SS
Broadley James	USA	L
Cellexus	UK	SUB
Cellscale	Canada	L
Cercell	Denmark	SUB
Centrion	South Korea	L SS Ph
Cesco	Taiwan	L SUB
Distek Inc.	USA	L SUB
EastBio	China	L SS
Ebers Medical	Spain	L SS
Electrolab	UK	L
Eppendorf	Germany	L SS SUB Ph
Fermentec	South Korea	L SS
Fermetec Resources	Malaysia	L SS
Finesse Solutions	USA	SUB
Flexcell International	USA	L SS
Frings	Germany	SS
GE Health and Life Science	USA	SUB
Heinrich Frings	Germany	SS
Infors	Switzerland	L SS Ph
Katalyst	India	SS
Major Science	USA	L
Medorex	Germany	L
Merck Milipore	Germany	SUB
Lambda	Switzerland	L
Lleal S.A.	Spain	SS
Novaferm	Sweden	L SS
Pall (Danaher)	USA	SUB
PBS Biotech	USA	SUB
Pierre Guerin	France	L SS SUB
Prime Care Technology	India	L SS
PRAJ	India	SS
Ritai	China	SS
Satake Multimix	Japan	SS
Sartorius	Germany	L SS Ph SUB

Scigenics	India	L SS
Shree Biocare	India	L SS
Solaris	Italy	L SS Ph
Solida Biotech	Germany	L SS Ph SUB
Sysbiotech	France	L SS
T.A. Instruments	UK	L SS
Techniserv Inc.	USA	SS
Thermo Scientific	USA	SUB
VTU Engineering	Austria	SS
Zenith	India	L
Zeta	Austria	SS

TE market comprehends application of material methods, cells and engineering, biochemical and physicochemical factors, thus bioreactor market is only a small portion of the many segments in this market. In Figure 2.5 the data from Table 2.1 is converted in a pie graph giving a better picture of how the bioreactor manufacturers market is spread around the world, having the bigger emphasis in USA, followed by India and Germany expressing the biggest market in Europe. Throughout all these companies, some stand out providing all the bioreactor existent technologies such as Solida Biotech in Germany presenting their systems as modular bioreactors and fermenters for fermentation and cell culture to Broadley James in USA with mainly spinner flask/stirred tank approaches for small to medium batch cultures.

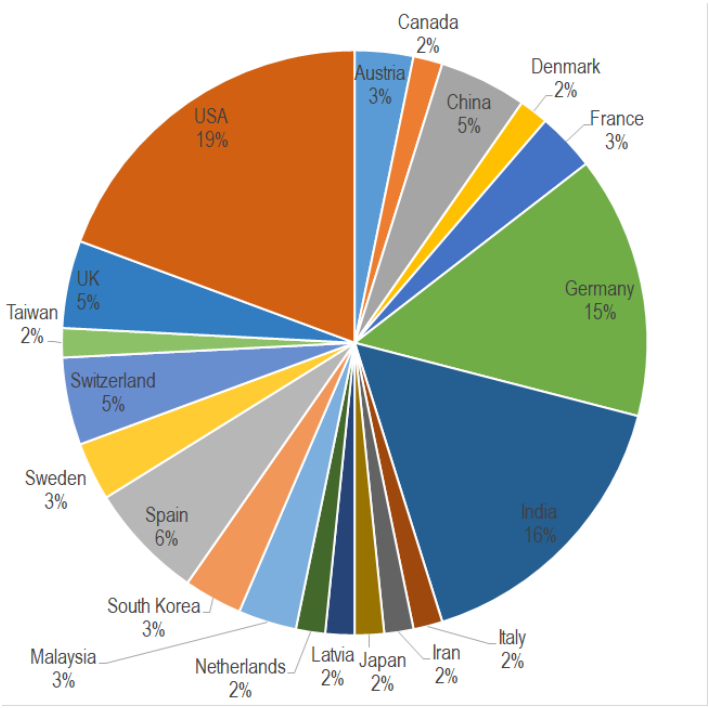

Figure 2.5 - Bioreactor manufacturers' worldwide (graph based on Table 2.1).

As many solutions are available in this engineering field, which encompasses many variables and market segments, the focus must be set in in specific aspects in order to be able to grasp and understand one of those single market segments. Thus, inside the scope of bioreactors for tissue culture of mostly bone, muscle and cartilage, commercially, it is possible to find bioreactors such as vacuum bioreactors the FX 6000-T (Figure 2.6a), which are being sold by Flexcell. These devices are used as a computer peripheral for control and are able to apply static or cyclic deformation (Tension Force) to cells in monolayer and 3D scaffolds. They claim it is possible to regulate the vacuum pressure and positive air pressure through a digital valve, for a given strain regimen. They aim to achieve with this product a biomimetic system for muscle, lung, heart, vascular vessels, skin, tendon, ligament, cartilage and bone cell tissues. Thus, this system allows to be controlled by software for multiple frequencies, amplitudes and waveforms on the vacuum stimuli, having two types of accessories according to equibiaxial or uniaxial strain to be applied to the scaffolds [112].

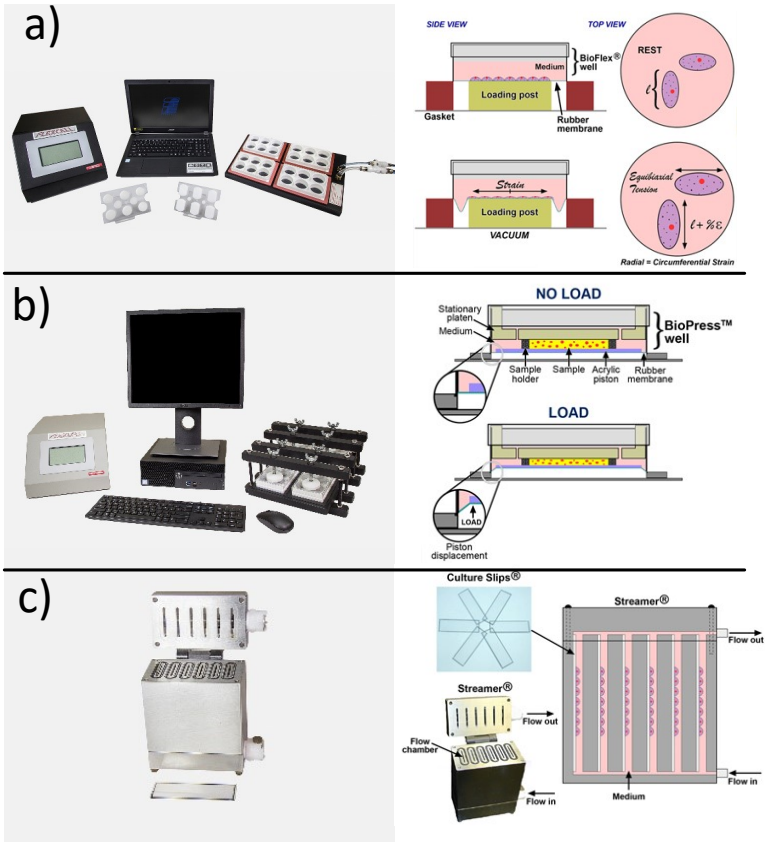

Figure 2.6 - a) FX6000-T vacuum bioreactor and application of equibiaxial strain with Flexcell® Tension Systems using their Bioflex® culture plates [112]; b) FX-5000C compression bioreactor and schematic of how compression is applied to tissue samples in this supplier developed BioPress™ well [113]; and c) Streamer® perfusion bioreactor and b) fluid shear applied to cells cultured on this supplier Culture Slips® in the device [114].

In their portfolio, they also comprise compression bioreactors such as the FX-5000C (Figure 2.6b) which regulate the compression through positive air pressure to compress plane or 3D scaffolds. The graft samples are compressed between a piston and fixed plate using their own commercial culture plates, being able to reach as high as ~6.35 kg of force [113]. As for perfusion, this seller provides regulated shear stress devices to cultures with laminar, pulsatile or oscillating flow through a peristaltic pump computer controlled (Figure 2.6c). They provide an extra device (Osci-Flow®) for oscillation or pulsatile frequency and pattern regulation [114]. TC-3F bioreactor from EBERS offers a refreshed design from a previous model bioreactor which can measure the force it applies on samples for each tension or compression force while running up to 3 experiments, having the force applied recorded, claiming to be the first of its kind (Figure 2.7a, b and c). The manufacturer states it can apply up to 400 N forces on samples with a maximum speed of 10 mm/s, although the sensors are only able to measure

forces up to 100 N. The three available culture chambers can harbor a maximum volume of 90 mL and are autoclave compatible [115].

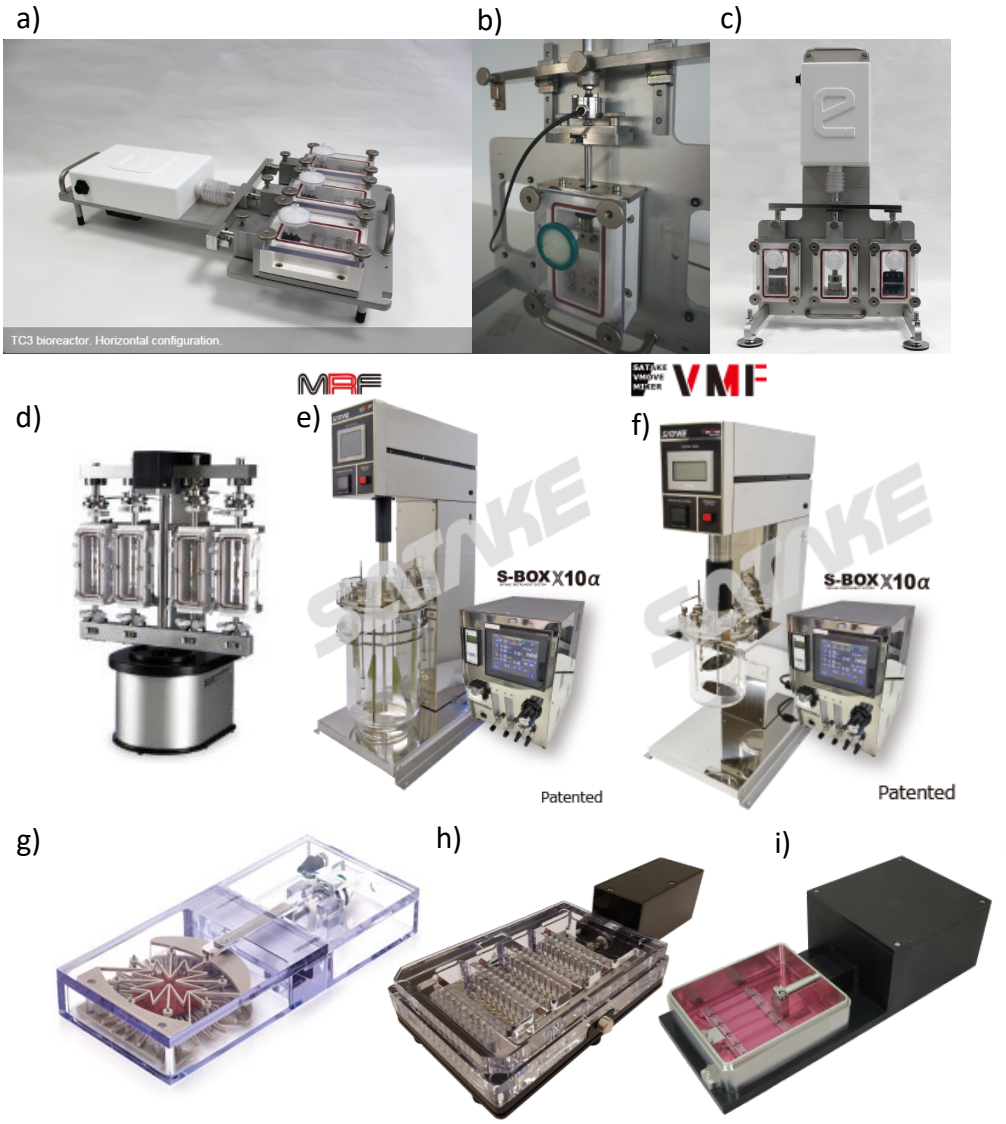

Figure 2.7 - EBERS TC-3F stretching and compression bioreactor can be used a) horizontally or b) vertically by adapting the c) standing supports [115]; d) ElectroForce BioDynamic 5200 series [116]; e) MRF stirred tank bioreactor for up scalable productions; f) VMF stirred tank bioreactor which enables high values of shear stress on cell cultures [117]; g) MCB1 biaxial stretching bioreactor; h) MCFX uniaxial mechanical stimuli bioreactor with real time imaging and i) MCT6 High force stretching bioreactor by clamp grips [118].

On the other hand, TA Instruments offers a different approach of high precision force stimuli devices, such as the ElectroForce BioDynamic 5200 (Figure 2.7d). It is a system, which can apply multi-axial loading on samples, such as compression through platens for stimulation and characterization of

biomaterials. These devices can be used on workbenches or conventional incubators [116]. It is stated to be suitable for characterization of the mechanical properties of bone, cartilage, intervertebral discs or any other disc-shaped tissues and biomaterials. The system allows the user to select the physiologic behavior to mimic some activities such as the loading a walking period provokes in cartilage joints. Furthermore, this bioreactor flexibility for other types of tissues, such as ligaments, tendons and skin, which can be stimulated through stretching by adapting optional tensile grips, providing the system with a higher range of stimuli available (traction, compression, torsion, static and dynamic forces). According to manufacturer, it provides low force testing capabilities until 200 N of force in independent chambers and medium from each other, enabling adaptation with independent perfusion circuits [116]. From Japan it is possible to find a manufacturer such as SATAKE Multimix, which produces from laboratory to industrial scale equipments, they identify themselves as a unique company who build custom systems according to customer needs, from research until the industrial production line. In their portfolio, they gather stirred-tank based bioreactors for small culture batches and up until the industrial scale. This manufacturer claims to be an expert developing high-performance mixing impellers and mixing methods, stating their experience is key in order to be able to replicate the lab scale results in the industrial scale results. They manufacture some bioreactor solutions for many situations, such as the MRF model (Figure 2.7e) which is designed for current production and for upscale from 1.5 L up to 20 kL. As for stimuli precision they provide the VMF model (Figure 2.7f), which provides vertical reciprocating motion combining the blending performance with gentle mixing by enabling severe shear stress control with productions up to 10 L, among many more [117]. A Canadian manufacturer CELLSCALE develops bioreactor structures such as the ones in Figure 3.16. Thus, in Figure 2.7g, it is possible to see the MCB1 model, which applies up to 20% biaxial stretch, with 10 N force at 10 mm/s and maximum of 2 Hz in monolayer or 3D scaffolds up to 35 mm size. In Figure 2.7h, the model MCFX provides uniaxial stimulation of cell culture with real-time imaging in a flexible silicone 16 wells plate, executing user-specified stretch protocols such as simple, cycle and intermittent stretch stimulation up to 12.5% strain, with 30 N force at 10 mm/s and maximum of 5 Hz. In Figure 2.7i the model MCT6 is a uniaxial cell culture stimulation device of 6 parallel samples and harbors a 200 N actuator and screw driven clamp grips to apply user-specified stretch protocols such as the previous device but with higher speed (20 mm/s) and loading capacity (200 N). The manufacturer states all assemblies can be sterilized and are suitable for long-term cell culture in a laboratory incubator [118].

Table 2.2 - Publications according to technology and tissue types being employed in literature.

Stimuli	Category	Technology	Tissue Type	Cell Type and Scaffold	Year	Ref.
Shear Stress	Stirred Bioreactors	Custom sample holder magnetic Teflon® disk stirrer	Cartilage	Rabbit MSCs seeded into fibroin sponge	2007	[119]
		Spinner Flask		Human adipose-derived stem cells seeded into fibrin gel	2012	[80]
				Trachea cartilage grafts using marrow MSCs seeded into PLGA	2010	[120]
				Bovine articular chondrocytes seeded into PGA	1998	[121]
				Human chondrocytes seeded into chitosan	2012	[122]
			Bone	Human bone marrow stromal cells seeded into coralline hydroxyapatite	2007	[79]
	Rotating Wall	Rotating Wall Vessel – Free Fall	Cartilage	Human articular chondrocytes seeded into a 3D porous material consisted of collagen, hydroxyapatite, and chondroitinsulfate	2012	[93]
				Bovine and human chondrocytes seeded into 2% alginate hydrogel	2006	[92]
			Bone	Rat calvarial osteoblast cells seeded into PLGA	2004	[94]
				Rat osteoblasts seeded into cytodex-3 micro-carriers	2007	[123]
			Skin	Human epidermal stem cells seeded into cytodex-3 micro-carriers	2011	[124]
	Perfusion	Continuous and variable flow rate within a controlled range	Cartilage	Human chondrocytes seeded into PGA	2011	[103]
		Closed loop continuous medium flow		Human Articular Chondrocytes seeded into Hyaff-11 non-woven mesh	2010	[102]
				Human articular chondrocytes seeded into polyactive foams and Hyaff-11	2003	[125]
				Bovine articular chondrocytes seeded into three-dimensional collagen sponges	2001	[126]
		Variable flow within a controlled range	Bone	Bone marrow–derived human MSCs seeded into fully decellularized bovine trabecular bone	2008	[101]

Shear Stress	Perfusion	Closed loop continuous medium flow	Vascular	Rat aortic smooth muscle cells seeded into decellularized rabbit aortas	2012	[127]
		Pulsatile bioreactor with endoscopic monitoring unit		Human vascular endothelial cells and fibroblasts seeded into polyurethane scaffolds	2012	[128]
Biomechanical Hydrostatic Pressure	Dynamic Hydrostatic	Air pressure-driven piston, custom-made stainless steel culture chamber and mechanical manometer	Cartilage	Bovine articular chondrocytes seeded into synthetic 3D porous degrapol	2008	[129]
	Dynamic Hydrostatic	Air pressure-driven piston with chamber and medium replenishing peristaltic pump	Cartilage	Human nasal chondrocytes and human adipose stem cells seeded into gellan gum hydrogels	2012	[130]
	Static Hydrostatic			Bovine articular chondrocytes	1994	[131, 132]
	Static and Pulsed Hydrostatic			Bovine articular chondrocytes seeded into agarose gels	2003	[133]
Electro-mechanical	Compression	Stepper motor displacement, uniaxial actuator	Cartilage	Human chondrocytes seeded into agarose disks	2000	[134]
				Rabbit chondrocytes seeded into chitosan/gelatin	2009	[135]
				Rabbit chondrocytes seeded into genipin-crosslinked chitosan/collagen	2013	[136]
	Compression			KUM5 cells seeded into macro porous poly(ε-caprolactone)	2015	[68]
		Stepper motors displacement, biaxial actuators		Porcine chondrocytes seeded into agarose gels	2013	[67]
		Linear variable differential transformer (LVDT), uniaxial actuator	Bone	Rabbit bone-marrow MSCs seeded into agarose disks	2004	[105]
	Stretching	Vertical tube chambers with attachment anchors with translational and rotational strain		Bone marrow aspirates (human or bovine) seeded into collagen gels	2002	[137]
		Linear motor-driven uniaxial stretching device	Skin	Human foreskin expansion	2008	[138]
		Controlled 3D left-ventricular stretching through inflatable latex balloon	Muscle	Rodent neonatal cardio-myocytes seeded into decellularized rat hearts	2017	[139, 140]
		Stepper motors pulling 4 holders for equibiaxial planar stretching		NIH 3T3 fibroblasts seeded into collagen gels	2018	[104, 141]

Electro-Mechanical	Electrical	Modified Cooper tissue culture disk	Bone	Osteoblastic cells (MC3T3-E1)	1997	[142, 143]
		Arduino Uno® controlling signals instrumented with digital potentiometers and amplifiers, with extra piezo-actuated micro pump for perfusion	Muscle	Cardiac cells seeded into collagen sponges	2013	[144]
		Silver electrode and platinum electrode in each end of scaffold	Nerve	Nerve stem cells seeded to polyaniline with poly (ε-caprolactone)/gelatin	2009	[145]
		Platinum mesh electrodes on culture chamber	Neural	Anionic dopant dodecylbenzenesulfonate seeded into polypyrrole	2015	[146]
	Electro-Stretching	Stepper motor displacing thin stainless steel rod inserted in syringe working as a seal against contamination, stainless steel electrodes at both sample grips	Muscle	Cardiomyocytes seeded into collagen gels	2005	[106]
		Electrodes wrapped around tube inflation controlled by solenoid valves		Mouse skeletal myoblasts (C2C12) seeded into aligned electrospun polyurethane fibers	2008	[74]
		Stepper motor-driven uniaxial stretching device and electrodes of Teflon-coated silver wires		Lewis rat MSCs seeded on decellularized porcine myocardium	2013	[147]
		PDMS coated magnets grips displacement through magnetic attraction controlled by linear motor, grips with platinum wires for electrodes connections		Cardiac adipose tissue-derived progenitor cells seeded into fibrin hydrogel	2016	[76]
Multi-stimuli	Electro-stretching-perfusion	Stepper motor controlling grips position with electrode contacts, including single pass perfusion system		Rat cardiac progenitor cells seeded into poly(glycerol-sebacate) cardiac patches	2013	[75]
	Stretch-perfusion	Cyclic distension achieved by pulsatile medium flow	Skin	Neonatal human dermal fibroblasts (Invitrogen) seeded into fibrin gel	2015	[148]

2.5 Summary

In this chapter, the main types and operating mechanisms being employed in bioreactors were listed and summarized. Systems were grouped in Table 2.2 regarding type of stimuli and technology used to employ such cellular tissue development incentives. Bioreactors technology can take several formats, which are suitable for one or more types of tissues, such as spinner flasks, stirred tanks, and rotating wall vessels are more suited for bone and cartilage constructs, which take advantage from the shear stress stimuli, so does muscle and skin constructs takes more advantage from stretching stimuli and neural constructs from electricity. However, each one of them still take advantages from the others stimuli, because they all happen in-vivo direct or indirectly. Thereby, many bioreactor variations are present, being developed and tested, to better mimic the native environment conditions, such as the perfusion systems where the medium flow providing shear stress, nutrients and oxygen to the scaffold constructs mimicking the blood flow of a body. This document section finishes with the commercial equipment available, which aims provide standardized tissue culture results aimed as well for research, mass production and production scale studies. There are big innovations in bioreactor devices both commercially and research, most of the innovations comes from joining multiple mechanisms to produce multiple stimuli to the culture while adding medium motion (a perfusion mechanism), which means a paramount variable for a TE biomimetic device according to literature. In a financial point of view, all of the research custom equipment can be optimized to reduce tissue production costs after the main culture variables are carefully identified and controlled (standardization) for higher scale production. Thus, until reaching that point, the more tools a researcher can get to test many types of stimuli while providing the most in-vivo like environment, the better chances to grasp the required system properties to design a more affordable production system. Although, not every tissue may be able to be massively produced and may require to be specifically custom designed for each patient, the research equipment will be the ones to use in those specific cases, working in a lean production method according to requirements, although more expensive and time consuming.

3 Bioreactor System Analysis

Bioreactors are devices which, in order to get the most suitable results should be designed/adapted for each specific TE experiment in order to promote cellular high proliferation rates and provide each process step, such as seeding or harvesting, while avoiding contamination [149]. However, in order to reach acceptable developing time and being financial viable for research purposes, performance/time/costs follows an in-between compromise in order to reach a viable solution with sufficient degree of freedom according to adapt for many types of experiments [149, 150]. Spinner flask is an example of a starting point of a lab scale experiment in order to access viability of a specific tissue growth, whereas is followed by scaling study to be produced in bioreactor such as a stirred tank or high production wave bioreactor. An important aspect relies in control and system variables awareness through closed loop control where the system reads its own actuation and acts according to the measured error leaning continually to the most suitable actuation, in order to provide the most accurate possible actuation on each culture [150]. The errors may have several sources, since internal or external vibrations, closure of bioreactor's door or incubator or simple system components aging or degraded from heat, which may influence tissue progression through non-intended mechanobiological signals being applied to the cells introducing bias in the analysis [150]. In the design of a device for TE, several requirements must be fulfilled, since the construction materials, which must be biocompatible and chemically resistant, but also able to withstand the sterilization process required before each culture, such as UV light radiation, autoclave and specific disinfection processes. Thus, each tissue-specific culture conditions requirements must be sufficed regarding also, experiment process, oxygenation method, nutrient supply and stimuli amplitude range [149]. The types of intended stimuli to be applied to the culture plates/chambers must be carefully studied in order to accomplish the most suitable range of stimuli according to the type of tissue targeted and respective geometry directly related to scaffold size, porosity, topography and stiffness [26]. In addition, scaffolds can be used as electromechanical actuators as well, when composed by smart electroactive materials [108], working symbiotically with a bioreactor for single or multi-stimulation operation on the tissue culture. The same type of stimuli can be applied through more than one method, as an example, stretching stimuli type of

bioreactors, can use motor driven clamps, pressurized fluids or gas pumps to apply uniform stretch on scaffolds. However, pumps can be used outside incubators to provide the mechanical stress instead of motors, gaining space inside the incubator avoiding interior generated heat [151]. These pump-based setups can be used to produce tissues such as heart, lungs, bladders or vascular, although, among stretching, some stretching movements can only be accomplished by motor driven clamps in order to produce rotation at one end while stretching in the other, which is useful for engineered tendons and ligaments, while applying direct contact to apply electrical stimuli [151]. The quality of force/stress measurement is key in order to precisely quantity the correct relation between stimuli and cellular growth in the scaffolds [150]. A very important aspect still relies in sensors used for precise stimuli control, transducer types such as: electromechanical; protein; electrical; optical; and light, in order to keep track of the closest possible quantification of the amount of stimuli applied to the cellular constructs to get a correct correlation between stimuli and cell proliferation/differentiation [26]. The same happens for biosensors for culture monitoring to maintain a healthy cellular environment; they can be divided in three main types: potentiometric, amperometric and conductometric, according the type of electrical properties they exhibit measuring their respective chemical variables [26]. However, in this type of experiments replications may become hard to accomplish if all similar conditions are not met, such as oxygenation, shear stress, mechanical force stimuli, nutrient distribution, medium pH related to waste quantity, among others such as scaffold properties as before mentioned [28]. Nevertheless, the most suitable conditions for each type of therapeutic grafts require further research to understand and define, using increasingly more complex and multi-stimuli bioreactor devices, in order to overcome these limitations. The study of anisotropic mechanical properties through real-time monitoring systems has been suggested [151], although the costs associated with digital image correlation and high speed cameras doesn't really tend for affordable medical implants production, it still may be an interesting approach for research and cellular behavior analysis only.

3.1 Tissue Engineering Physical Stimuli Study

As mentioned before, TE main components can be condensed in cells, scaffolds and stimuli, whereas the latter is a bioreactor task to provide besides the required environment. Thus, those same stimuli and more are provided *in-vivo*, through walking, running, breathing and any other daily routines that increases cellular growth, maturation and differentiation of stem cells (Figure 3.1), which is a process a bioreactor aims to mimic as a biomimetic system.

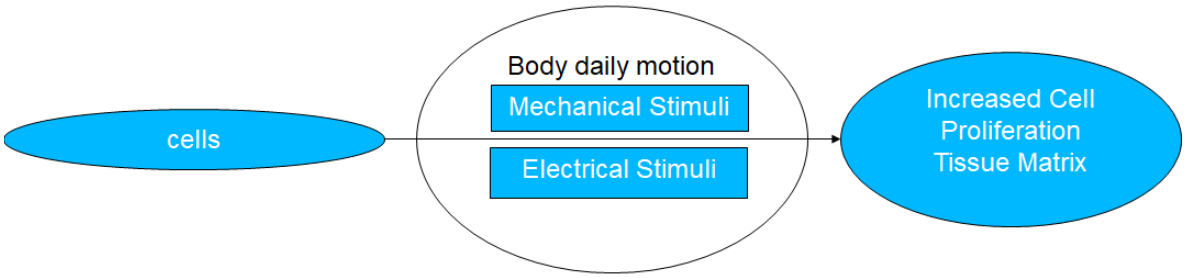

Figure 3.1 - In-vivo daily stimuli and cellular maturation and differentiation.

In some cases of medical therapy required for a patient to recover through generated tissue matrix, produced *in-vivo* through those natural stimuli is not possible due to physical limitations of patients or severe injuries, which may get worst with motion increasing the recovering time, due to lack of stimuli. Thus, a biomimetic system such as a bioreactor, which provide such stimuli to produce in-vitro grafts to be implanted on patients, may represent a solution to such cases where the recovery presents difficult slow results. In order to mimic *in-vivo* environment and stimuli, a human daily routine is analyzed and translated to active cycles and repose cycles within two time lines in order to have an active long time divided between short active periods and short resting periods, finalizing with a long resting time mimicking sleep hours without any activity (Figure 3.2) [108].

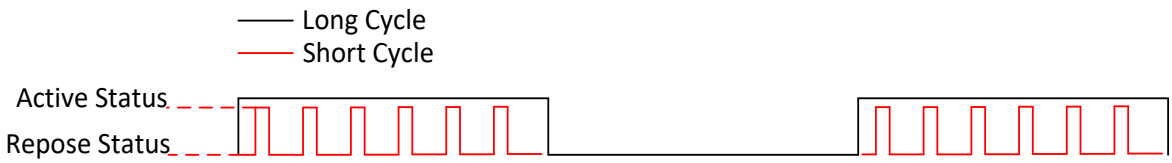

Figure 3.2 - Bioreactor culture active and repose time sequence dynamics.

Thus, the system must have these features regarding active and repose time calibration of long and short cycles, where the stimuli is initiated and terminated according to repose and active periods of the

bilayer timeline (Figure 3.2), allowing to explore several operating time conditions. Consequently, in order to achieve a modular affordable system which can work symbiotically with smart polymer-based materials as scaffolds for both bone and muscle TE an approach centered in a motor driven magnetic remote force was employed. For bone TE using ME scaffolds it is possible to avoid invading the culture chambers/plate while providing the physical stimuli and reducing the contamination chances and damaging the culture using a mechanical-polymer transduction process taking clues from [45]. As for muscle TE, it is not possible to provide stretching force and electrical impulses without invading the culture due the scaffold holders required contact for both stretch force and electrical connection, joining a similar approach from [76] with the previous one, it is possible build a modular system for both case scenarios. Thus, this system sets the stage for more complex systems that this base may harbor at later developments. Thereby, the system must comply with cell culture requirements and every material must comply with the whole process, depending on their level of contact or influence to the culture. Accordingly, the device was designed to meet experiment requirements through careful analysis of the whole process, which includes being placed in an incubation chamber with controlled temperature and humidity (37 °C and 95%, respectively). Therefore, a critical parameter must be followed, which is not increasing the scaffolds temperature while applying sufficient stimuli to the culture which, will be a paramount property in both cases either for bone and muscle TE experiments.

3.1.1 Magnetoelectric Bioreactor

The magnetoelectric bioreactor setup settles in an indirect stimuli provided by a magnetic field, which is transduced into mechanical stress and piezoelectricity transmitted into the cell sites. This transduction is possible through ME materials acting as scaffolds, which are composed by two types of materials: magnetostrictive and piezoelectric particles working synergistically to produce a composed stimulus. Piezoelectric materials act as an electromechanical transducer, by converting pressure variation into electrical charge thereby, an alternated mechanical stress such as vibration produces piezoelectricity as a response. As aforementioned, scaffolds, besides biocompatibility, are required to be flexible so the best type of magnetoelectric scaffold must be polymer based, resulting in a single co-material to act as the piezoelectric particles, which has the highest piezoelectric response among polymers being the P(VDF-TrFE) [152]. Magnetostriction can be defined as a material, which

generates mechanical stress with the presence of an alternated magnetic field and comprehends materials such as Terfenol-D, Metglas or Cobalt Ferrite [40, 153]. The ME composites can be laminated and particulated micro and nano composites, having significant response magnitudes difference between them, 4 orders of magnitude lower on particulated composites [108]. However, particulate composites offer higher flexibility, simpler fabrication, miniaturization and degradation absence of the ME interface [40, 154, 155]. In Figure 3.3 it is schematized how the magnetic field to electric field transduction operates in particulate ME composite materials.

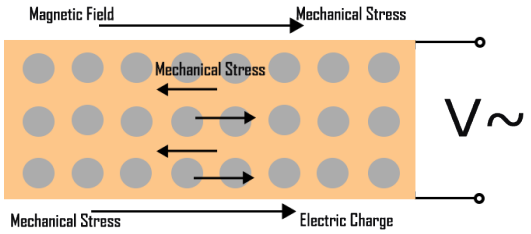

Figure 3.3 - Particulate magnetoelectric composite transductions.

Thus, through a time variant magnetic field it is possible to generate a mechanical stress and electrical charge at the material surface transmitting it to the seeded cells in this ME scaffolds. In order to achieve it, the culture plates must be analyzed to study how to apply such a magnetic field, regarding mechanical distribution and scaffolds positioning during the culture. Therefore, in Figure 3.4, the culture plates to be used are displayed, in this case, for 24 and 48 culture wells, where the medium will be involving the scaffolds and cells to keep them in their surviving environment inside an incubator at 37 °C, temperature that cannot be compromised by the system at risk of culture failure. In order to apply evenly the time varying magnetic field to make the ME scaffolds vibrate at the desired frequency, there must be a magnetic field source available immediately bellow each culture well.

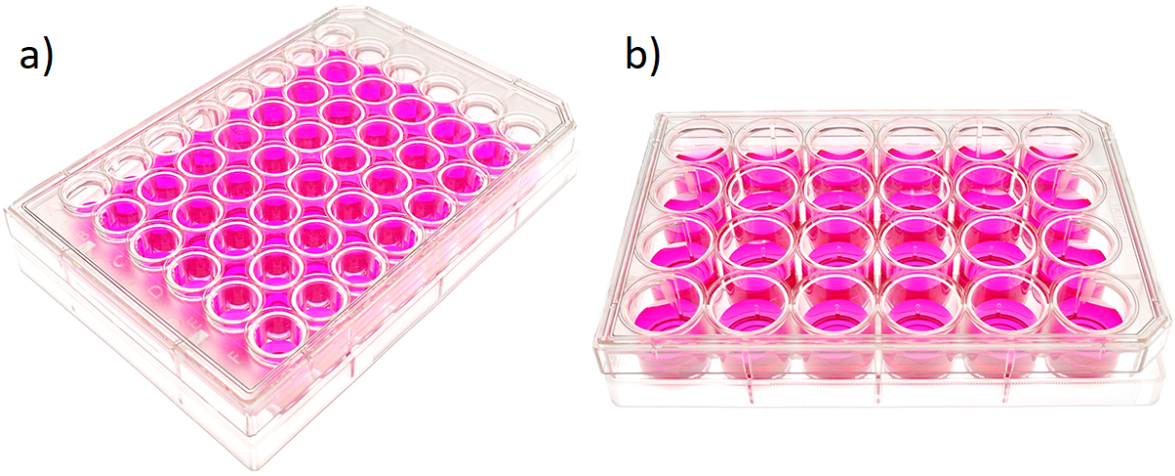

Figure 3.4 - Commercial culture plates being used with a) 48 and b) 24 culture wells.

The magnetic field could be provided by electromagnetic actuators such as coils or by permanent magnets, although in each there are advantages and disadvantages. Electromagnets provide the most flexible method in terms of magnetic output control, which can be digitally controlled with high precision with electronic control over amplitude, frequency and magnetic waveform. However, in order to produce the required magnetic field an amount of considerable current in the coils windings will be required, producing as well considerable heat. This cell hazardous environmental variable (heat) can be attenuated by increasing coil wire section and reduce current electrical resistance and heat loss, but the tradeoff will result in a bulky system as the current amplitude and number of windings will dictate the magnetic field force. Either way, higher current means higher heat losses, whereas higher number of windings results in the same outcome as higher length means higher resistance. Thus, in Equation (1) it is possible to see how to calculate the magnetic flux density and how the relation between the number of turns and current are important to generate enough magnetic field amplitude.

$$B = \mu_0 \frac{NI}{L} \quad (1)$$

Where μ_0 is the magnetic constant, N the number of turns, I the current and L the length of the coil [156]. Thus, in order to reduce heat, the electromagnetic actuator windings resistance must be reduced and in order to achieve that, either the length must be reduced or wire section increased, the tradeoff is lower magnetic field production or bulky apparatus, respectively, for the same current amplitude. In addition, conductor section must be higher for higher currents, or may overheat the conductor wirings, melting the isolation varnish and provoking a short circuit between windings. In opposition, permanent magnets have a static magnetic field, which weakens with distance from source the same way as

electromagnets, providing an inflexible magnetic force that cannot be changed or provide magnetic field variation through time, which could be done with electromagnets by applying a sinusoidal wave current to them. However, permanent magnets can still produce an alternated magnetic field through the aid of an auxiliary mechanical system to displace them. In addition, they can produce the required magnetic field strength with lesser current, which is applied to a motor as the mechanical actuator to displace several magnet clusters instead up to a frequency limited by mechanical constraints, which electromagnets doesn't have. The magnetic field generated by a permanent magnet is easily stronger at a given *z* distance from source, by comparison with fair current amplitude within a fair size coil for this system, and it can be calculated for a cylinder type permanent magnet using Equation (2).

$$B = \frac{B_r}{2}\left(\frac{D+z}{\sqrt{R^2+(D+z)^2}} - \frac{z}{\sqrt{R^2+z^2}}\right) \quad (2)$$

This way, magnetic flux density can be calculated at a certain distance in cylindrical permanent magnet, where B_r is the remanent field, independent of the magnet's geometry, *z* the distance from a pole face on the symmetrical axis, *D* the thickness (or height) of the cylinder and *R* the semi-diameter (radius) of the cylinder (Figure 3.5) [157].

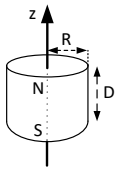

Figure 3.5 - Cylindrical permanent magnet variables for magnetic flux calculation.

Thus, permanent magnets displacement as magnetic actuators of the cell seeded scaffolds were selected, rather than electromagnets in order to avoid high current flow to generate the required magnetic field, which results in radial heat from the electromagnetic windings and a bulkier package to install in the system. The operating principle is schematized and can be seen in Figure 3.6, where the system working method is explained, how the mechanical motion is employed and which sensors will control and keep the system and culture protection in closed loop.

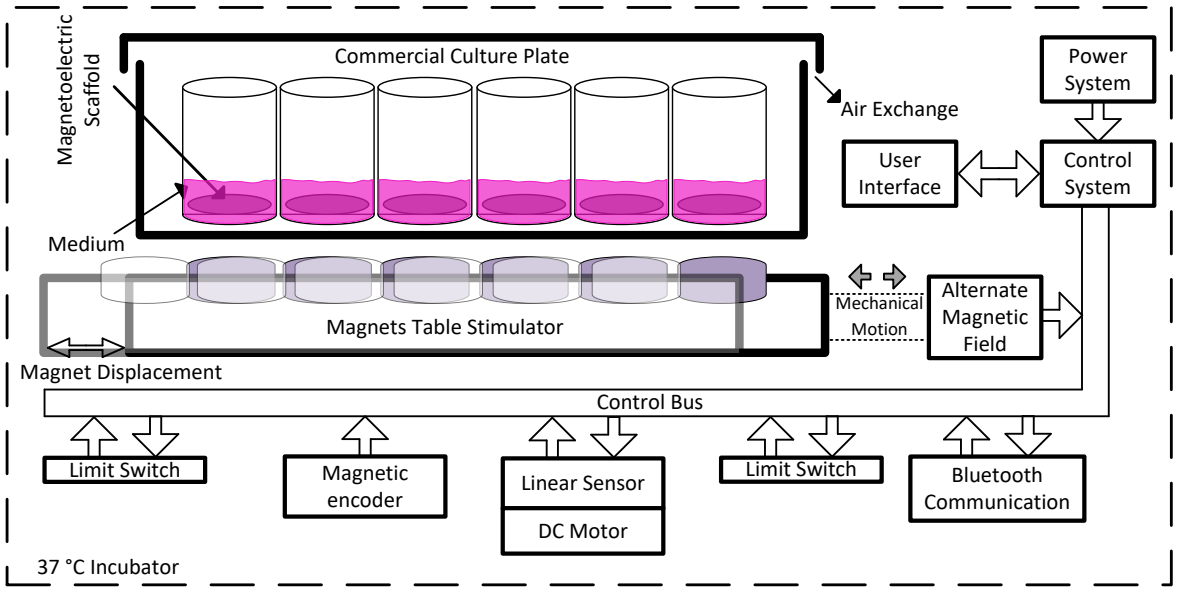

Figure 3.6 - - Magnetoelectric bioreactor operating principle through the use of electrical and mechanical controls through sensors and actuators to produce an alternated magnetic field in order to stimulate the magnetoelectric scaffolds and, in consequence, the bone cells.

The system principle of operation relies in using a commercial culture plate with respective medium with cell seeded ME scaffolds inside the wells, placing the experiment batch at the top of the bioreactor required to be a magnetically inert material. As the magnetic field value must be oscillating at a near sine wave signal at a frequency controlled by the displacement speed of the motor, the magnets must be arranged as it is displayed in Figure 3.7 (ANSYS® Simulation Software) with alternated magnetic poles directions to reach such a magnetic distribution. However, in order to have a controlled alternated magnetic stimuli to the ME scaffolds, the starting position of the magnets is user-defined as well as its displacement and motion frequency, that's how the user can control the complete magnetic curve and with how much continuous magnetic field is applied during repose time. The permanent magnets distance to the culture wells, and magnets size or number of magnets can be selected to fit within the necessary magnetic field range for particulated ME scaffolds actuation [108].

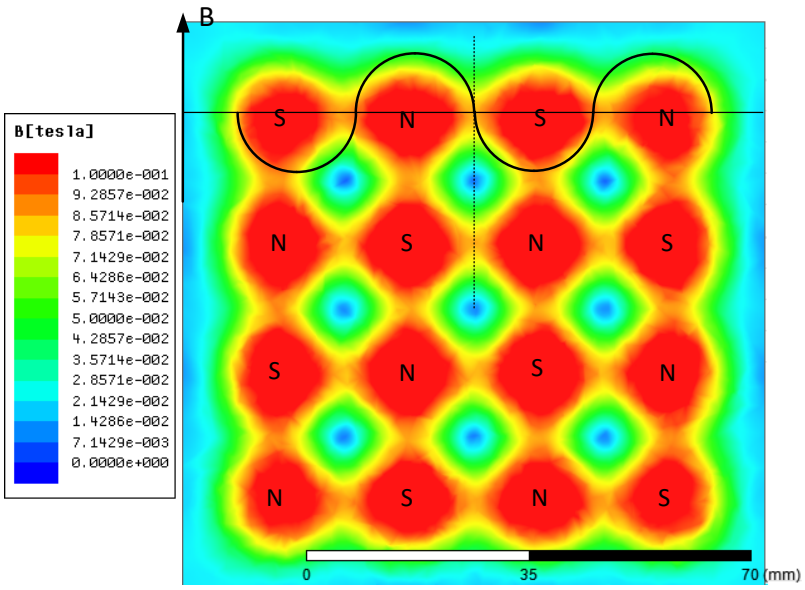

Figure 3.7 - Permanent magnets configuration to achieve alternated magnetic field distribution with platform displacement (magnetic field distribution at 5 mm distance plane from equidistance disk magnets of 15 mm diameter and 3 mm thickness). Magnets properties set as Neodymium magnets grade N52 and B_r value from equation (2) provided by manufacturer in [158].

It is important to note that the displacement will influence the magnetic curve start value and end value, and the frequency will transpose into the vibration frequency of the ME scaffolds. The magnetic field peak values are directly dependent on magnets grade and distance to the scaffold, which can also be calibrated mechanically by adding extra elevation layers below the magnet table. The DC motor must be controlled by a custom electrical system and designed for the purpose of this application, taking the role of controlling the magnet displacement, displacement frequency, user interface and culture cycles for active and repose times.

3.1.2 Electro-Stretching Bioreactor

The same type of contamination protection obtained in the ME stimulation bioreactor, cannot be achieved in this bioreactor setup due the skeletal muscle TE, involving stretching and electrical contact to the scaffolds, invasive supports (clamps) to hold the scaffolds are required for stretching and electrical current signals to be applied. As the scaffold, clamps will be submerged in the medium stored in the culture plate such as the one in Figure 3.8. Thus, the materials must be chemically resistant, oxidation free and with an electrical conductive contact to guide the electrical current through the scaffold. The non-conductor materials must be biocompatible and chemically resistant such as acrylic, nylon, Teflon®, PLA, among others, whereas the conductive components can encompass biocompatible metals such as stainless steel, gold, platinum, palladium or titanium.

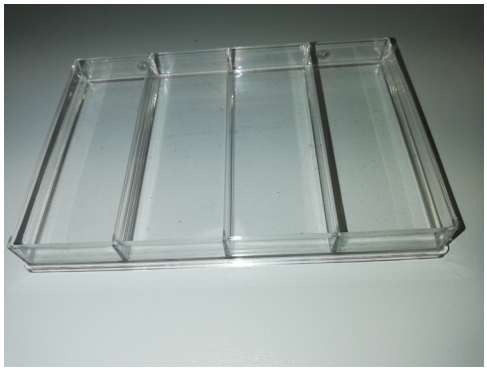

Figure 3.8 - Commercial culture 4 well plate.

For this type of commercial culture plate, the most adequate permanent magnets would be a block-like geometry, and in order to calculate the magnetic flux density at a given distance for this shape through Equation (3).

$$B = \frac{B_r}{\pi}\left[\tan^{-1}\left(\frac{LW}{2z\sqrt{4z^2 + L^2 + W^2}}\right) - \tan^{-1}\left(\frac{LW}{2(D+z)\sqrt{4(D+z)^2 + L^2 + W^2}}\right)\right] \quad (3)$$

Where B_r represents the remanent field, independent of the magnet's geometry, z the distance from a pole face on the symmetry axis, L the length of the block, W the width of the block and D the thickness (or height) of the block (Figure 3.9) [157].

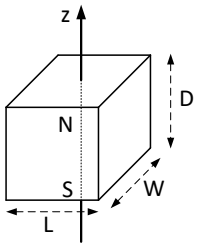

Figure 3.9 - Block permanent magnet variables for magnetic flux calculation.

As illustrated in Figure 3.10, the mechanical stretch can be achieved by magnetic force created by permanent magnets, keeping one end static and the other pulling the other side. Through the use of a similar approach as employed in [76] where the authors approximate a magnet to pull a PDMS clamp coating a permanent magnet, while also using electrical stimulation through platinum wires. Thus, the previous system operation can be converted to a similar purpose with same type of actuation and using the permanent magnets ready structure. Electrical current is transmitted also through wires connected through stainless steel screws used to both fix the scaffolds to the clamps and make electrical contact. Two methods can be employed to apply current signals into the four wells commercial plate, in parallel and series, although parallel gives higher control over each scaffold electrical stimulation, it requires a 4-channel current output system and more wiring with the control system. Thus, by setting a connection of every scaffold in series, it is possible to use a single current channel to apply the stimuli to all scaffolds using the same current as long as the scaffolds electrical resistances are suitably low for the maximum voltage supply to comply. One difficulty is common to both methods, the current path is divided by the scaffold conductive nanoparticles and the medium salts, which knowing the scaffold's electrical resistance is a vital variable, to be able to calculate how much current, is theoretically being crossing the scaffold and reaching the cellular sites, and how much is lost through the medium salts.

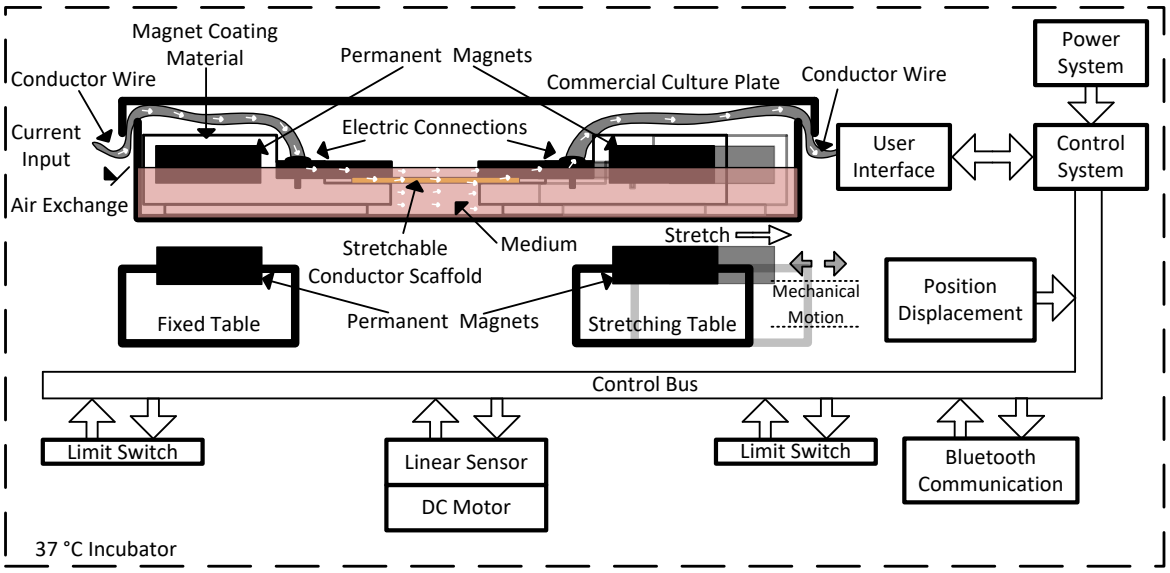

Figure 3.10 - Stretching Bioreactor operating principle using electrical and mechanical controls through sensors and actuators to produce a stretching push through a remote magnetic force.

Thereby, the medium and scaffold conductivity difference should be as low as possible, in order to only divide the electrical by the minimum possible with the medium. In order to reach this suitable condition, highly conductive scaffolds should be built using highly conductive biocompatible metal/carbon powders to take most of current paths from the medium salts conductivities. Following the magnetic stimuli counterpart, the system will be operating inside an incubation chamber with controlled temperature. Thus, if the mechanical stress produces extra heat to the culture plate, the system turns off the mechanical movement if it reaches a critical temperature value. The scaffolds seeded with cells are held by the clamps that are placed inside the commercial culture plate (Figure 3.8), which is located at the top cover of the system. Each of the scaffold clamps coat a permanent magnet with magnetically inert biocompatible material such as PLA, PDMS, acrylic, among others. The remote magnetic force is the driving force for the stretching being pulled by a bottom structure with a moving platform and a fixed one both filled with permanent magnets (Figure 3.10). As it is displayed in Figure 3.11, the force between two block magnets can reach up to almost ~370 mT in a distance of 5 mm and lower down to ~180 mT at a doubled distance. The simulation software calculated forces at those distances of ~9.5 N and ~2.6 N, respectively, making every millimeter closer count in terms of force in the exponential force curve it provides.

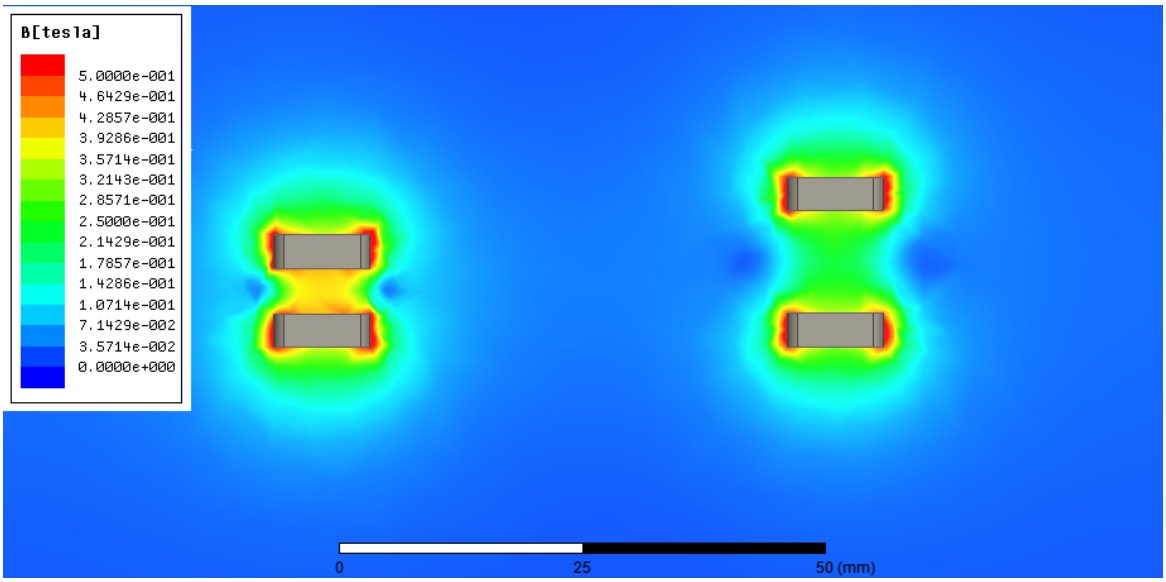

Figure 3.11 - Magnetic force between magnets grade N52 Neodymium magnets at a) 5 mm resulting in a magnetic flux of ~370 mT (force of 9.456 N in the z-axis) and b) 10 mm from each other resulting in a magnetic flux of 180 mT (force of 2.553 N in the z-axis).

As the how to operate in this device, the user attaches the scaffolds to the clamps with the fixing surfaces and screws, followed by setting the point of the starting position where the scaffolds are set steady, and then to be stretched further with the defined displacement. That position is considered the resting position for repose time in each cycle. The culture and mechanical system closed loop control follows a similar approach as the magnetic bioreactor, which is considered to take advantage of every common part in the design this modular system.

3.2 Types of Scaffolds and Processing Methods

Regarding ME film scaffolds construction many materials were considered, although depending on tissue culture type and stimuli, they must be tailored for each one, so a film construction approach was followed based on [159]. Briefly, as it is schematized in Figure 3.12, the solution for the films construction starts by dispersing magnetostrictive nanoparticles in the solvent through an ultrasound bath for 8 h, followed by adding the filler polymer and keep the solution being mechanically agitated to dissolve the polymer for another 2 h. After, the solution can be spread in a glass sheet to build the liquid film, which the solvent is then evaporated at an oven at 210 °C, during 10 min, cooling

down at room temperature to achieve polymer crystallization. However in order to get oriented dipoles for piezoelectric response, the film needs to be poled at 120 °C with a 10 kV electric field for 120 min by a method such as corona in order to enhance its piezoelectric properties. Thereafter, the scaffolds are then washed with ethanol and PBS, finished with UV light exposure for 60 min on each side for sterilization purposes and ready to be cell seeded for the a TE experiment [108, 160, 161].

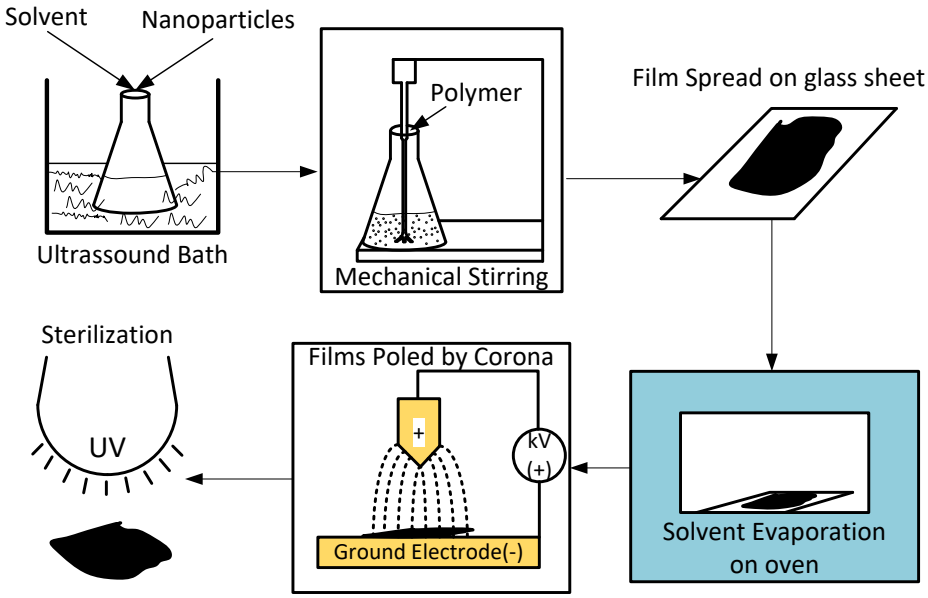

Figure 3.12 - Smart scaffold film building for ME response and sterilization process flow chart.

Many materials can be used as solvent, nanoparticles and polymer, although only a few will come out with the proper final material response and required biocompatibility for a TE experiment. Thereby, for the experiment schematized in Figure 3.12 to build the ME scaffolds, the solvent is N, N-Dimethylformamide (DMF), the magnetostrictive nanoparticles are Terfenol-D and polymer is P (VDF-TrFE) [108]. Concerning electro-stretching scaffolds, besides the conventional films, in order to better resemble muscle myofibers geometries, the fibers can be built by using a similar approach as in [162]. Although the solution follows the same pattern as in Figure 3.13, instead of spreading it as a film in a glass sheet, it is inserted in a syringe to be shot through a flow control system. The flow control system is set in an electrospinning apparatus where the solution strings are thrown by the needle and conducted through a high voltage electric field between an electrically positive conductor needle and a ground connected aluminum foil. The foil is rotating in motor driven drum so the fibers become aligned with the motion of the aluminum collector, resulting in a more muscle-like geometry scaffold [161].

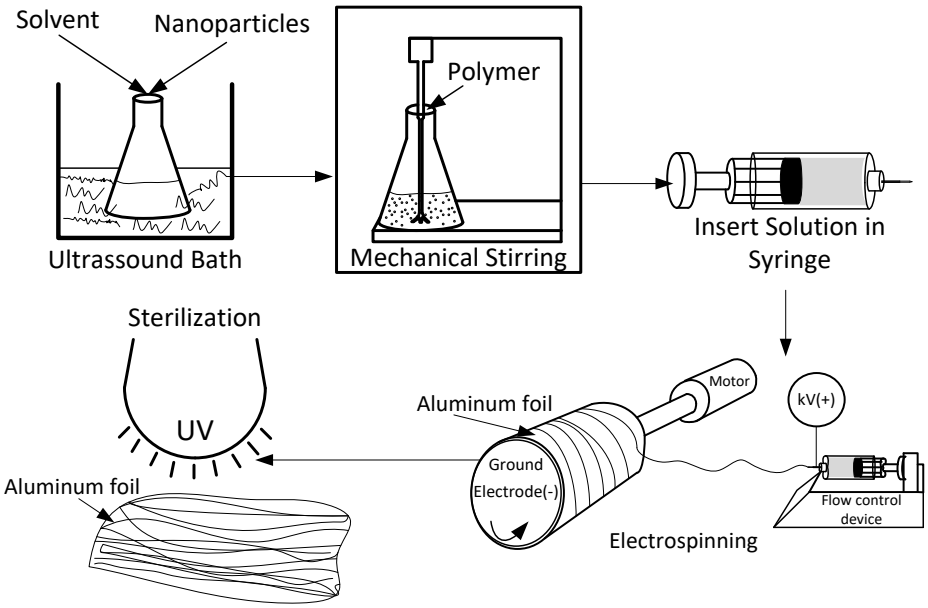

Figure 3.13 - Aligned fibbers for fibrous scaffold construction method through electrospinning flowchart.

Thus, the materials employed in this case to build the fibrous scaffolds is usually DMF as solvent, conductive nanoparticles such as gold, titanium, carbon, among others and filler polymers, for instance PVDF or SEBS. After the electrospinning process, the fibers are detached from the aluminum foil and cut into the desired size in order to be washed and sterilized before being seeded for the following TE culture in a culture plate or petri dish. Furthermore, 3D scaffolds can be developed using solvent casting methods such as the ones that can be observed in Figure 3.14.

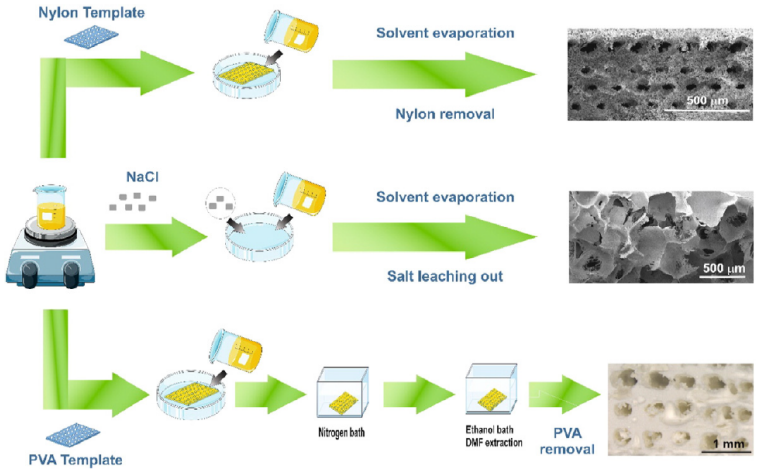

Figure 3.14 – Different procedures for PVDF three-dimensional scaffolds production [163].

3.3 Electrical Analysis

In order to accomplish the electrical control of this system, a custom electronic design is required, so in this chapter the electronic methods and potential supporting circuits are analyzed and discussed accordingly. Therefore, it is imperative to have the physical variables electrically controlled, though they must be measured through voltage or current variation for quantification. Thus, electrical control relies mostly in sensors and actuators, those two components work perfectly together when the application requires so, like the one being developed, where the actuation must be measured by sensors in order to correct any misbehavior from the system and possibility to adapt to potential unforeseen conditions, where this type of control is commonly called closed-loop. On the other hand, an open-loop system relies on highly optimized systems, human control or simply non-critical applications, being still viable for short operating time applications or with constant human monitoring, resulting in cheaper electronics with no control circuits or complex programming. Therefore, this system operating backbone is the control it provides that will make it viable for the planned tasks, although more digital components are important, such as the user interface, power source, communications and system responsiveness. Whereas the system interface with the user can be through mechanical pressure buttons, capacitive detection or remote communication input methods. On the other hand, the output of the system could be through LED lighting, 7-segment display or a LCD with a touchscreen encapsulating both input and output such as a common smartphone. In the case of the power source, the use of outside transformers are a nowadays-common practice due its tremendous advantages regarding the obvious replacement, space which is no longer required inside the system and the heat production due to normal energy loss from the AC/DC transformation which is kept outside and not adding up to other further energy transformations. Concerning the digital components, they communicate mostly by high frequency square waves comprehending data and control bits and flow firmware protocols such as SPI, I^2C and USART, which are highly flexible to communicate/control thousands of possible peripherals and are industry standards. Finally, the system responsiveness is what the sum of all those components result on, where all components are important variables to result in a functional electrical ecosystem. In order to achieve that, good design practices must be employed in order to keep electrical noise to compromise other components of the system, such as fast square wave electrical transitions from the digital communication, which may compromise analog signals with noise. Furthermore, quick power draws of components from the power lines may introduce noise in

sensitive integrated circuits and should have a capacitor holding charge the nearest possible to their power pins to suffice those peaks. Thus, these are a few of many concerns to be taken into consideration, and following manufacturer's instructions is of paramount importance to get the desired results and performance, in terms of speed and lower heat production.

3.4 Acquisition System and Sensors

Data acquisition is the process of data gathering from physical phenomena from the real world converted into discrete electrical signals so they can be digitally processed, analyzed and stored in a computational platform. Usually, in most applications where data acquisition is used, the system used the data for actuation control just like in the one being developed. A platform with computational capabilities, which processes the digital discrete signals in order to get a digitally suitable value from the physical volume measured. Thus, the process is composed by three fundamental components: sensors that convert physical volumes into discrete electrical signals, the signal conditioning instrumentation that partly filters the signals to the intended frequency (in an AC signal case), and the ADC peripheral that samples and holds the voltage value to be digitally quantified before discharging the sample capacitor for the next reading. Then, through a digital code such as binary, it is possible to process the signal and move every digital "cog" accordingly for the most appropriate system behavior. Having materials which respond from physical stimuli with electrical response is then a very important electronic component in order to build reliable system which no longer require human monitoring. Varying on sensor type, the output may be in voltage, current, resistance, capacitance, among others or a junction of many electrical or physical variations such as heat. Nowadays, a considerable range of sensors that enables the measuring of plenty of physical grandeurs (Table 3.1).

Table 3.1 - Sensing and transducing components well established on commercial technologies being employed nowadays.

Sensor	Physical Measure
Thermocouple, Thermo-Resistance, Thermistor	Temperature
Photoelectric, Photodiode, Phototransistor	Light
Microphone, Hydrophone	Sound
Extensometer, Piezoelectric, Piezoresistive	Force and Stress
Rotary and Linear Potentiometer, LVDT, Encoder	Position and Displacement
Accelerometer	Acceleration
pH Electrode	pH
Hall effect, Magnetometer, Magnetoresistance	Magnetic Field
Anemometer, Flowmeter, Turbine	Liquid flux

Therefore, sensors present an electric signal level variation tending to the respective physical phenomenon being measured through linearization or calculating equation. However, the way they are employed will dictate how accurate they can be so sensors can be intrusive and interfering with the measurement itself such as flowmeters through turbine, which are directly introduced in the flow. Whereas, non-intrusive examples can be the ones such as temperature and magnetic field sensors.

3.5 Signal Conditioning

Analog voltage signals generated by sensors or transducers in some cases require a dedicated instrumentation circuits in order to condition the signal to be read with the most suitable or safe voltage levels, frequency range and noise-attenuated state, which must be done in order to reach the most accurate type of system. Sensors with alternated current response may suffer from signal distortion caused by many electromagnetic sources, including the system itself, causing signal contamination. Therefore, for a known interesting signal frequency, which contain the information required, a hardware tuned filter can be employed or even by software with digital filter calculations. Thus, it is not necessarily with the exact processing order as displayed in Figure 3.15, where the hardware filtering happens before the ADC samples the signals, as it can be done posteriorly after getting the discrete values. Although, both techniques can be employed when the system operates within a hazardous electromagnetic environment that contaminates sensor signals heavily.

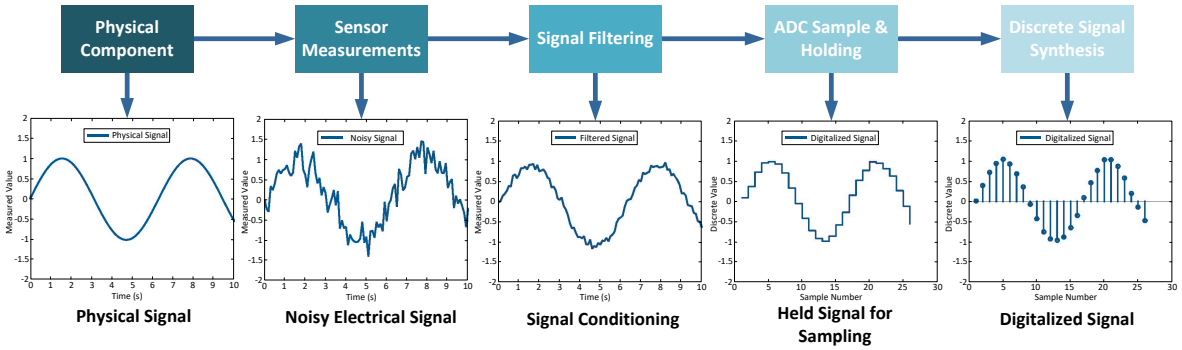

Figure 3.15 – Diagram Block exemplifying the possible signal transformations throughout a data acquisition system (adapted from [164]).

Thus, signal conditioning is required in most cases to attenuate the noise levels through hardware and/or software filters, amplify small signals, isolate from noise sources, apply electrical excitation in passive sensors and linearize through software. In the case of DC sensor response, usually a hardware employed low-pass filter only is enough to avoid fast transitions usually generated by the digital high frequency communication.

3.6 Closed-Loop Control Methods

System actuation can be controlled by software or hardware, although for precision it is better to do it by software, as the control options are hugely higher, easier to develop and improved over hardware. Regarding hardware control, it has the advantage of providing a faster hardware response with no processing time spent in data gathering and digital processing, however it results in a limited control system with no control flexibility for any future improvement. Regarding control methods, a simple one is the ON-OFF control, which usually relies in a single variable being measured by a sensor or group of sensors with an averaged value, and an actuator, an easy example is a greenhouse with a heating mechanism. Whereas, the temperature is the variable being controlled, thus the system turns on the heating mechanism to reach the desired temperature and when the variable surpasses the value it is turned off until it goes below the temperature to turn it on again and so on (Figure 3.16) [165].

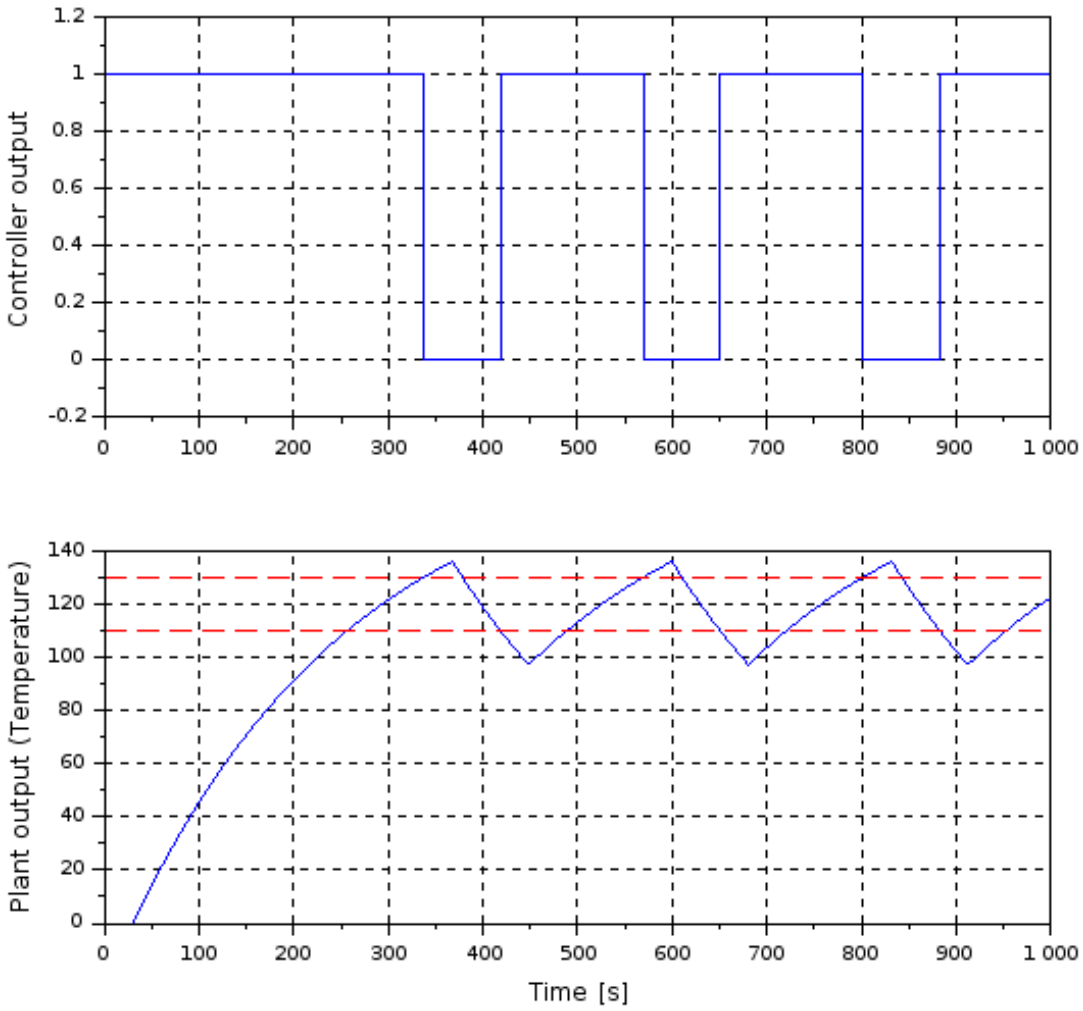

Figure 3.16 - On-off control applying a hysteresis limit values regarding system actuation times [166].

Turning the actuator on and off though, provokes fast wear on the actuator, thus it has added a hysteresis to the control where the controlled value is in an acceptable range for the application to reduce actuator commutations over time. This control presents itself as simple and easy implementation, but many disadvantages are related to a controller that shuts down the actuator repeatedly further than wear, which is related to the application inertia and the system reaction time to recover from higher error margins in the control variable. A robust control system is provided by a PID (Proportional-Integral-Derivative) control method, which is tremendously effective and widely used by industry standards (Figure 3.17). As the name implies this type of control relies on three types of control actions, each with its own advantages and disadvantages.

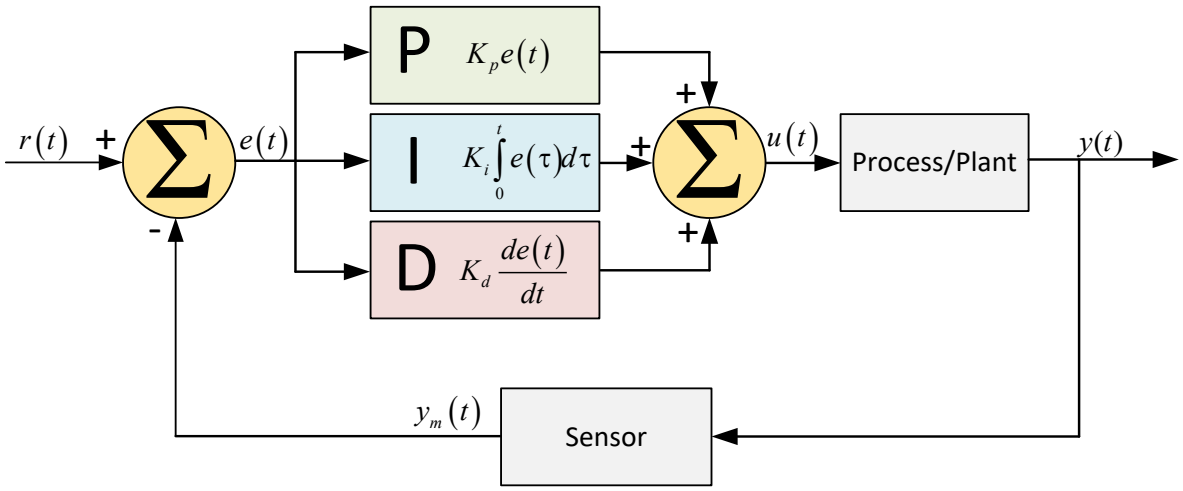

Figure 3.17 Closed-loop method with PID control, whereas: r(t) is the control reference value; e(t) is the error measured; u(t) is the control value to be applied; y(t) is the system output; and $y_m(t)$ is the measured output by the sensor to be compared with the reference value for system error control.

The proportional gain is the always-present component of PID control and can be perfectly enough in some applications. This starting component of the control is based on error multiplication by the respective controllers gain (K_p), whereas the controller responds proportionally to the system error. The system may get unstable if not calibrated properly or always oscillate around a reference value such as an ON-OFF control system. Thus, in order to improve this type of control over a common multiplied variable it is used the integral component, which aims to remove the error in steady state [165, 167]. This type of control compromises system stability so is not very often used without the proportional gain. With this component included, the sum of previous errors within a defined time constant are taken into consideration. Therefore, the steady state error attenuation and rise time reduction are important advantages of this component, although overshoot and settling time are increased (Figure 3.18).

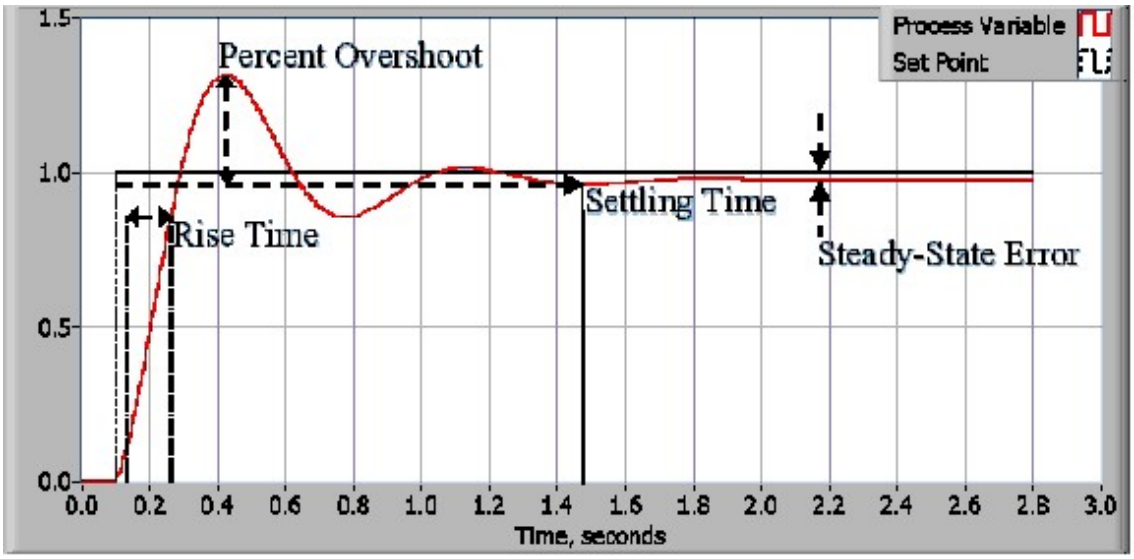

Figure 3.18 - Closed loop response of typical PID control system [168].

Concluding, the PI control is still far superior to just a P control with an improved steady state stability. Thereby, PID control were developed to address the disadvantages introduced by the in integral component and make a faster system reaction. This derivative component acts on the values of the previous errors by multiplying the error's derivative by the derivative time constant. Thus, the main advantages of this component are the fact of speeding system response stabilization, attenuating overshoot, which can be damaging on system start when dealing with high currents, and settling time, resulting in a final Equation (4). However, in some applications this component is just excluded from control because of high susceptibility to electrical noise produced by high frequencies requiring expensive shielding.

$$PID_{control\ value} = K_p e(t) + k_i \int_0^t e(\tau)dt + K_d \frac{de(t)}{dt} \quad (4)$$

Finally, the K values can be figured through two approaches: trial-error method and Ziegler-Nichols method. Trial-error follows an approach of stabilizing a component at a time, and starting with the proportional gain K_p, followed by K_i and then K_d. Whereas the most scientific method is Ziegler-Nichols by using a small set of rules for each type of control case depending if it is P, PI or PID. Their method ended up being used as the standard due the fact of setting stable gain values for integrative and derivative variables quickly, after finding the critical proportional gain just as in the trial-error method. This situation happens due to small physical differences from equal components in production that require slightly different parameters for the most tuned control possible, a comparable method to

processor overclocking on computers because of the tiny differences related with lithography-made products that result in substantial performance difference [167].

3.7 System Circuits Design

The system circuits must encompass power, actuation, sensing, user interface and remote communication, therefore the main working principles are analyzed in this document section. Thus, power is the starting component and must be designed in order to be stable, reliable while producing low heat. As it is the system only source of energy, it is important to consider a robust component from which the system will take energy from a power outlet. Following the system operation principle discussed in the previous chapter, a motor will take the role as main actuator, so an H-Bridge circuit will be required, this type of circuit allows digital input to control motor rotation direction and intensity through PWM input. As for sensors, the system will require a temperature and positioning system, as well as a magnetic field sensor, thus many ADC channels may be required within the used microcontroller. Continuing, the input user interface is better suited with capacitive interface to avoid fissures and leaks and most microcontrollers nowadays already are integrated with capacitive input channels lifting the development time and improving this type of technology widespread. As for the output user interface, it can be better accomplished by a LCD display, such as the ones in printers nowadays. However, even though some LCDs already bring a capacitive input layer, there is a thickness limit and, to protect system components from liquids the display will have to be placed in the back of a protection layer, which will add too much thickness for proper operation of a capacitive panel. Thereby, the most suitable solution is to use a dielectric material with the best range of thickness for capacitive interface and transparency, such as glass or acrylic in the frontal system cover. As for “under the hood” firmware communications, many types of communications can be employed, since a simple voltage level to bitwise communications with information exchange protocols, such as I^2C, SPI, USART and USB, with many methods in-between. Finally, remote communications rely mainly in protocols such as Ethernet, Bluetooth® or Wi-Fi. However, for the current system the one that could be more useful would be a close range communication such as Bluetooth®, as it enables easy and implementation for a direct communication with a smart device and does not require wiring from inside the incubator.

3.7.1 Motor and Actuation

Magnets platform motion requires motor polarity reverse for moving it for both sides, thus it creates the need for a suitable circuit to create current path, which may reverse. The common type of circuit is known as an H-Bridge and is an industry standard used for motor actuation, thus it is already under production as integrated circuits for many power levels and features. However, in order to select the appropriate power requirements related to voltage and current level, the motor must be selected to fit the system space, provide the required torque, while reducing the most possible size and weight. For instance, Nylon 6/10 has a density of 1140 kg/m^3 and the magnets platform takes a predicted volume of less than 3.84 x 10^{-4} m^3, thereby resulting in a weight less than 500 g shared with system bottom, as it will not be lifting, just pushing and pulling. To this weight, it is required to add permanent magnets weight, which is going to be the double of the required magnetic points, as they are going be stuck by another magnet below to keep everything fixed. Each magnet for 24-wells culture plate comprehends a weight of ~7 g each, considering 56 magnets results in an extra weight of 392 g, which outcomes with a total weight of 892 g, but as other small components are included like screws, threaded attached nut and linear bearings thus a 1000 g weight was considered. Considering also, the worst case scenario where the platform is being lifted, thus using gravity acceleration value and the expected motor coupled screw diameter of 8 mm, thereby using Equation (5), it is possible to calculate the a required torque of a slightly less 40 mN.m.

$$\vec{\tau} = m.\vec{g}.r\ (N.m) \tag{5}$$

Where τ is the torque value in N.m, m is the mass in kg, g is the acceleration in this case of gravity, and r is the rotating radius of the ball screw topology in m. Thus, a 12V, 250 mA motor with up to 150 mN.m torque is more than enough force to move the required mechanical system. As for angular speed, which will be converted to linear speed through a ball-screw assembly, a 200 rpm motor with coupled screw with 8 mm lead of thread already achieves more than 25 mm/s linear speed if all the mechanical constraints allow it, such as friction, motor sliding, sensing and control system response time. Thereby, a given DC motor can perform the task by the application of PWM signals at the MOSFETs gates of an H-Bridge integrated circuit [169], which will work as the interface between microcontroller and motor. In few words, an H-Bridge integrated circuit is composed by four transistors (Figure 3.19) of any kind

might work (Bipolar, MOSFET, IGBT, among others) although MOSFETs and IGBT are the most suitable due to higher commutation speed on gate and wider current levels support.

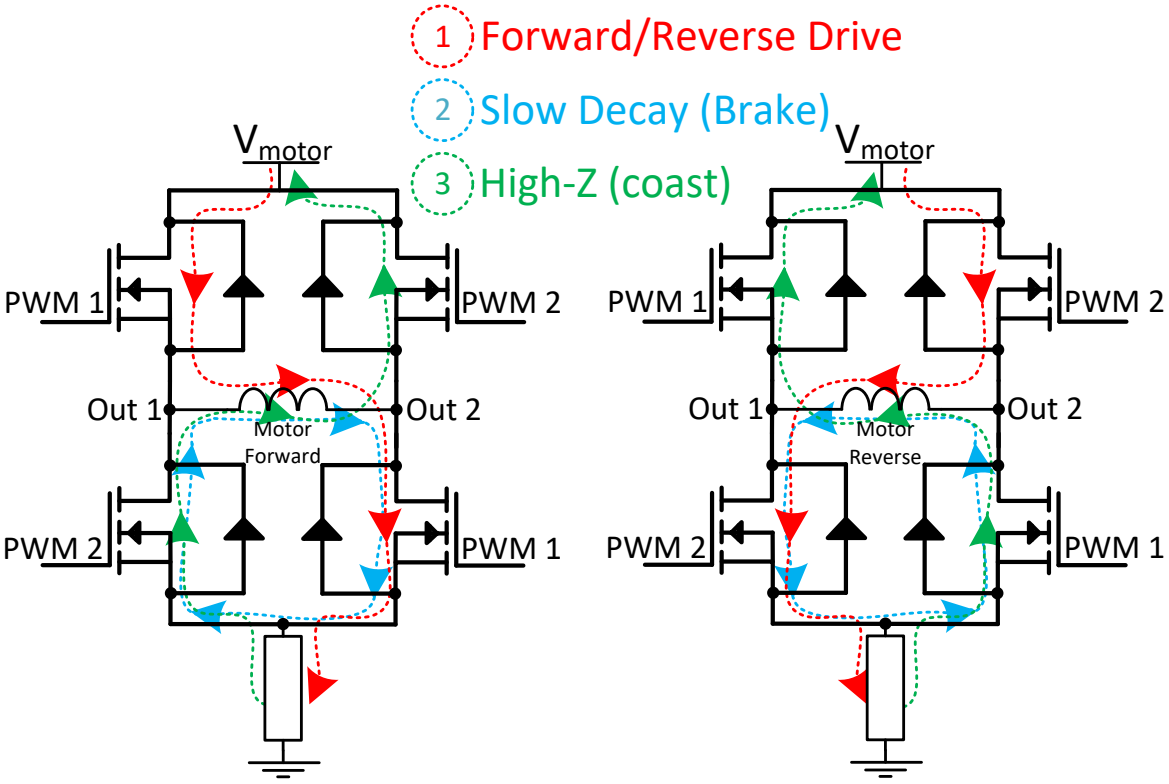

Figure 3.19 - H-Bridge circuit configuration with four transistors setting current flow direction over motor windings.

The digital control applied to the gates of transistor work as switches to open or close the circuit points, thus the four transistors operate to create a double path for the current to flow for one side or the other. This double path can be even used to close both circuits simultaneously to create an electrical braking mechanism for motor sliding attenuation, which is important for this application for precise magnets positioning.

3.7.2 Sensing Components

As previously mentioned, sensing is an important method to keep the system in the suitable/critical operation range through a closed-loop method, in order to avoid/attenuate system error or even system damaging. Thus, for this type of system five types of sensors have been analyzed, regarding temperature, magnetic field, motor rotation, platform positioning and platform limits. Whereas, the temperature sensor is one of the most important ones, has it is the one that will protect the cellular culture from overheating and damaging the tissue culture. Following with the magnetic field sensor that alongside the temperature sensor can be a small integrated circuit by using a Hall Effect sensor, and will measure the magnetic actuation of magnets platform by quantifying the magnetic field value over time. The platform displacement, however, require control for speed motion, positioning and mechanical boundaries, thereby three sensors are under analysis as for speed motion a magnetic encoder, for positioning a linear sensor and for mechanical boundaries two end-stop optical sensors in each mechanical end. Therefore, the platform would be fully controllable and fail-safe from mechanical issues. The list of sensors being employed can be seen on Table 3.2, they were selected after analyzing their features regarding size, full-scale range, resolution and compatibility.

Table 3.2 - Sensors to be employed in the thermomagnetic environment and displacement mechanism.

Sensor Reference	Manufacturer	Physical Measure
LMT85	Texas Instruments	Temperature
AD22151YRZ	Analog Devices	Magnetic Field
9610R3.4KL2.0	Sensata BEI-Sensors	Linear Positioning
AS5030-ATST	AMS	Rotation
HY301-19	Generic Component	Mechanical Limits

LMT85 presents a linear response and, when matched with a conventional 12 bit-resolution ADC channel, it results in a grandeur resolution of 0.1 °C. According to manufacturer guidelines, temperature/voltage conversion calculation follows the Equation (6) [170].

$$V_{Temp}(mV) = 1324.0mV - \left[8.194\frac{mV}{°C}(T - 30°C)\right] - \left[0.00262\frac{mV}{°C^2}(T - 30°C)^2\right] \quad (6)$$

Thereby, through software it is possible to calculate the temperature through the voltage reading performed by the ADC with the predicted typical level of precision of ±0.4 °C (Figure 3.20a). As for the Hall Effect sensor, using a similar conventional 12 bit-resolution ADC channel as it presents a

voltage output as well, the AD22151YRZ presents a compact form (Figure 3.20b), and through a circuit topology with a gain of 1, it presents a magnetic field sensitivity of 0.4 mV/G, with a full-scale of 10000 G. The gain can be calibrated at the integrated circuit output amplifier pins through the relation of two resistors, where it will increase resolution and lower the full-scale and vice-versa, working as a trade-off according to what is more important for the application. In this case, the gain of 1 was selected, which is more than enough in terms of resolution and full-scale, where at maximum 5000 G will be produced by each magnet at a given distance. A resistive response sensor is the linear positioning sensor 9610R3.4KL2.0, which works through the traveling distance of a tip being pushed and let loose by the moving structure, and that changes contact position within a rheostat-like compact structure (Figure 3.20c), changing resistance. Thus, this sensor resistive variation must be excited by voltage and measured with the same method as the previous two sensors, by a conventional ADC channel input, 12 bit-resolution as well, resulting in a linear resolution of more than 10 µm. Following, the AS5030-ATST rotation sensor requires a magnetic disk at the tip of the rotating screw, so the magnetic rotation can be perceived by this transducer through the permanent magnet North Pole variation (Figure 3.20d).

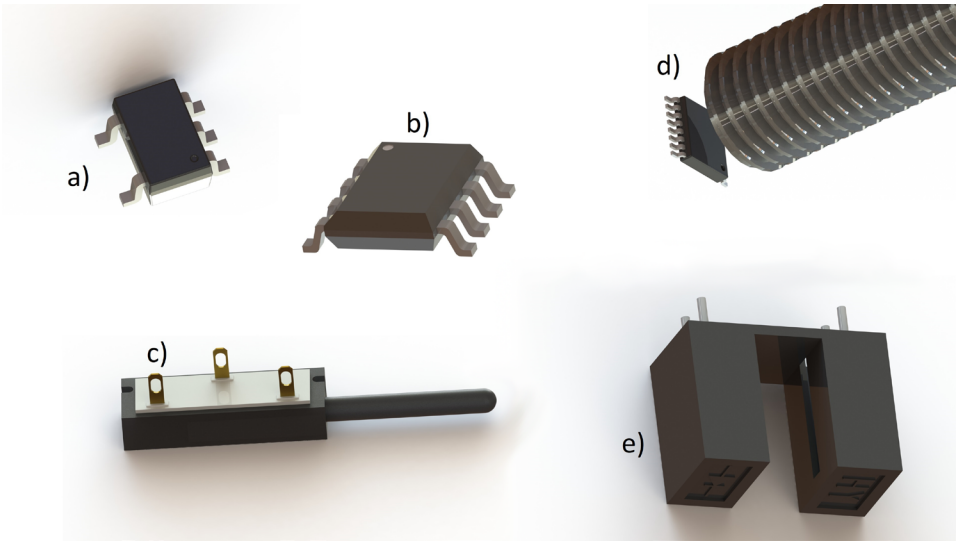

Figure 3.20 - Employed sensor mechanical formats a) temperature, b) Hall Effect, c) Linear sensor, d) Magnetic encoder positioning according to rotating motor shaft with a disk magnetic at the tip and e) optical end stop sensor structure.

Furthermore, it must be positioned with the correct orientation right in front with the least required distance for the most precision. This integrated circuit sensor has 8-bit resolution digital output response, being able to read with many methods, including SPI, custom digital protocol and even

voltage variation through an ADC channel by configuring the hardware instrumentation around it. For this case, and for simplification, a SPI communication protocol was employed as it features more speed, less CPU time consumption and higher firmware reliability over the others. Finally, the HY301-19 optical end-stop sensor is a simple, yet robust solution, which changes its response instantaneously when any object cuts the light path between its two supports (one containing an emitter IR LED and other a receiver IR LED as can be seen on Figure 3.20e). This type of response is suitable to be used with a microcontroller external interrupt pin, generating an interrupt routine inside the programing to turn off immediately any motion of the platform in the respective direction to avoid mechanical damage. This can be observed as a safety measure with no mechanical wear, as mechanical contact or travel does not happen with this type of light using sensors.

3.7.3 User Interface

The system required user input and output, thus it is necessary to add components for each, which can be achieve by sensors and actuators such as capacitive or pressure sensors, lighting panels or remote communication for a terminal, respectively. Therefore, an output interface composed by an LCD display (Figure 3.21a) for information display and RGB LEDs lighting for more expressive exhibition of bioreactor operating status colors to act more quickly according if required. On the other hand, as input interface, it was decided to add capacitive copper panels in a custom designed PCB to be placed in the back of the frontal bioreactor cover, restricting the set of materials to use in the front panel for the effect, as they must be dielectric materials. The capacitive technology can be employed in waterproof system without sacrificing usability, speed and precision on user touch input, thereby it is the best solution to avoid any type of system fissure for its interior.

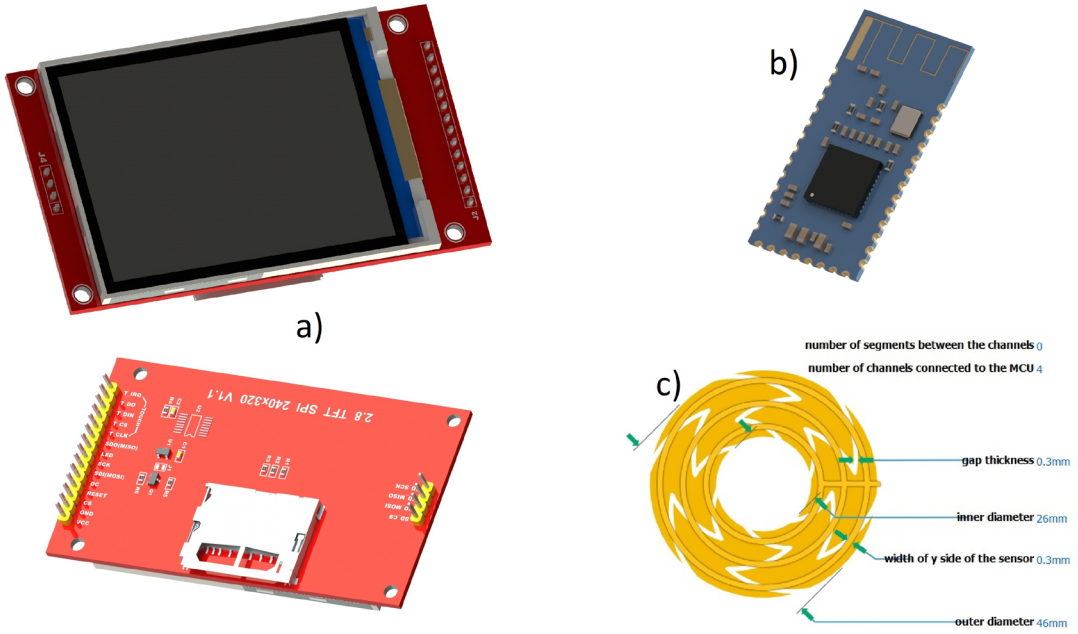

Figure 3.21 - User interface components a) LCD, b) small Bluetooth® PCB module for PCB integration and c) Q-Touch library for circular capacitive linear sensor design on PCB copper pads.

Thus, for this case it was used a design library for capacitive sensor design on PCB copper pads as showed in Figure 3.21c, which can detect capacitive variation from conductive object approximation such as skin, with the aid of a microcontroller with capacitive input pins as peripherals. Finally, in order to finish the user interface, another input/output method will rely with a wireless interface to trade information with the bioreactor from a remote terminal through a Bluetooth® communication using an HM-10 module (Figure 3.21b).

3.7.4 Firmware and Communications

Digital electronics has brought new methods and features to how electrical signals are controlled nowadays, providing increased precision, logic control and a new complete layer over electrical design and equipments. Thus, even though analog electronics still play important roles in power transmission and physical signal measurements and actuation, the logic engine behind, is each more digital and discrete signals through time. Therefore, regarding the current system development, it is going to require microprocessors for digital data treatment and processing of communications,

precise timings of operations and process control through digital signal communications. In this system there will the need to control system actuators such as a motor through an H-Bridge circuit, which requires a sensing pin and two PWM signals derived from timer peripherals present in each microcontroller. Furthermore, there is the requirement of communication with the LCD display, which communicates through SPI encompassing 3-wires for unidirectional communication and several more digital pins for further control of parameters such as display brightness controlled through PWM. Concerning sensors, most of them will work through an analog voltage reading, thus requiring at least three ADC channels for temperature, Hall Effect and Linear position sensors, although encoder communicates its readings through an SPI communication, whereas the end-stop sensors best approach are with external interrupts triggered by their ON and OFF state. External interrupts are important mechanisms in order to make the processor interrupt any on-going operation to attend that specific external signal, which, in this case, is very important because the mechanical limits have been reached and the motor must be stopped to avoid mechanical wear or damage. Thus, all of these peripherals require a powerful arm processor to control them and even further system operations such as actuation control timings, remote Bluetooth® communication through USART, among others. Furthermore, operations should be handled by other processors, which is required for RGB led lighting and capacitive buttons readings with a featured processor for the task. Having two microprocessors contributing to the same mechanism where one assumes actuation, sensing and timing tasks and the other assumes light actuation tasks and user input, they must communicate with each other and exchange information, thereby a communication between them such as USART can be employed. Further external microprocessors, present in external modules can use the same communication channel with the main processor, which must be faster, more powerful and resourceful, in other to handle every required task and “responsibility” to each peripheral and any other not so powerful task tuned microprocessor communication.

3.7.5 Power Design

DC power is required for the system to perform properly, thus it is required to convert from a regular AC power outlet through a commuted power source. However, this energy transformation generates heat due to power losses in commutation on present semiconductors. Thereby, the best approach is to do the task, outside the system and outside the incubator through a regular power transformer brick just as it has been used nowadays with any other consumer electronics, as it brings many advantages regarding replacement and less heat generated inside the devices. The highest DC voltage required is set by the motor, which can be either 12 or 24V for fair sizeable motor for these system mechanical requirements, thereby it required to select a transformer with those respective type of voltage outputs while providing enough power for the system to perform properly. That would be the power design first step, before moving to the next set of power requirements, as there will be components requiring 5 and 3.3 voltage levels. Whereas, 5 V is required for sensors, LCD display and RGB LED lighting, and 3.3 V the standard level for SMD logical components such as microprocessors and Bluetooth® module. Thus, in order to lower the voltage to 5 V while providing enough current without requiring a heatsink to avoid overheating, a Texas Instruments LM2596 buck regulator was selected due its high voltage input range up to 45 V and stable output of 5 V with the aid of external passive components (C2, D3, L2, and C3 from Figure 3.22).

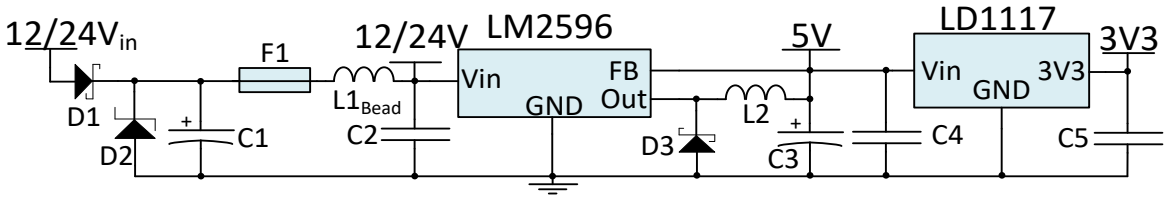

Figure 3.22 - Complete power circuit scheme.

Whereas, for the transformation from 5 V to 3.3 V it only requires and input capacitor (C4) and output capacitor (C5). Additionally, a protection circuit that provides input isolation through a Schottky diode (D1), against overvoltage peaks through a TVS diode (D2), local energy storage (C1) for fast energy transitions solicitations, against overcurrent through an input fuse and against high frequency noise through a ferrite bead ($L1_{Bead}$). The values of each component were calculated using manufacturer guidelines directly related to the input power to be drawn from this circuit and consequent circuits powered by this circuit voltage levels.

3.8 Summary

This chapter states the issues related to each type of culture design according to their stimuli requirements and system planning constraints. Thereby, in the case of ME bone TE, the system must provide an alternated magnetic field which, in order to make the ME scaffolds vibrate inside the culture plate at the magnetic field frequency. As for possible electronically controlled alternated magnetic field sources, can be found with electromagnets (mostly coils or solenoids) being crossed by a controlled current in amplitude and frequency and the other choice would be with permanent magnets being displaced by an electronically controlled motor in speed and frequency. Due to lower current requirements and heat generation, a permanent magnet displacement mechanism was employed. The stretching mechanism employs permanent magnets as well, as the stretch driving force using a motor to move a platform holding the magnets, thus pulling the scaffold holding clamps, which coat permanent magnets that create the force attraction with the ones from the bottom platform inside the device. The system then is planned to use the same interface and box cover, only replacing the mechanical interior, which will use different motion axis of each permanent magnets platform to comply with the commercial culture plates' different layout to one another. This point is important to keep the device modular for these two systems and future ones to be adapted which rely on magnetic stimulation and magnetic force stretching. Some smart scaffold construction methods are also briefly explored in order to clarify idea how to embed electroactive properties to regular biocompatible polymers, which provide several scaffold formats. Furthermore, the electronic components were analyzed accordingly to system electromechanical requirements for operation, system protection and stability. The main control principles were described according to firmware and hardware features, which in this case the best approach relies in in closed-loop firmware controlled system using a linear, end stop, temperature and rotation sensors for the whole ecosystem to work together synergistically in order protect cells and mechanical components. The PID control is the most suitable in order to attenuate wasted energy in abrupt transitions and motor dispositioning due to sliding on the shaft. The H-Bridge motor control configuration allows to be controlled in many ways such as PWM signal variation over time, step motion and braking for an exact position within a fair error margin, thus it is an important component to add. The magnetic field produced by the system can be measured by the Hall Effect sensor and keep record of the variation error over the culture in order to take effect on data analysis, as many sources can influence the magnetic input from the system. The user interface is going to rely in remote control

through Bluetooth®, local interface through a capacitive frontal panel and LCD where the user will be able to navigate the menus, set variables and start/pause/stop the cell tissue culture, while the system still offers protection against liquids spill and functionality. Furthermore, the ecosystem hardware will be managed by microprocessors, which will monitor, temporize system actions, warn user through lighting a remote messaging while exchanging information between each other in order to provide a smooth user experience with task division. The power transformation will rely a conventional AC/DC transformer brick in order to provide the DC voltage levels required for the system, while other circuits take care of further DC/DC conversions for each voltage level required by system electronic components.

4 Bioreactor System Design

Bioreactors can take several shapes according to which type of objective they are being designed to such as research, custom built of a tissue for a specific individual at lab-scale and mass production of general-purpose tissues or bio-construction bases for more complex tissues or organs and which type of technology they employ achieve the environment and/or stimuli. This project aims to design, develop and build a bioreactor for research purposes with static medium environment and electromechanical stimuli. Thereby, the system was designed in order to accomplish two types of cultures by exchanging mechanical modules, which are accommodated in the device interior. In order to amplify its potential, the external modules possibility was taken in consideration, so the electrical impulses component was developed as an external module, which can be replaced by any other module for future different purposes and cultures to work with other setups and methods. As cell culture require sterilized environments, the system must be sterilized before each culture through a method such as an autoclave, requiring a waterproof enclosure, while withstanding the temperature. A principal module of the design can be seen in Figure 4.1, as the main appearance of the device holding the 24 wells culture plate.

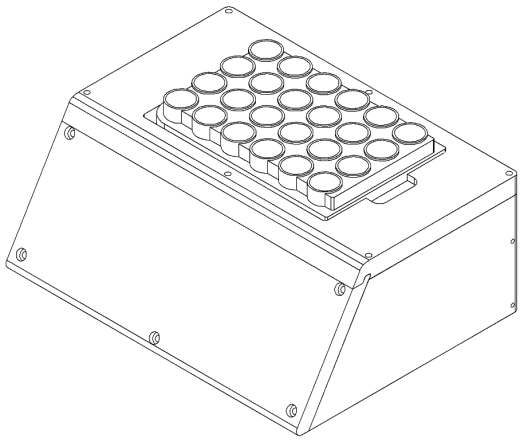

Figure 4.1 - Conceptual model of waterproof system appearance providing the mechanical motion in its interior on the commercial culture plates, which fit at the top if the device.

The dimensions and appearance were considered according to culture, incubator, the commercial culture plate sizes and man-machine functionality. In addition, the mechanical and electronics dimensions that would have to fit in the device interiors such as motor, couplers, bearings, spindle shafts and permanent magnets table. The local user interface was defined to be in a 60° inclined plane, in order to achieve a more comfortable interaction with the user from a predictable superior position to the mechanism.

4.1 Mechanical Design

The mechanical design was planned following the main components of the system, which needed to be placed and fit at certain points of the enclosure. The variables taken in consideration were the culture plate sizes, type of stimuli to be employed and respective mechanics, sensor positioning, electronic board sizes as well as user input, feedback components and wiring.

4.1.1 Main Module

The main module size, which will be the base of the device, must comply with the culture size requirements such as culture plates/chambers and incubator being used, while providing enough space to accommodate mechanics, sensors, electrical connections and outer connectors, while providing a hermetic enclosure for all its content. Although, every part must be designed in order to be able to be manufactured with conventional tools through machining a project compatible material. The waterproof ability is enabled by adding contact rubbers present with every opening for the top and frontal fitting covers and waterproof power connectors with IP68 grade (Figure 4.2).

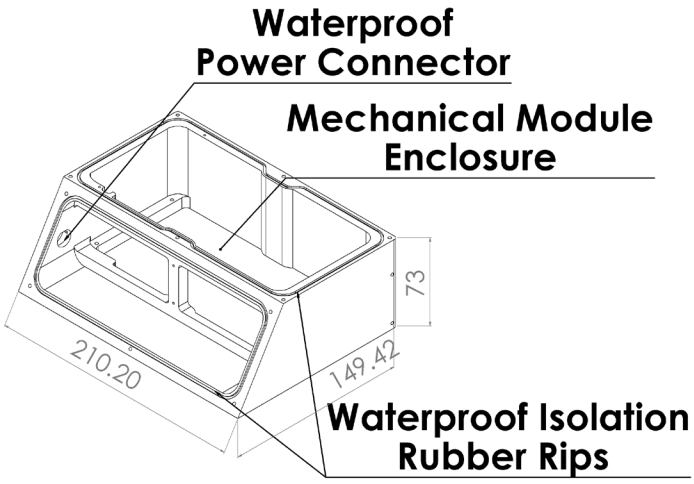

Figure 4.2 - Main enclosure design regarding which will operate as the main base for the system to stand on (measurements in mm).

Nylon was selected as the main base material for construction due its properties to be able to withstand high temperatures, easily worked, being electrically and magnetically inert, also its soft nature and opaque view on the sides of the system fulfills the most suitable requirements.

4.1.2 User Interface

The user interface is a sensitive part of the design, as the device needs to withstand sterilization processes and operate in high humidity environment inside an incubator, so a waterproof interface is mandatory for mechanics and electronics protection. Thus, the system is divided into two main control points behind a waterproof protective transparent frontal cover, where one controls user inputs and the other takes the task to display positioning, sensors and any other system feedback. The local user interface was defined by a LCD display and a side capacitive touch wheel with a central button and a sliding circular panel for selection, variable increase/decrease and option confirmation. The setup allows the user to locally stop, start or change the culture control parameters. A remote interface was also installed by Bluetooth through where the user can monitor the culture status and sensor information from outside the incubator from an external terminal. The system was designed in order to be liquids resistant, thus, a connector with rubber protection in the joints and a capacitive touchscreen was used, avoiding mechanical buttons and leaks to the system interior mechanics and electronics. Thereby, the enclosure frontal cover (Figure 4.3) is the main source of interface with the

user that contains the information display, receives user input through a waterproof keyboard, and assembles mechanically with the main base and top cover.

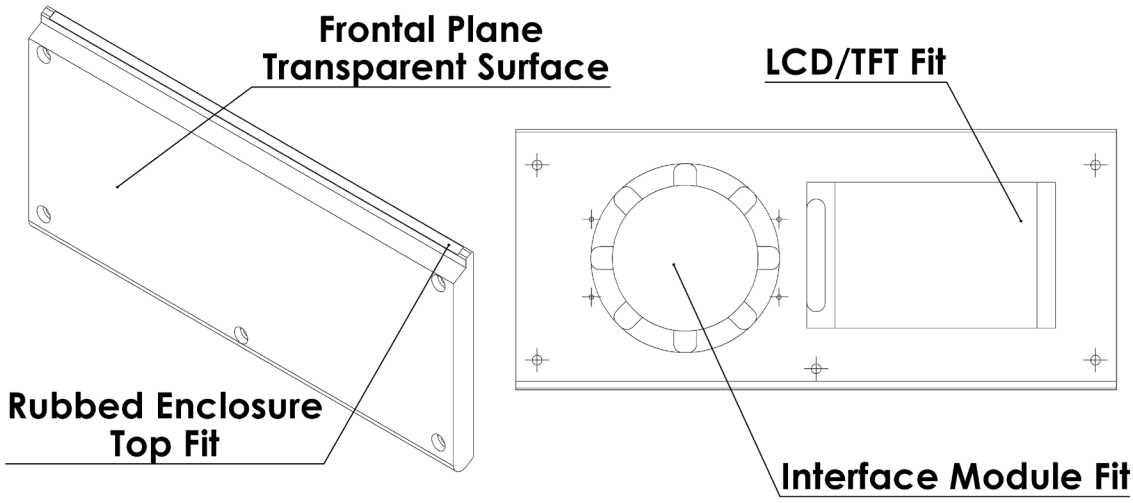

Figure 4.3 - Frontal main system cover, which accommodates the interface module and TFT display.

The frontal cover required the same characteristics as the main enclosure although some extra requirements were needed, which were being transparent in order to enable the view to the LCD screen in the interior of the enclosure and being a dielectric material to use as a capacitive surface, so acrylic was selected as an harder material with well-defined worked finish.

4.1.3 Top Plate

The top cover is where the culture plates/chambers stands and where the temperature sensor must be placed to control the nearest possible to the culture (Figure 4.4). In this case, as permanent magnets are being employed, a Hall Effect sensor is also useful in order measure the magnetic field value at the system top, in order to keep the variable controlled.

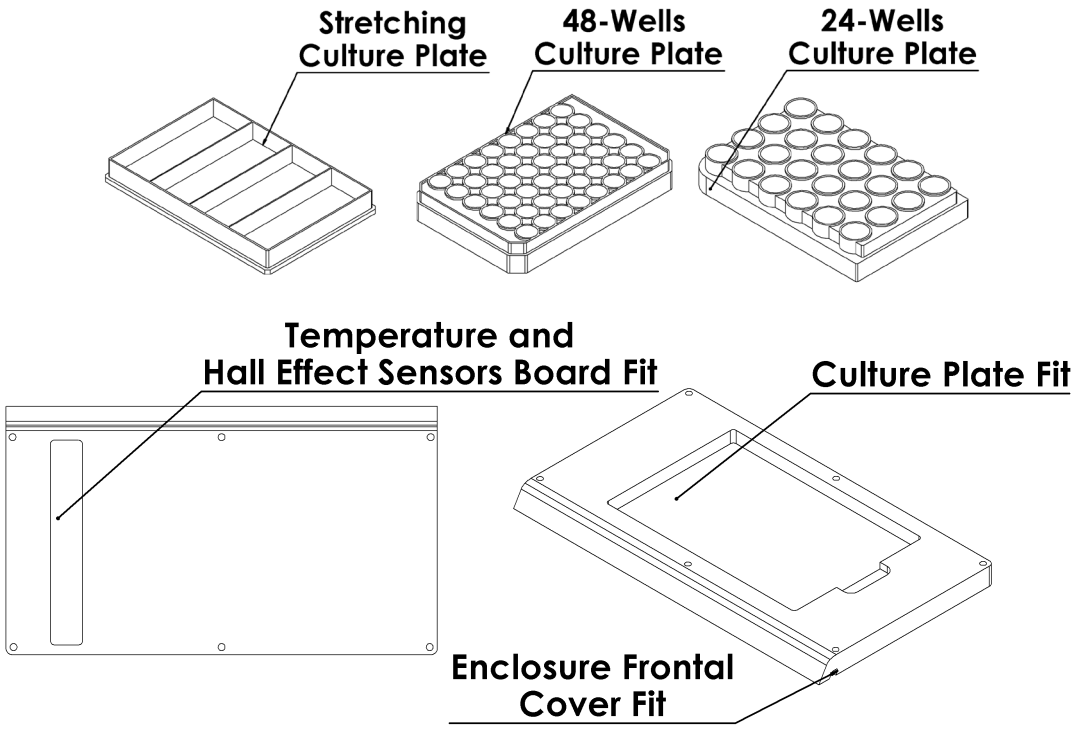

Figure 4.4 - Culture plates that hold scaffolds for magnetic and electro stretching stimuli, and main system top cover displaying mechanical fittings with frontal cover and culture plates.

The top cover follows a similar approach to the frontal cover being composed as well by acrylic instead of Nylon such as the main enclosure in order to control magnets starting position according to each type of culture plate, which are as well transparent but built with polycarbonate plastic.

4.1.4 Internal Mechanical Modules

The mechanics followed a conventional approach regarding a surface displacement through a precision digital control, using a motor with screw attached rotating and moving a surface in a ball screw assembly topology. However, for each case, magnetic displacement or stretching it would have to be in perpendicular axis to each other and still fit in the main enclosure. Thus, for the magnetic module the displacement will operate in the longitudinal axis just as displayed in the Figure 4.5, requiring a surface to attach a motor with a coupler and screw and a moving surface balanced by two spindle shafts supporting it through four linear bearings to reduce the displacement attrition and load in the motor.

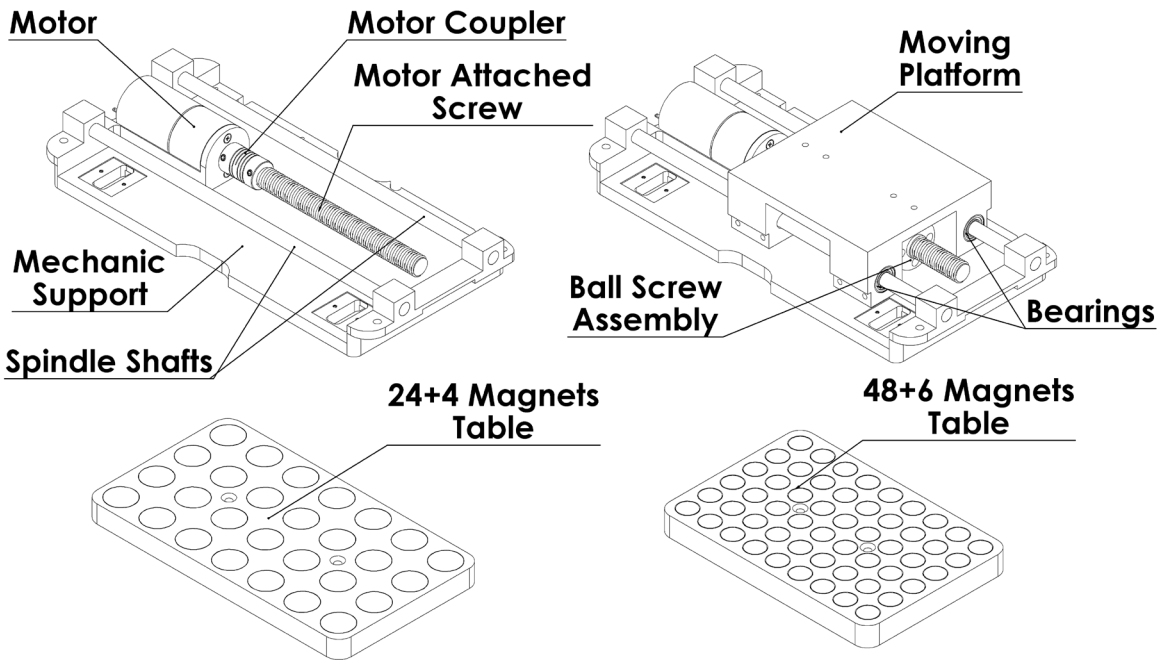

Figure 4.5 - Magnetic table motion interior mechanism.

The displacement surface was designed in order to be screwed any type of permanent magnets table with several number of permanent magnets with any type of magnetic grade and size till the max bearable size of the system component. The number of magnets columns in the table have one more extra than the respective well culture plates in order to keep the magnetic field stable always in the edges of the culture, being fixed to it by a bottom layer of magnets with a separating support to keep all of them attached by magnetic force to the structure. In addition, as the required magnetic field for the ME samples to vibrate and produce piezoelectricity must reach values within a range of 20 to 50 mT [108], the distance between the culture bottom and permanent magnets influence on the magnetic field intensity was analyzed through simulation on the previous used software ANSYS® Simulation Software. The Figure 4.6 displays the more appropriate distance according to each culture wells plates setup, which is different according to number of magnets and radius being used, resulting with a distance of 10 mm for 24 wells plate and 5 mm for the 48 wells plate.

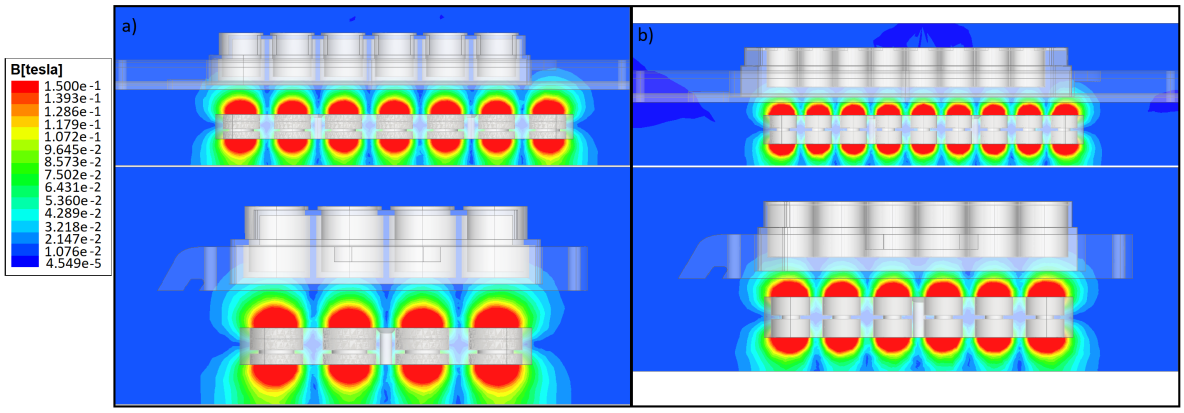

Figure 4.6 - Magnetic field intensity simulation in frontal and side planes on a) at 10 mm from the 24 wells culture plate (magnetic table of 4 x 7 permanent magnet points) and b) at 5 mm from the 48 wells culture plate (magnetic table of 6 x 9 permanent magnet points).

Thus, the number of magnets, thicknesses and orientations influence the magnetic field output on a given distance, in this case in order to keep several magnetic intensity value points, varying from maximum and minimum values, the magnets were distributed by alternating between north and south poles both in lines and in columns. Thereby, the Figure 4.7 displays the magnetic intensity distribution alongside the wells in both types of plates, with the near zero values placed between wells and the highest values at the center of the wells, where the displacement of those values will produce a constant alternated magnetic field as previously mentioned.

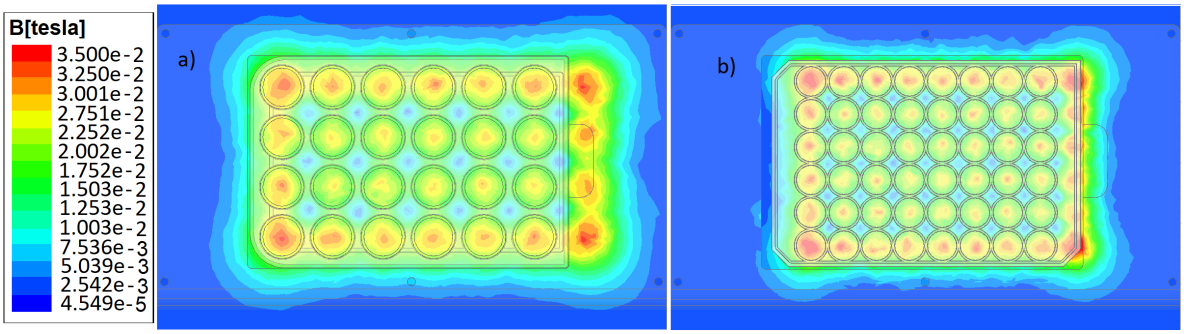

Figure 4.7 - Magnetic field intensity distribution at the bottom of culture plate wells on a) 24 wells culture plate within a distance of 10 mm from permanent magnets table and b) 48 wells culture plate within a distance of 5 mm from permanent magnets table.

Through magnetic force field, it is possible to pull or push a magnetic component at the top of the bioreactor structure from a bottom position in the system interior so the magnetic component for stimulation can be used as the driving force for stretching. Thus, stretching interior module was designed as schematized in Figure 4.8, although the nature of the stimuli requires that components must be inserted inside the culture plate to take advantage of the magnetic force, hold the scaffolds,

and simultaneously make electrical contact for electrical impulses. The stretching force operates through keeping a fixed side while the other pulls through permanent magnet displacement, for this specific experiment, the pulling clamp was built differently in order to minimize the support attrition to the culture plate wheels. In this setup, the mechanical transmission is through toothed wheels with a timing belt and the screw rotation support makes contact with a regular rotation bearing, completed with the same ball screw assembly in the moving surface and two linear bearings to reduce attrition with the spindle shafts.

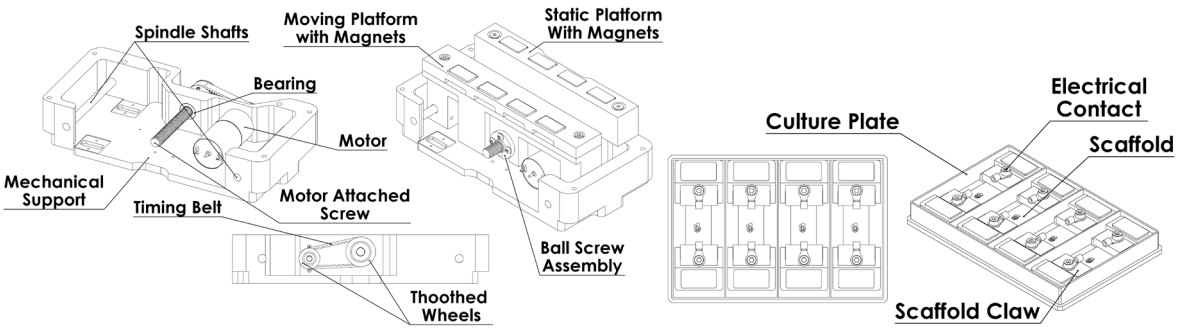

Figure 4.8 - Stretching mechanics interior module and culture plate setup to hold and stretch scaffolds.

The claws or clamps, present in the culture box do the job of holding, stretching and make an electrical contact to the scaffolds (Figure 4.9). Thus, the materials required to build them must be biocompatible, sterilization and chemically resistant and must be composed by conductor materials such as: stainless steel, gold, platinum, palladium or titanium and isolation materials such as Teflon, acrylic or PLA. In this case, the clamps were 3D printed in PLA using stainless sell as conductive contact plate and screw with the scaffold. Furthermore, for modular compatibility, the mechanics must comprehend a displacement in the transversal axis, also the displacement requirements are a few millimeters representing 5 to 10% scaffold stretching.

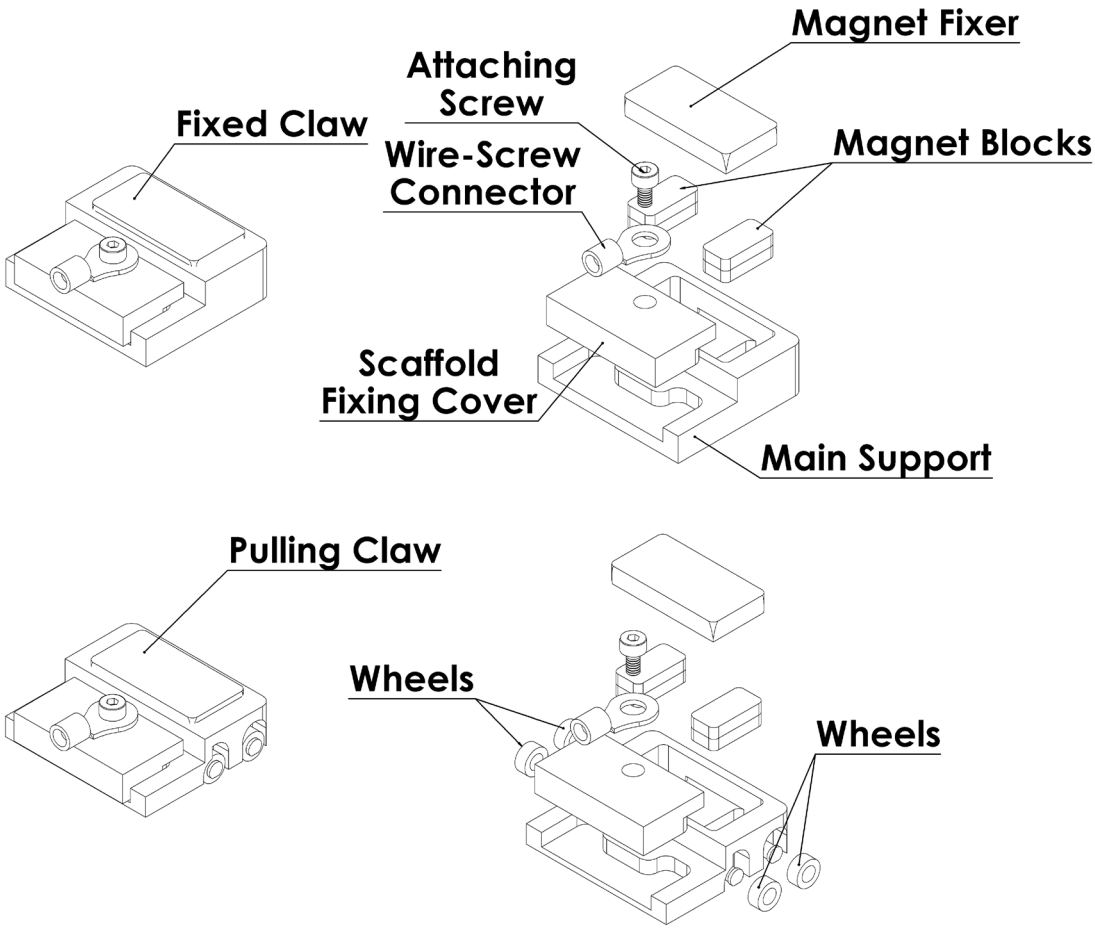

Figure 4.9 - Stretching scaffold supports for fixed and pulling ends.

Thus, for this mechanical module in question, the stretching force is provided by magnetic attraction from the magnets integrated in the bottom mechanics to the magnets coated in the clamps interior, which are placed in the culture plate wells. The two-block magnets approach with smaller magnets inside the claws was taken in order to keep two points of force in each side avoiding claw rotation around the magnetic force axis. In order to measure how much magnetic pull force strength it was used the 3D model in the same electromagnetic simulation software. As it can be seen in the Figure 4.10, the field intensity reach up to 250 mT while not reaching 0.7 mT at the scaffolds to be stretched, reducing to minimum the magnetic influence in the cultured cells as it was not planned stimuli.

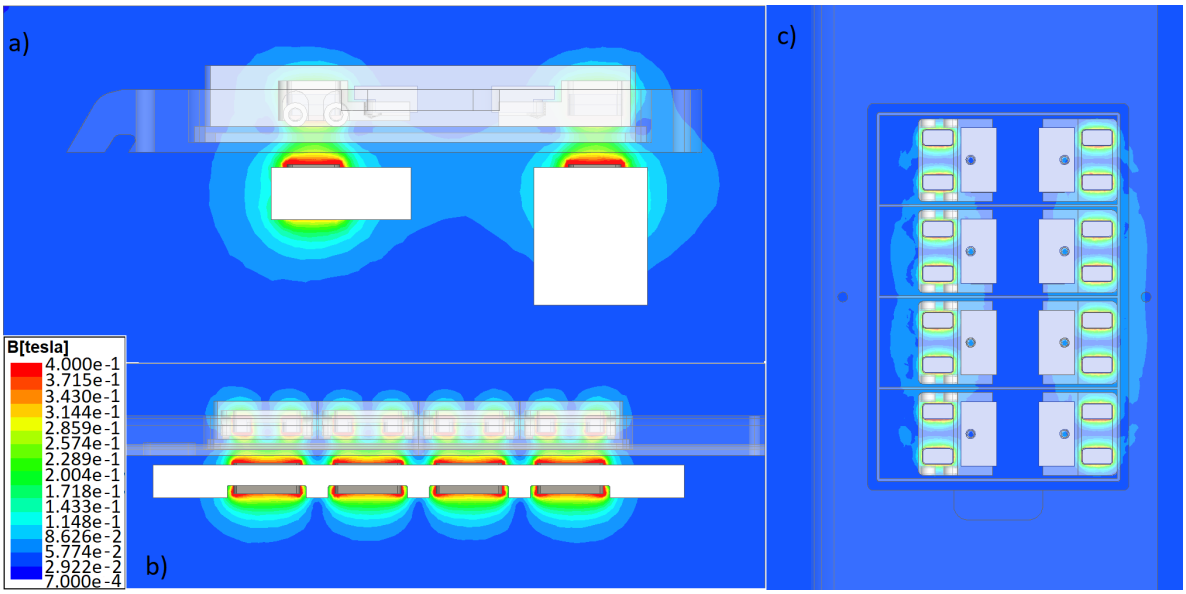

Figure 4.10 - Magnetic field strength for stretching forces applied in the scaffold clamps between magnets: a) side view of magnetic field lines, b) complete magnetic interaction between each pair of clamps inner magnet blocks and bioreactor inner blocks and c) magnetic field at culture plate bottom.

4.2 Electronic Design and Control

In this section of the document the electronics component will be described according to their role and requirements, although many possibilities would be valid, these electronic solutions were decided to give the system power robustness, flexibility for further hardware integrations and high speed of firmware communications for many types of sensors and operating mechanisms. The main system communication and control between modules is illustrated in the diagrams of Figure 3.6 and Figure 3.10. Thus, an electrical system was designed according to the machine mechanical and user interface operational requirements. Further, the designed circuits and PCBs were implemented using commercial available integrated circuits, LEDs, connectors, microcontrollers and passive electric components. The main electrical circuits designed are represented in the schematic of Figure 4.11. These circuits can be divided between power conversion, interface, sensors and main control of operation.

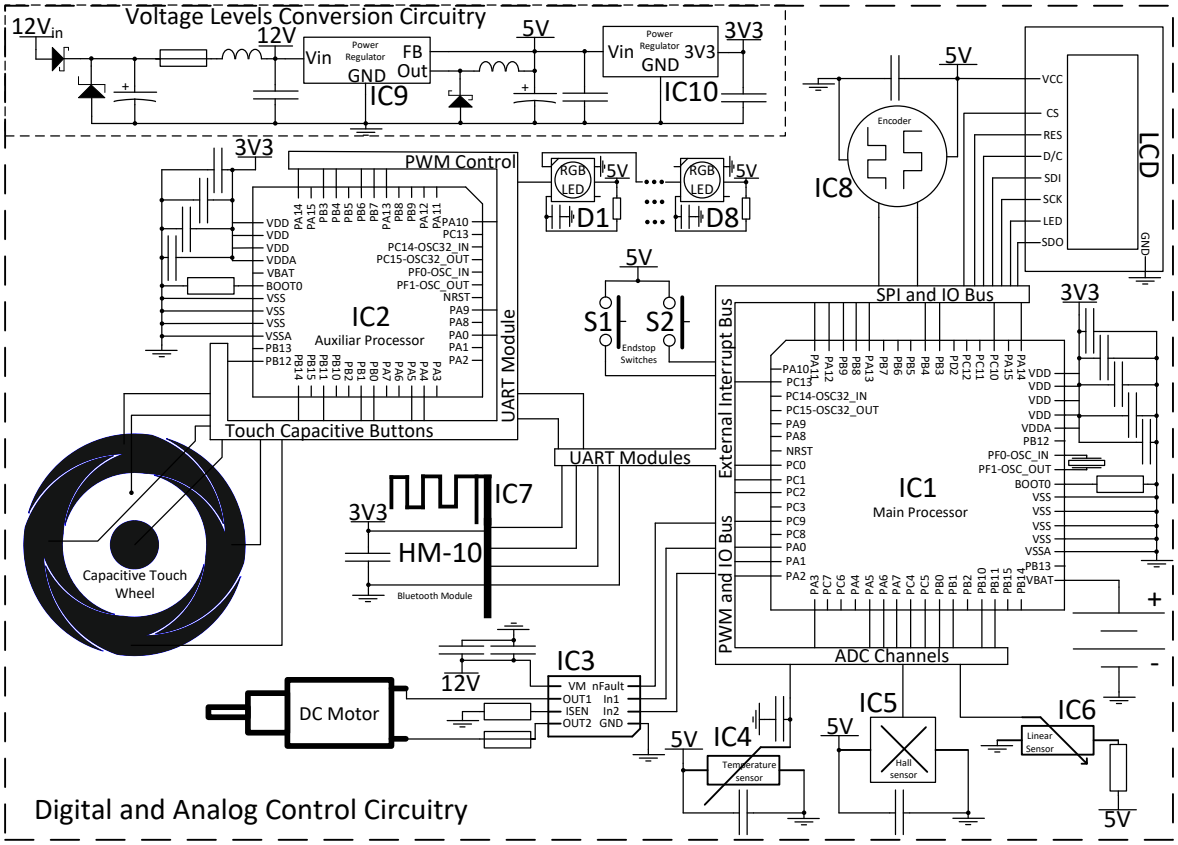

Figure 4.11 - Main circuits used for the power conversion, control and communication between sensors, actuators and interface.

Power conversion is required in order to comply with three different voltage levels, whereas the motor operates with 12V, LED lighting and sensors with 5V and logical CMOS level of 3.3 V. The interface was designed in order to be intuitive and waterproof with no leaking fissures to the device interior, so a capacitive interface was selected with a dedicated microcontroller STM32F091CBT6 (IC2) ARM® 32-bit Cortex® M0 CPU frequency up to 48 MHz for both RGB LED WS2812 lighting (D1~D8) and capacitive detection handling. Figure 4.12 displays the assembly of the capacitive touch buttons board to the interface control board with respective microcontroller and RGB LEDs.

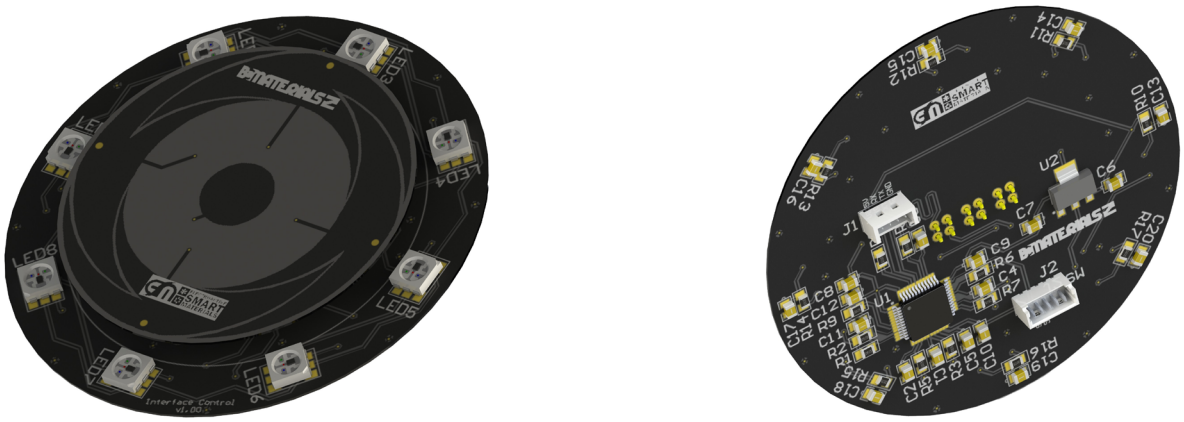

Figure 4.12 - Touch Module board two PCB assembly composed by a copper board for touch capacitive buttons and interface control board composed by IC2 and D1 to D8 RGB LEDs from circuit in Figure 4.11.

The main control of operation is performed by STM32F303RET6 (IC1) ARM® Cortex® M4 32-bit CPU with 72 MHz FPU, which controls overall firmware architecture. The main board contains the main DC power transformation, main microcontroller IC1, Bluetooth and H-Bridge motor control circuit as it can be seen in Figure 4.13. Thus, IC1 controls motor operation through the aid of an H-Bridge DRV8872-Q1 (IC3) with high range of operation up to 3.6A and 45V, interface communication with IC2 and Bluetooth HM-10 (IC7) through UART, LCD screen design through SPI, sensors input through ADC channels and system-timings for culture operation.

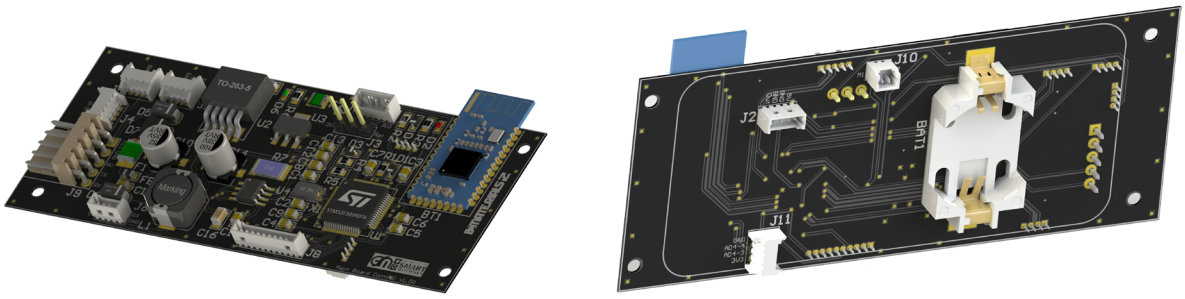

Figure 4.13 - Rendered picture of main control board composed by the majority of integrated circuits from Figure 4.11 (IC1, IC3, IC7, IC9 and IC10).

A CR2032 battery holder (coin size battery) were added in order to power the logic system only in order to keep system parameters such as clock and machine state in case of energy failure. The system was designed in order to employ a closed loop control using sensors, regarding temperature, magnetic field and displacement. An extra board was designed in order to house a LMT85 temperature sensor (IC4) and an AD22151 magnetic field sensor (IC5) being placed at the top of the main enclosure and in an entrance of the top cover to stay the closest possible to the culture plate (Figure 4.14).

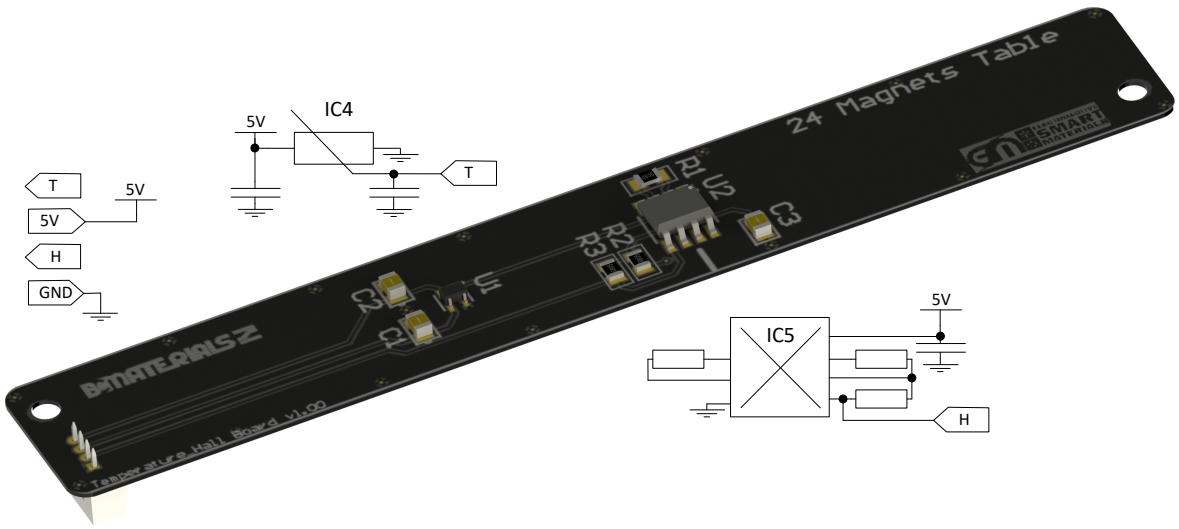

Figure 4.14 - Rendered picture of temperature and hall sensors board (IC4 and IC5 integrated circuits from Figure 4.11).

Other two types of boards were designed in order to be used to control the displacement system, relying on optical end-stop sensors (HY301-19) placed at the moving platform limits and a magnetic rotation encoder (AS5030) at the end of the motor screw, which would provide the angle of rotation (Figure 4.15).

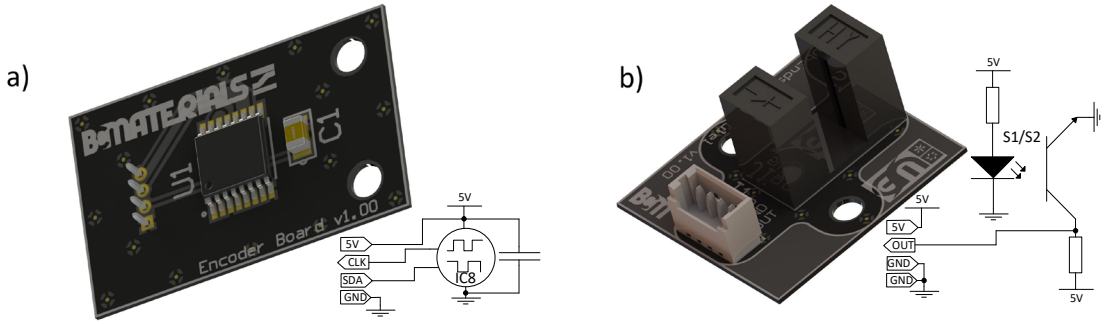

Figure 4.15 - Rendered picture of a) encoder rotation sensor (IC8 from Figure 4.11) and b) optical end-stop sensor (S1 and S2 from Figure 4.11).

This approach was considered in order to reduce the mechanical wear produced by contact, but there was lack of information regarding the platform position unless it were in the limits detected by the optical end stop sensors, requiring more components, higher processing time and resulting in slower system response. In order to overcome it, a linear position sensor 9610R3.4KL2.0 (IC6) was employed being easily integrated with an ADC channel input in the microcontroller, and replacing simultaneously end stop optical sensors and rotation encoder. This sensing device still provides more than 5 million cycles,

however the system is able to harbor all sensors simultaneously. All integrated circuits were designed with their respective decoupling capacitors in order to avoid high frequency power transition noise produced by the digital communications to dwell in the rest of the circuit power lines. The 5V regulator LM2596 (IC9) is a switching step-down power source with 80% efficiency, being important for this application by comparison with linear regulators, during long periods of use the amount of heat produced is considerably less for this level of power required. In order to power the logic circuits at 3.3 V, a LD1117 voltage regulator (IC10) was employed. The previous components described were designed in order to stay inside the main system enclosure, whereas for the electrical external module, to be placed in the back of the system with electrical connections, an extra circuit board was designed (Figure 4.16). Thus, the main components of the external circuit are composed by another dedicated STM32F091CBT6 microcontroller (E-IC1) used in the control of the electrical impulses module and respective communication handling with main system. In order to use a single-channel current output it was decided to link every scaffold in series according to number of scaffolds (Culture Plate section in Figure 4.16), taking the most advantage of a single controlled current source. This system can be scaled into multi-channel future approaches with singular control over every current running in each culture well, although with higher costs in dedicated hardware.

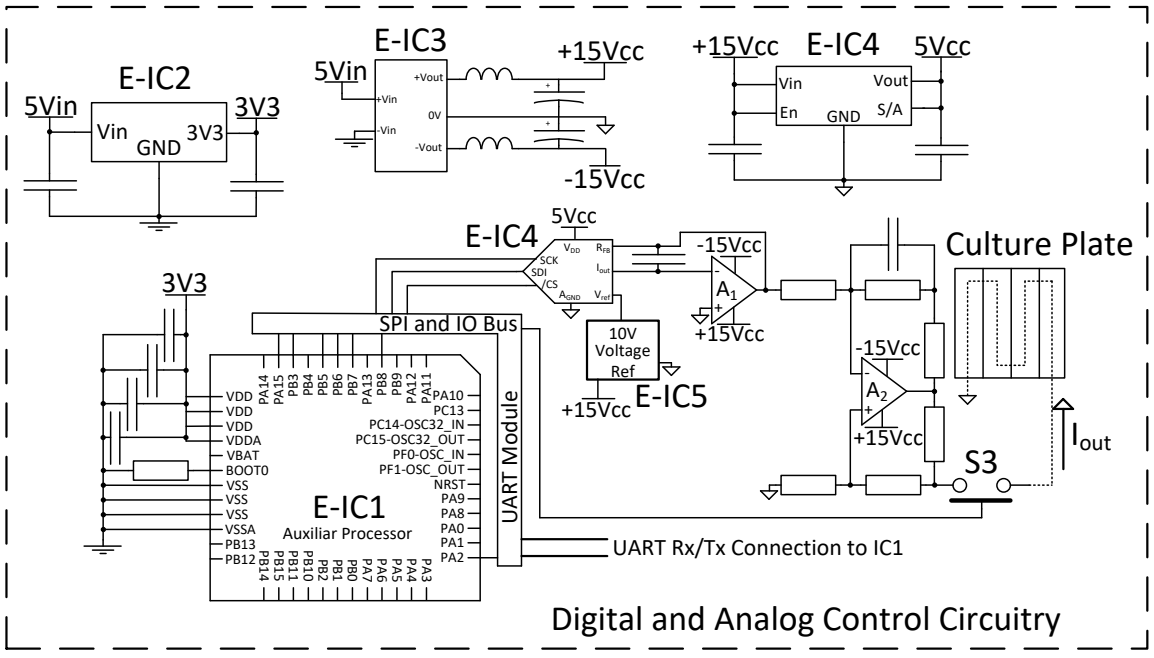

Figure 4.16 - Main extra circuits used for power conversion, control and communication between main system and external module.

Therefore, the instructions are received through UART from the main board (Figure 4.13) microcontroller (IC1 – circuit of Figure 4.11) regarding current amplitude, type of wave and frequency, as well as turn impulse on and off according to culture state. In order to follow a high precision approach a bipolar current source based on the Howland Current Source was employed [171]. This circuit is composed by a DAC with 16 bits resolution AD5543 (E-IC4) which communicates directly with the microcontroller (E-IC1) through SPI communication. In addition, it requires a voltage reference (employing 10 V ADR01AKSZ (E-IC5)) and high precision double amplifier (employing AD8512 (A1, A2)), which provide an output current up to 20000 µA with 300 nA resolution. Transforming the circuit from Figure 4.16 into a PCB, a rendered picture of the external module control board can be observed in Figure 4.17.

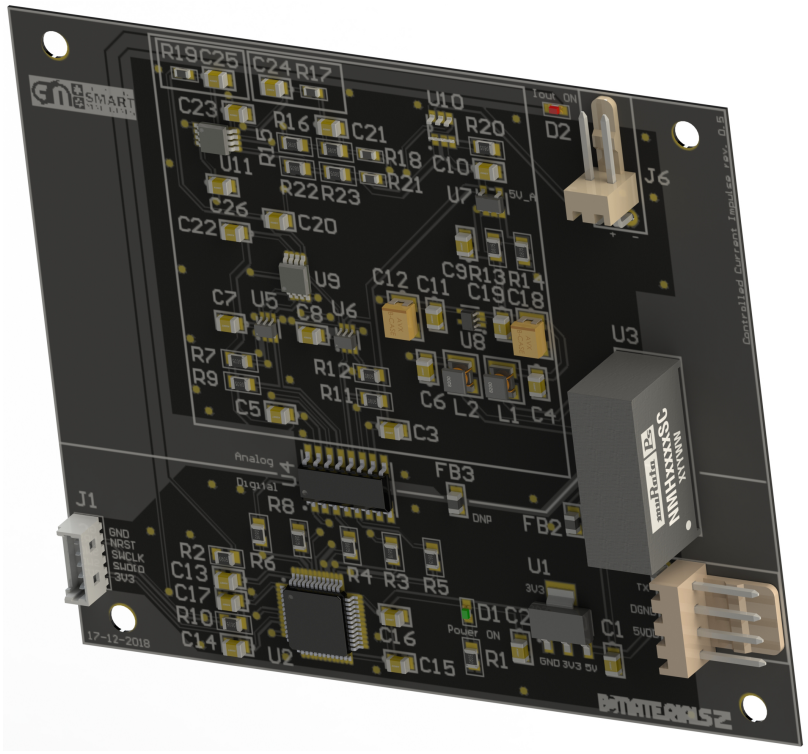

Figure 4.17 - Rendered electric impulses control and actuation board.

The output is controlled according to the active and repose cycles through the output switch ADG752 (S3) with ultra-low leakage currents of up to 250 pA according to manufacturer. This parameter is very important in order to have enough electrical precision when applying sub-µA currents, as it can become unpractical to use some components due to the current leakages and noise level surpassing the level of the signal intended to apply, requiring superior electromagnetic shielding and each more expensive hardware. The main power source is taken from the 5V transformation circuit on the main board

conditioned by IC9 (Figure 4.11) and lowered back to 3.3 V by another LD1117 voltage regulator (E-IC2) to power the microcontroller (Figure 4.16). However, due the different operating nature of both analog and digital electronics, as good practice the digital and analog voltage supplies and respective ground planes should be separated, as digital electronics produce high-frequency noise due to the very fast communications. The currents produced by digital communications are reflected in the voltage supplies and ground planes, reducing stability in the power-source and reflecting in the analog circuitry, which is prone to be corrupted by such noise, especially in small currents power sources as the one being employed. Thus, the isolated power converter Murata NMH0515SC (E-IC3) was employed, establishing the analog voltage supply and ground levels providing higher voltage and digital-to-analog isolation. However, there was a requirement to connect the digital and analog ground planes, in order to have compatible voltage levels in the communication between the digital and analog circuitries, so a ferrite bead was used to connect both ground planes, as it attenuates high frequency noise generated by the high frequency digital communication [172]. Thereby, a 4-channel optical coupler was considered in order to avoid connecting both planes physically, although the system did not require such signal isolation for currents higher than 0.6 μA for the time being (measured with a Keithley® 6487 picoammeter).

I

4.3 System Electromechanical Assembly

The main electronic PCB components regarding control, environment and electrical connections were screwed to the main enclosure as schemed in Figure 4.18. The enclosure was designed in order to harbor mechanics, sensors, magnetic actuator surfaces and wiring, so some openings and edges were added to pass wires from PCBs connections. The waterproof rubbers were fitted in oval rips in the top and frontal side of the enclosure. As previously mentioned, the bioreactor was designed with IP68 system in order to be water resistant for the sterilization process, through a waterproof power connector, rubber protection in the joints and capacitive touch avoiding mechanical buttons and leaks.

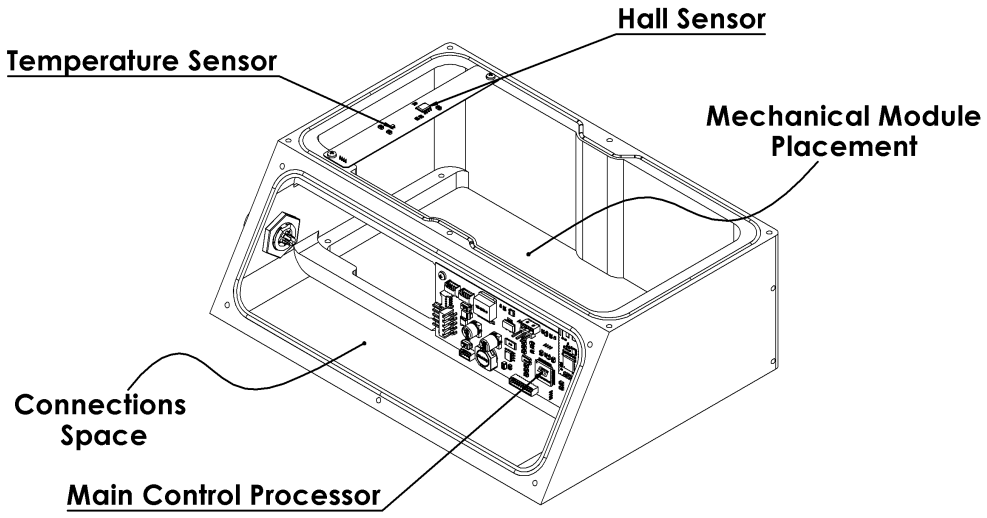

Figure 4.18 - Main enclosure with main electronic control board and temperature and magnetic sensor boards assembled.

Local user interface is composed by an LCD ILI9341 board providing a 240 x 320 resolution in a 2.8'' size and a capacitive sliding wheel. With these two components, the user can interact with the system while getting the system feedback. The fittings were machined in the acrylic frontal cover to fit with both electronic boards (Figure 4.19).

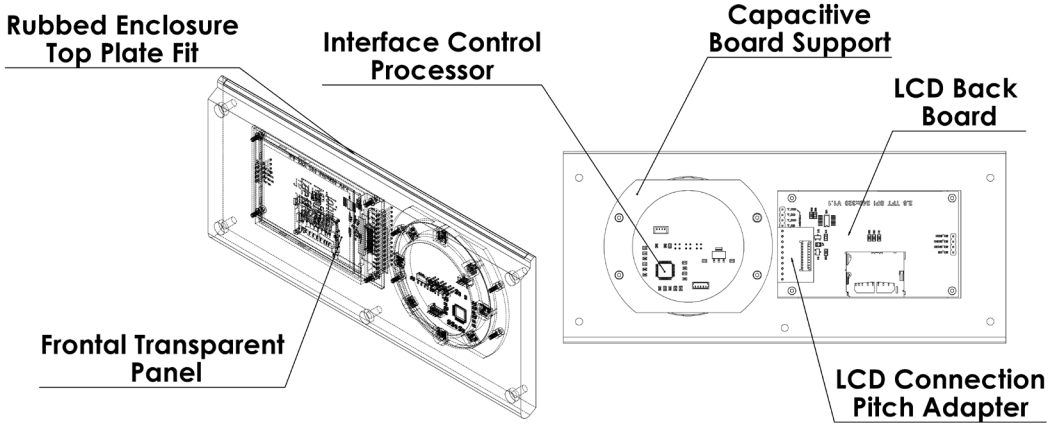

Figure 4.19 - Frontal cover with LCD display and interface module screwed and attached. LCD display is complete commercial module, which required an extra PCB for pitch adapting for the interface with main control board, whereas the capacitive interface module required a fixing support for a better contact from the capacitive buttons with the acrylic cover.

The mechanical modules were finished by the installation of displacement sensors. The magnetic encoder requires a disk shaped magnet at the tip of the ball screw in order to sense the magnetic field variation an then perceive the magnetic angle when motor is activated and rotating. Whereas, the

optical sensors and linear displacement sensor requires a mechanical tip to trigger their sensing mechanisms in order to communicate electrically to the microprocessor IC1 (Figure 4.11). The Figure 4.20a display the magnetic table mechanism where the alternated magnetic stimuli is produced and provided to the ME scaffolds, achieved by the movement variation along the longitudinal axis of the magnets table, below the culture plate. In this setup, the permanent magnets table can be replaced with higher or lesser number of magnets to fit the culture plate and apply an even magnetic field to all scaffolds, in this design, the system operates with 24 and 48 wells culture plates. It should be noted that the permanent magnets are selected according to the magnetic field level required for the magnetoelectric scaffolds to vibrate and generate the mechanical stimulus.

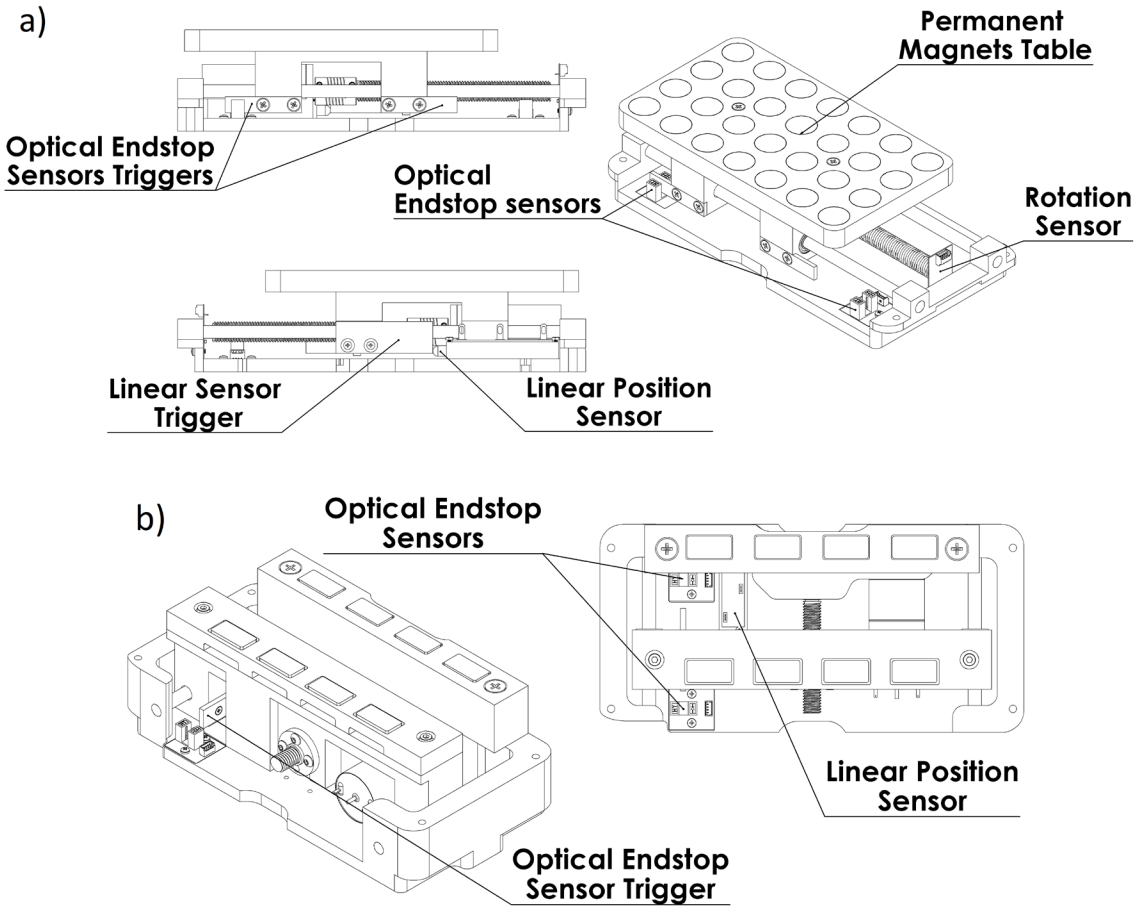

Figure 4.20 – Mechanical modules with respective linear and rotation sensors and end stop optical triggers assembled a) magnetic table mechanical module and b) magnetic stretching mechanical module.

The movement along the horizontal axis is achieved by using two side supports and a central motor shaft coupled with the DC motor as it is possible to observe in the device sectional detail in Figure

4.22d. The mechanical setup is implemented with a 25GA370 DC motor with 400 rpm, and is controlled through an H-Bridge at 20 kHz square wave regulated by a pulse width modulation (PWM) technique. The permanent magnets position moves along the longitudinal axis and table position is controlled by a linear displacement sensor (9615R5.1KL2.0), through the use of IC1 (Figure 4.11) peripheral ADC with resolution of 12 bits resulting in a theoretical linear resolution of 0.01 mm. As for the stretching mechanical module, the operating axis is the transversal axis through the threaded shaft coupled to a DC motor (25GA170) with 200 RPM, through a timing belt and cogs (Figure 4.20b). The stretching force is applied by mechanical pulse steps for higher displacement accuracy (better control of motor motion slip) whereas the feedback loop readings are taken from the linear position sensor. The displacement is controlled with a similar linear sensor and can be coupled with the same main system, resulting in the same linear resolution as the magnetic table module. The completed modular system is finished with the electric impulses external module, to be used optionally with the stretching module, providing the electrical output to the stretching scaffolds and can be attached by screws in the back of the main system. It is important to note that the system was designed to work with or without it, so the power cable is connected to either of them, if connecting both, the power cable connects to the electrical external add-on and an auxiliary waterproof connection cable provides the power and communication from the external module to the main system (Figure 4.21).

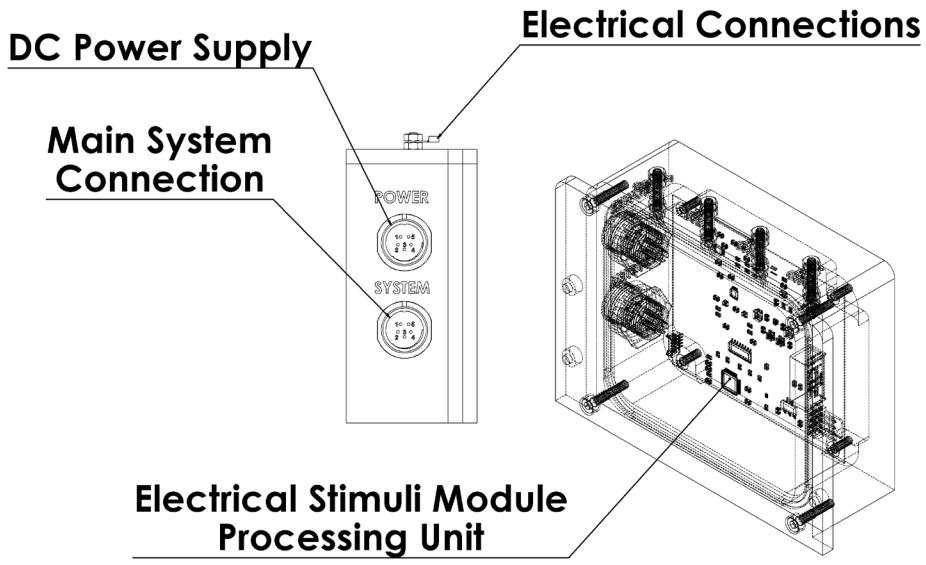

Figure 4.21 - Electrical external module enclosure with electric impulses board assembled, waterproof connectors and top culture electrical connection points.

The electrical contacts, as before mentioned, are provided by electrical connections with biocompatible conductor metals such as stainless steel, gold, palladium, platinum or titanium wires. Every scaffold terminals are arranged to be electrically connected in series, controlling a single current amplitude and frequency, which will be the same in every stretching chamber.

4.4 Final Assemblies

The result of the assembled system is a simple, compact and sealed design focused on a simple interface with the user. The device has been designed in order take a modern aspect using state-of-the-art interface and waterproof electrical connections, in order to take its purpose to higher levels of development and easier operation from specialized users in TE experiments. In this project in particular, two types of bioreactors can be assembled such as the magnetic bioreactor, which enables the application of an alternated magnetic field through the displacement of permanent magnets in a surface fit to the culture plate (Figure 4.22).

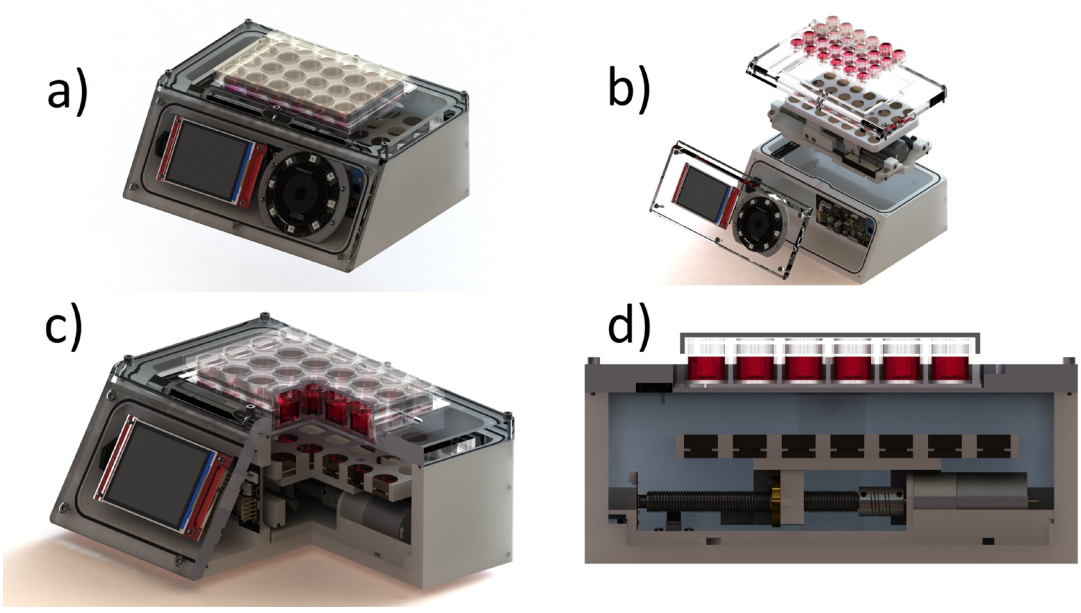

Figure 4.22 - a) Bioreactor assembled with tissue plate and culture trimetric view, b) dissembled with all main electric and mechanical components, c) L-cut view and d) transversal cut with the display of the mechanical component.

In the Figure 4.22 is possible to see the 24 wells culture plate configuration, although it works within the same principle for the 48 wells culture plate, with a smaller radius for the magnets disk sizes according to the radius of the culture plate wells. Through the system assembly, it is possible to see how every part fits with each component and how they will interact mechanically. The Figure 4.22a shows the complete assembled magnetic bioreactor with the 24 wells culture plate filled with medium simulating the operational look of the device, whereas the Figure 4.22b and c and gives the internal view of the system subassemblies. In Figure 4.22d the main operating principle is summarized, displaying how the magnetic field amplitude can be worked by changing the distance from the permanent magnets to the culture plate or the magnets grade. The simple principle of operation gets more complex through the indirect stimulus provided by the magnetoelectric scaffolds, which convert the alternated magnetic field to magnetostrictive and piezo-electrical stimuli. Following a different nature of stimuli, the electro-stretching mechanism in Figure 4.23 is assembled and dissected the same way as the previous mechanism, harboring every piece of hardware and mechanism required. Thus, in Figure 4.23a it is possible to see how the electro stretching configuration looks like with all the required components for the purpose. The displacement exchanges to the sagittal axis and the magnetic force is used to drive the scaffold holders to push and pull the scaffolds seeded with cells in order to provide the stretching stimuli, while taking advantage of the physical contact to make, simultaneously, electrical contact enabling a path for electrical impulses. Figure 4.23b shows every subassembly and how positioned they are according to system construction, whereas the L-cut view in Figure 4.23c displays how the motor transmission works through a timing belt, cogs and bearings.

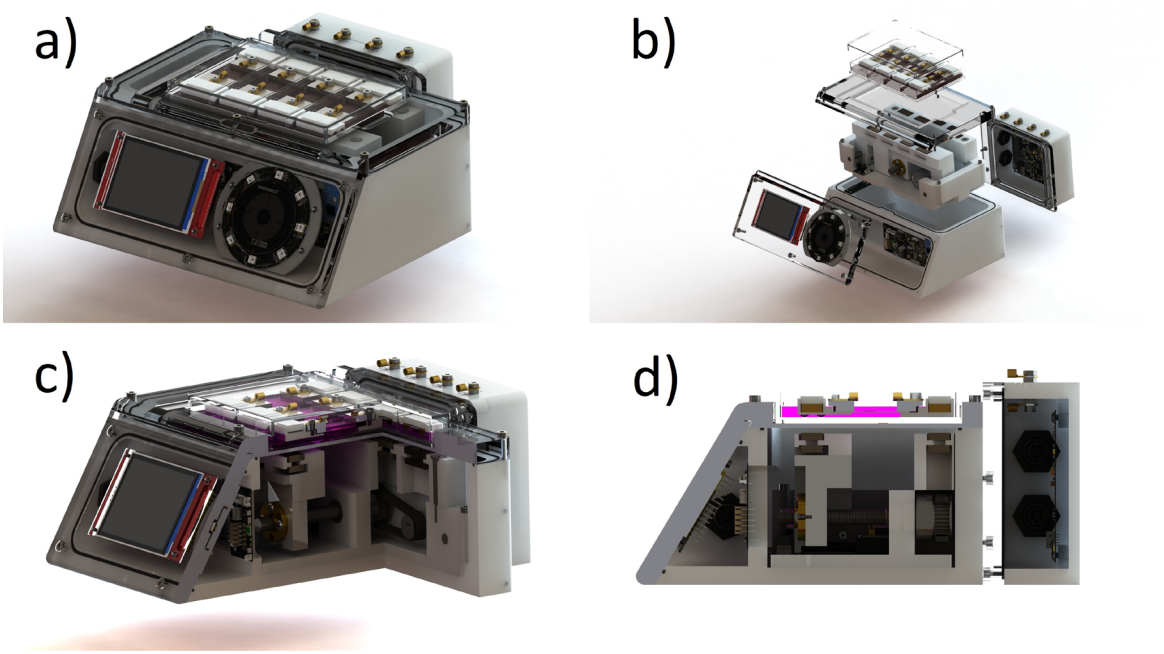

Figure 4.23 - a) Bioreactor assembled with tissue plate isometric view, b) dissembled with all main electric and mechanical components, c) L-cut view and d) sagittal cut view.

The main operating stretching mechanism relies in a line of permanent magnets displacement attracting the scaffold clamps, which coat as well, permanent magnets, as it can be better seen in Figure 4.23d, while providing the electrical contact to be wired to the backwards PCB terminals. This modular system main objective resides on micro-scale cultures to test new scaffold materials, analyze cellular behavior and culture methods according to the variable testing such as stretching percentage, pull force, magnetic field amplitude and frequency, active and rest periods, current amplitude, frequency and waveform, among others. Thus, set the stage for higher-productions on specific cultures with already mastered techniques obtained with a research sandbox-like device.

4.5 Firmware and Stimuli Control

Nowadays the digital era took over as it can provide new interface methods and functionalities, thus the circuit developed is based on microcontrollers and digital communication with every electronic component on the control boards. As the firmware is programmed according to each physical connection, the processor source code must be programmed, or in this case, generated in order to communicate with every electronic component. The microprocessors were programmed through Keil® µVision 5 to write and debug the programs and STM32CubeMX, which generated the source code with its associated libraries according to each peripheral/functionality being used for each microprocessor. ST electronics provide a utility to generate the source code according to requirements of peripherals, communications type, main oscillator and clock speed frequencies (Figure 4.24).

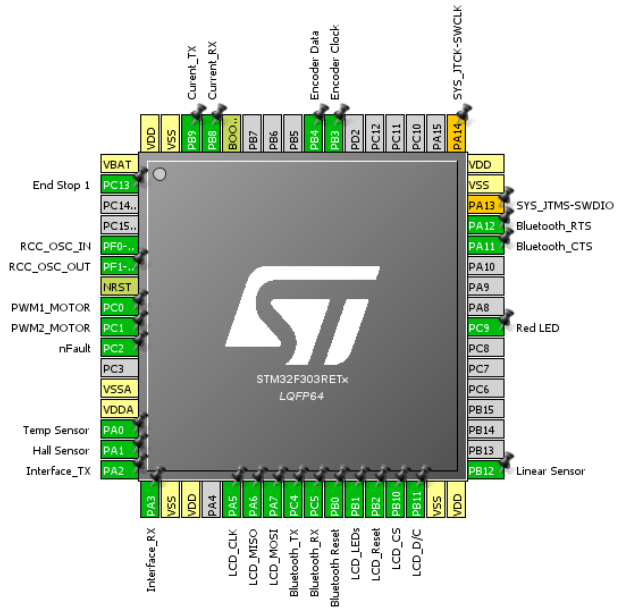

Figure 4.24 - Main processor configurations setup in STM32CubeMX for source-code generation of every pre-activated microcontroller module by software.

The main internal peripherals being used are analog-to-digital (ADC), universal asynchronous receiver-transmitter (UART), serial peripheral interface (SPI) modules and pulse width modulation (PWM) signals controlled by microcontroller oscillator derived timers. The ADC modules are being used to take analog readings from Hall, temperature and linear sensors, which measure the physical components by transducing it to a voltage signal or electronically instrumented to output a voltage signal within the ADC voltage range. As the main source of bi-directional external communications, the UART modules

are being used for the main processor to exchange data with other two microprocessors (interface control and external electric module) and through Bluetooth with remote terminals. Although SPI is a bi-directional method of communication employed in firmware communications between microprocessors and peripheral devices, it is commonly configured to transmit or receive data only from actuators and sensors such as reading-only from the magnetic encoder or sending data to actuators such as the display LCD. As for motor control, two PWM signals were set for each direction to be applied in the H-Bridge integrated circuit, which drives the current direction according to the intended motor rotation direction. Another PWM signal is being used as well to control LCD LEDs brightness, alongside with its respective SPI communication and DC signals. Peripherals such as ADCs, timers, UART communication and external signals are also being handled by interrupt service routines (ISRs) being executed on system demand according to electrical and mechanical requirements, alongside other secondary tasks such as menus, LED lightning and capacitive interface, which can be halted for some processor time, so they are being controlled by a pooling method. All these connections and driving source code is chained in order to work together symbiotically as an electromechanical device with several operating states which provides user with the interfacing tools to operate it. Each machine state (seen in Figure 4.26) dynamics were developed by building the programming for each microprocessor according to their own respective tasks. The different machine states allows the user to interface with each system functionality, which is bound according to system operation point in order to do tasks such as calibration, variable settings and running culture. Summarizing, the device operation relies on scaffold construction options such as materials and process, which will dictate how the scaffold response will be better suited for stretching, electrical discharge or magnetically responsive, followed by respective sterilization through several phosphate buffered saline (PBS) and ethanol washing cycles before being seeded with any kind of living cells [160, 161]. As it can be seen in Figure 4.25, after the biological supports are seeded and introduced with the bioreactor, the system can then be calibrated according to intended type of stimuli by placing the mechanical components on the most suitable position and selecting the intended variables, which will be described later in this section. The system can be started, and according to variable entry, applies the selected stimuli while monitoring temperature to terminate mechanical motion if temperatures are higher than cell safety values and issue warnings to a remote terminal wirelessly.

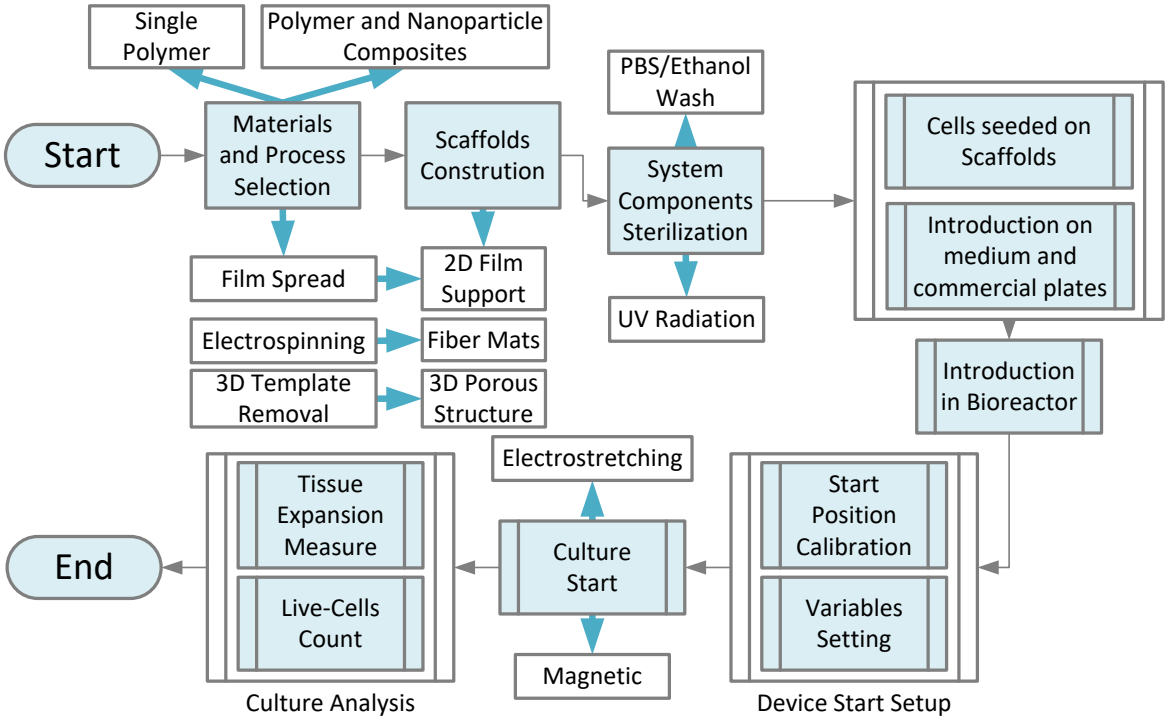

Figure 4.25 - Complete operation flowchart disclosing scaffold construction, scaffold sterilization, cell seeding and bioreactor operation.

The device works through 4 main states: menu state (1) where every state returns to and consists of the core control of the device; calibration (2) where the user sets the moving surface starting position; the parameters (3), which are the culture programs where the user sets the culture variables; and running (4) where the system performs the programmed culture by the user and displays the culture state variables taken from sensors.

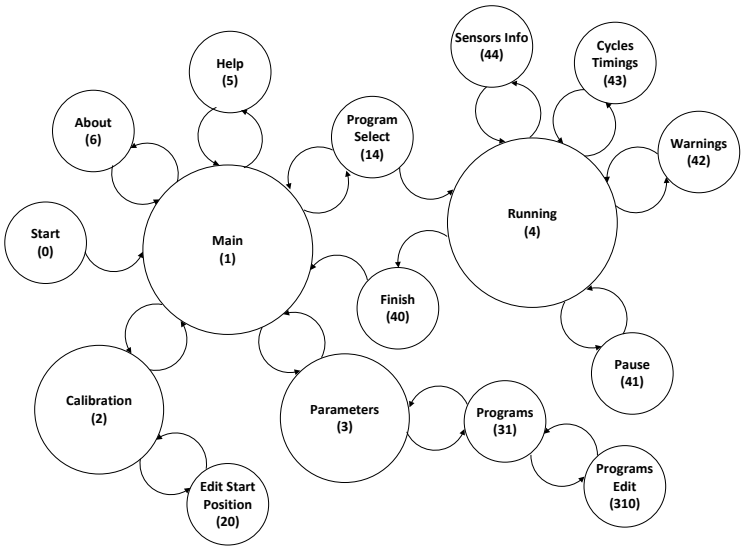

Figure 4.26 - State machine control nodes.

Thus, through the capacitive interface it is possible to navigate menus and adjust the culture parameters such as whole culture duration, the active- repose cycles duration, which work embedded in two temporal levels (short and long cycles), set mechanical shutdown temperature, operation frequency and displacement. It was reserved in program memory to store up to three culture programs through emulated electric erasable programmable read only memory (EEPROM). The firmware is adapted depending on the mechanical module operating, as the available displacement and frequencies are different due to the different nature of stimuli transmission and mechanical attrition. Thus, in the case of the magnetic module, it is possible to move the magnets up to 25 mm at a speed of up to 8 mm/s; in the case of the stretching module, it is possible to move the surface up to 12 mm at a speed of up to 4 mm/s. The firmware provides these limitations in order to protect the cells and hardware from human error by calculating hardware limits according to distance and operating frequency. The user can define various stimulation parameters such as critical temperature, displacement, frequency and different stimuli cycle timings to adapt the culture to the cells native environments such as it can be seen in Table 4.1.

Table 4.1 - Bioreactor user control variables to be set in the programs menu.

User Control Variables	Description
Displacement (mm)	Distance traveled by the respective permanent magnet platforms
Frequency (Hz)	Frequency of stretch or magnetic field stimuli signal to be applied
Runtime (hours)	Culture total running time
Cycle 1 active time (min)	Active time of sublayer cycle included in main layer active time
Cycle 1 repose time (min)	Repose time of sublayer cycle included in main layer active time
Cycle 2 active time (hours)	Active time of main layer cycle
Cycle 2 repose time (hours)	Repose time of main layer cycle
Shutdown temperature (°C)	Temperature value, which shuts down stimuli until culture temperature lowers to safety values again.
Current Amplitude (μA)	Current range from 0.6 to 2000 μA with 0.3 μA resolution
Current Waveform (Type)	Square, Triangular, Sinusoidal, DC
Current Frequency (Hz)	Non-DC wave form current frequency

The displacement in the case of the magnetic field stimuli will create an influence over the magnetic field curve, especially if starting or ending in a non-zero magnetic field position, whereas in the stretching stimuli case will determine the percentage of stretching applied according to scaffold size. Frequency will determine the mechanical speed to be applied, which will be directly dependent on the displacement, as longer distances at higher frequencies will require faster movement to comply with the timings. As for the culture runtime and bilayer cycles, those timings will set the respective total culture time, a longer active period filled with small periods of active stimuli and repose, and finally, a longer period of total repose. As previously mentioned the shutdown temperature value will disable every stimuli in the case of overheating at cell culture box. Lastly, the current control encompasses three variables in order to select one of the many types of current waveforms, amplitudes and, excluding the DC mode, frequencies up to 20 kHz.

4.6 Summary

In this chapter, the electromechanical design of the system was presented from system requirements to software operation, covering design decisions in both mechanics and electronic circuits. The system aesthetics was also decided in order to be easy to interact with, as well as intuitive to prepare scaffold samples to use on each type of TE culture. The Figure 4.27 resumes the various system assemble possibilities according to culture type and commercial culture plate layout, although

not only the electromechanical design must be modular, the software also must be designed to adapt to every configuration and assembly possible.

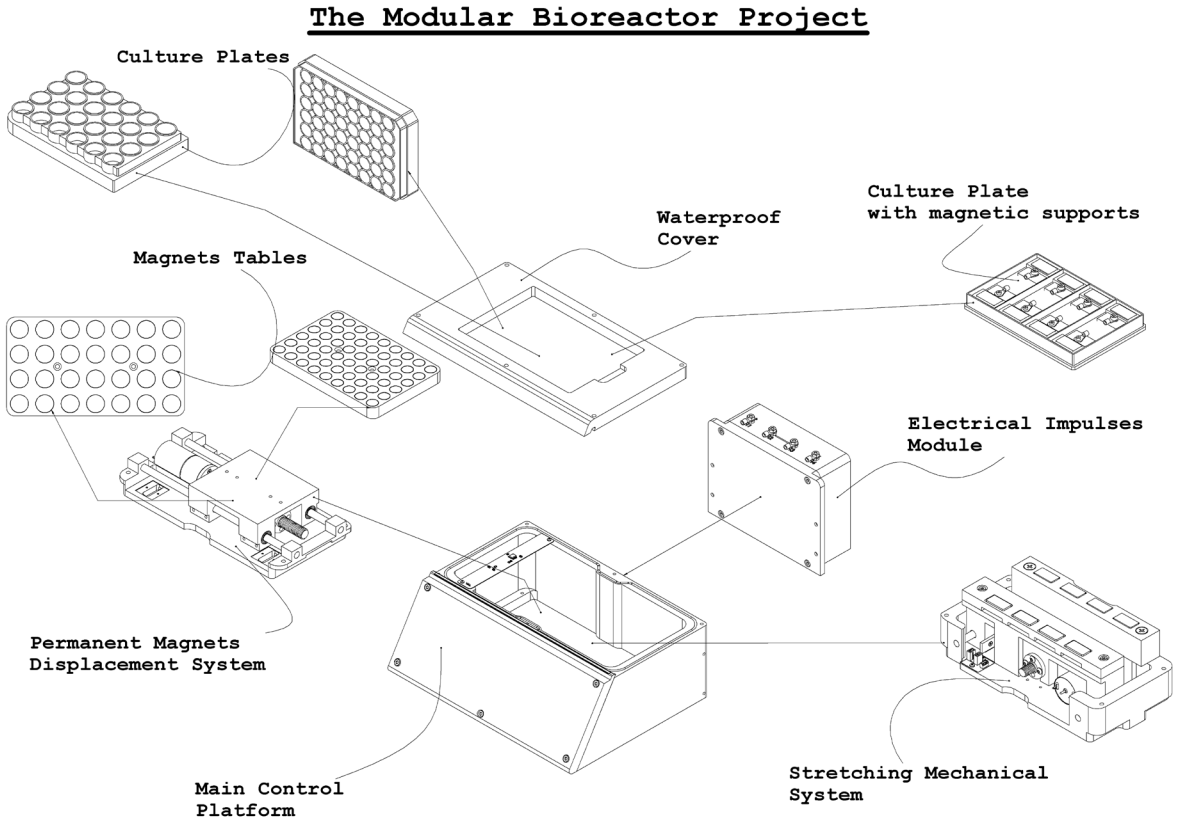

Figure 4.27 - Complete bioreactor modules for assembly possibilities.

This system relies on user input when electrical connections does not differ, as the software will not be able to perceive such differences, by selecting stretching or magnetic stimuli or even 24 or 48 magnets table when magnetic stimuli is selected. The system is able to detect the electrical stimuli module, as there are electrical connections differences though, when operating in electro stretching mode. After device planning, design and construction, the device was hardware and software operational, leaving the cytotoxicity tests and a TE culture performance to be executed as it is described in the next chapter.

5 Results and Discussion

Once the bioreactor has been designed and built, the remaining steps rely on device approval to bear cells and to keep them in the necessary environment. Thus, in the following chapter, the bioreactor electromechanical tests, the used methodology, cytotoxicity and viability tests are presented. The complete bioreactor system encompasses different mechanical variables, including scaffold physical size, which is directly related to the culture plate used. In the case of magnetic stimuli the samples can take shapes such as cylindrical/round in film or 3D porous scaffolds with the maximum size of the culture plate wells of 12 mm radius and a height of 15 mm for the 48 wells plate, and 16 mm radius and a height of 18 mm for the 24 wells plate. On the other hand, the stretching culture plate provides 4 large rectangular wells with 80 x 30 x 12 mm sizes. The whole group of components enable scaffolds to take a size with maximum length of 35 mm and width of 20 mm, in order to leave room for stretching and fitting the clamp limits. The electromechanical tests performed verifies system repeatability in terms of platform positioning and standard deviation error related with the increase of speed, as well as current output with a precision measurements instrument. Furthermore, bioreactor viability is a key factor to determine before any TE strategy can be planned, and will settle the starting ground for future module developments and improvements on the existing ones. This bioreactor device aims to provide new or reinvented tissue culture stimulation methods through clever remote force and state-of-the-art magneto-electro-active biocompatible scaffold materials in order to outline the processes and most important control variables for higher scale TE constructions. Thereby, in the case of bone, TE experiments rely on a piezoelectric scaffold, based on the fact that bone also show piezoelectric response. Thus, piezoelectrically responsive polymers are adequate due not only to their flexibility but also to their tailoring feature to be passively tolerated by the organism [15, 108]. Regarding muscle tissue engineering as this type of tissues takes advantage from stretching and electrical stimuli, the use of materials that comprehends elastic features is an advantage, as well as able to be tailored to assemble with conductive materials in order also to enable electrical stimuli. Thus, the use of polymeric materials and hydrogels are already being employed in the literature as previously mentioned, and is therefore important to build suitable stimuli-tissue interfaces as the one presented

in the present work. However, as the TE stretching culture is perturbed by extra materials, which will hold and stretch the scaffolds seeded with cells, those materials, must be analyzed in order to confirm if they are biocompatible before proceeding into further cultures.

5.1 Electromechanical Tests

The electromechanical tests were performed in order to check the performance, precision and repeatability that each cycle performs. The position of the platform, according to the frequency variation for the same distance (Table 5.1), shows a clear increase of the displacement according to speed due to the motor slip and sliding motion between the screw and the nut (mechanical backlash). The travel measurements were taken from the linear sensor maximum and minimum reading outputs of the 20 cycles testing on each frequency for the same given distance of 4 mm. It is show that, the faster the speed, the higher drift in platform positioning is observed. Thereby, the system is applying firmware braking techniques (same amount of energy in both motor directions for short periods to get a greater precision stop or reverse the direction) in order to attenuate those drifts. However, higher precision may be achieved with further firmware control (more complex control with speed analysis) and mechanical backlash compensation (using an axial method with a spring between two half-nuts or a radial method with a nut wrapped with a spring in its outer body).

Table 5.1 – Bioreactor mechanical displacement testing, according to frequency for the same travel distance of 4 mm.

Cycle Frequency (Hz)	Speed (mm/s)	Average Travel Distance (µm)	Standard Deviation (µm)
0.2	1.6	4022	54.16
0.3	2.4	4071	74.15
0.4	3.2	4032	146.88
0.5	4	4019	188.00
0.6	4.8	4011	211.26
0.7	5.6	4232	222.3
0.8	6.4	4138	232.56
0.9	7.2	4318	269.85
1	8	4259	294.90
1.5	12	4525	624.65
2	16	4839	881.87

Thereby, for each module it was set different maximum speeds. For the magnetic module, as it is not a critical force on the scaffold and only at the magnetic field signature, the 8 mm/s speed was set with 7.4% standard deviation not representing a significant variation on the stimuli. Although higher speeds could be achieved, according to the graph in Figure 5.1, the standard deviation would be difficult to reduce and keep it below the 10%. However, for the stretching module as it applies a force in the scaffolds indirectly, it requires higher precision to avoid tearing the scaffolds or over-stretching them, and therefore, the speed was limited to half. Thus, up to a speed of 4 mm/s it is possible to obtain a standard deviation below the 5% margin, being set as a maximum for the stretching mechanism because the stretching should not exceed the 10% of the size of the scaffolds. It should be noted that these restrictions do not limit application, as further speeds are not so interesting according to literature, as biomimetic approaches are related to low frequency stimuli, as experienced in the body. It should be also taken into account that with further improvements it could be possible to achieve higher speeds by adjusting firmware control and respective braking mechanics.

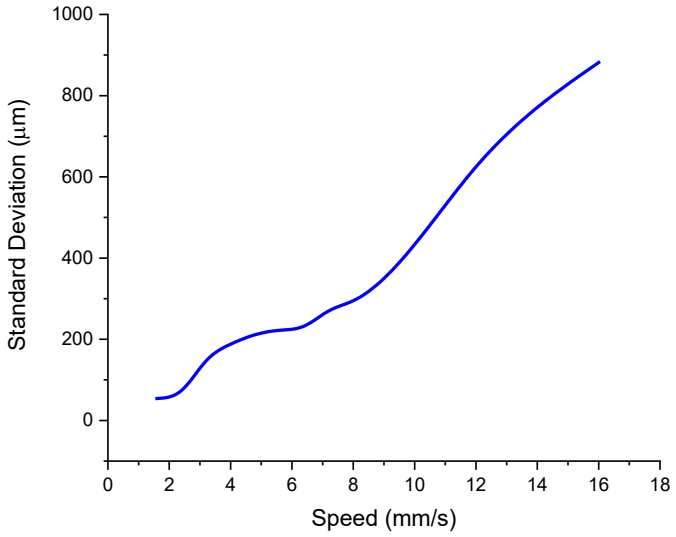

Figure 5.1 – Standard deviation according to speed graphical analysis.

Due to electromechanical tolerances, the variations throughout the speed increase are not linear, but clearly follow a tendency of further error, which is expected as it presents higher energy requirements to stop the slipping of the whole mechanical assembly. Thereby, depending on the displacement distance required, the maximum final frequency of the cell culture stimuli could be higher for smaller displacement distances and vice-versa.

5.2 Electrical Actuator Tests

Regarding the electrical external module, DC current tests were performed following several current levels from 1.9 to 1000 µA. However, due to the nature of the stimuli with very small current levels, in some cases smaller than electrical noise, further components such as current sensors and an ADC channel for closed loop control, would introduce noise especially in the sub 10 µA range, thereby it is being applied in open loop. The several variables that will influence the final application such as the medium and scaffold conductivity, must be externally measured in order to access the most possible approximation to the real current that flows through the scaffold, and consequently the cell culture. In order to achieve the current source output performance, a sample resistor of 10 kΩ (reaching a maximum of 10V with 1 mA, within a current source limit of 15 V) was used to simulate the scaffold/medium parallel resistor and, in series, a Keithley 6487 picoammeter. The difference from the reference current to the output measured are presented in Figure 5.2.

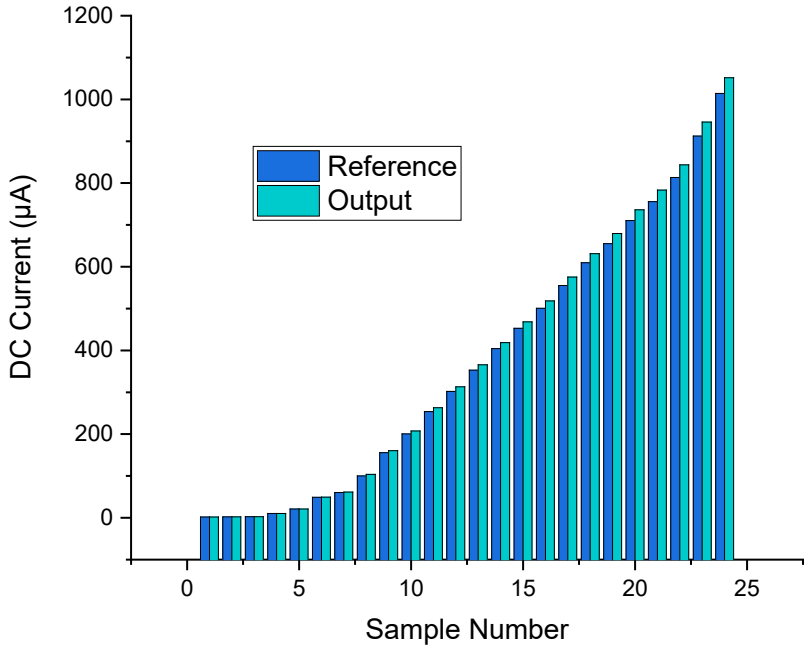

Figure 5.2 – Open-loop measurements of electrical impulses actuator with several DC current levels.

The DC current values at the lowest amplitudes, do not present so much difference from the reference, probably because of the smaller scale variation, although it can be observed to steadily increase with

current amplitude until reaching a maximum of 3.7% variation from reference in the sub-1 mA range, as presented in the last column of Table 5.2. The tested values present a current fluctuation below the 100 nA, with a fair small error. The current controlled approach still relies in higher precision and safety for the cells than a voltage approach, which can drain very high currents from source and kill the cells in the case of high quantity of salts are present in the medium or conductive fillers are included in the scaffolds.

Table 5.2 – Detailed electrical DC current measurements, according to the applied reference value.

Reference (µA)	Maximum(µA)	Minimum (µA)	Fluctuation (µA)	Average Error (µA)	Average Error (%)
1.9	1.95	1.89	0.06	0.02	1.05%
2.2	2.24	2.2	0.04	0.02	0.91%
2.8	2.85	2.77	0.08	0.01	0.36%
10.5	10.51	10.47	0.04	0.01	0.10%
21	20.98	20.94	0.04	0.04	0.19%
48.9	49.19	49.16	0.03	0.275	0.56%
60.3	61.34	61.28	0.06	1.01	1.67%
100	103.87	103.82	0.05	3.845	3.85%
155.6	160.29	160.26	0.03	4.675	3.00%
200.5	207.61	207.57	0.04	7.09	3.54%
254	263.06	263.02	0.04	9.04	3.56%
302	312.97	312.93	0.04	10.95	3.63%
353	365.62	365.57	0.05	12.595	3.57%
404.3	418.52	418.47	0.05	14.195	3.51%
452.9	468.54	468.49	0.05	15.615	3.45%
500.6	518.34	518.29	0.05	17.715	3.54%
555.3	575.29	575.25	0.04	19.97	3.60%
609.5	631.31	631.25	0.06	21.78	3.57%
655.2	679.45	679.4	0.05	24.225	3.70%
710.4	736.26	736.2	0.06	25.83	3.64%
755.6	783.19	783.13	0.06	27.56	3.65%
813.3	843.45	843.38	0.07	30.115	3.70%
912.2	946.02	945.97	0.05	33.795	3.70%
1014.3	1051.85	1051.77	0.08	37.51	3.70%

5.3 Biological Analysis

As main materials and methods, polymers can be processed in the form of small fibers to films and to 3D porous structures. These materials show tailoring flexibility, being suitable for TE scaffolds construction. They can be used as simple polymer construction or also include electroactive materials which will provide another layer or layers of functionalities, becoming an increasingly important source of possibilities for TE field nowadays. The scaffolds construction and corresponding characterization was performed at BCMaterials in the Scientific Park in Leioa, Bizkaia, providing an important contribute for the validation of the system with knowhow, facilities and equipment for this application. However, every component must be biocompatible and every new material or composite, which presents useful features for TE cultures, if not yet assayed for cytotoxicity, the step must be taken as starting point. Thus, the cytotoxicity analysis can take different approaches according to scaffold material or composite of materials and cells to be employed. Thereby, for these two particular cases, which are going to be presented, the process follows a standard scaffold sterilization based on scaffold multiple immersions on ethanol, followed by several periods of 5 min of scaffold washing on PBS, finishing with UV light exposition on each scaffold side. Cell culture process follows the sterilization and, when the number of required cells for cytotoxicity analysis is reached, the assay can be performed. This assay is a method that measure mitochondrial activity of cells being an indirect assessment of the number of viable cells. It can be performed by replacing the culture medium with a reagent such as (3-(4, 5-Dimethylthiazol-2-yl)-2, 5-diphenyltetrazolium bromide) also known as MTT or (3-(4, 5-Dimethylthiazol-2-yl)-5-(3-carboxymethoxyphenyl-2-(4-sulfophenyl)-2H-tetrazolium) also known as MTS. In the case of MTT, it interacts with viable cells and produce a colored formazan product, which after some incubation time, may be measured by dissolving with dimethyl sulfoxide (DMSO) the formed crystal within the cells outputting cell survival rate. The cytotoxicity is set by the ISO standard 10993-5 where the culture medium in contact with the components, when put in contact with the cells, they suffer a viability reduction greater than 30%. Furthermore, in order to also measure the number of cells, depending on the type of cells a LIVE/DEAD kit is used instead such as for mammalian cells, bacteria, yeast and fungi, although this method is costly by comparison when just measuring survival rate with MTT or MTS. Regarding the next phase of analysis, they follow an approach as schemed in Figure 5.3, for each type of module for biological validation. The biological tests were carried out at the Biological Engineering Department at the University of Minho, Braga, Portugal, with the contribution of the

Electroactive Smart Materials group biomedical engineering team, providing knowhow and insight in the system design and helping designing the requirements to use it as TE device for regular cell cultures.

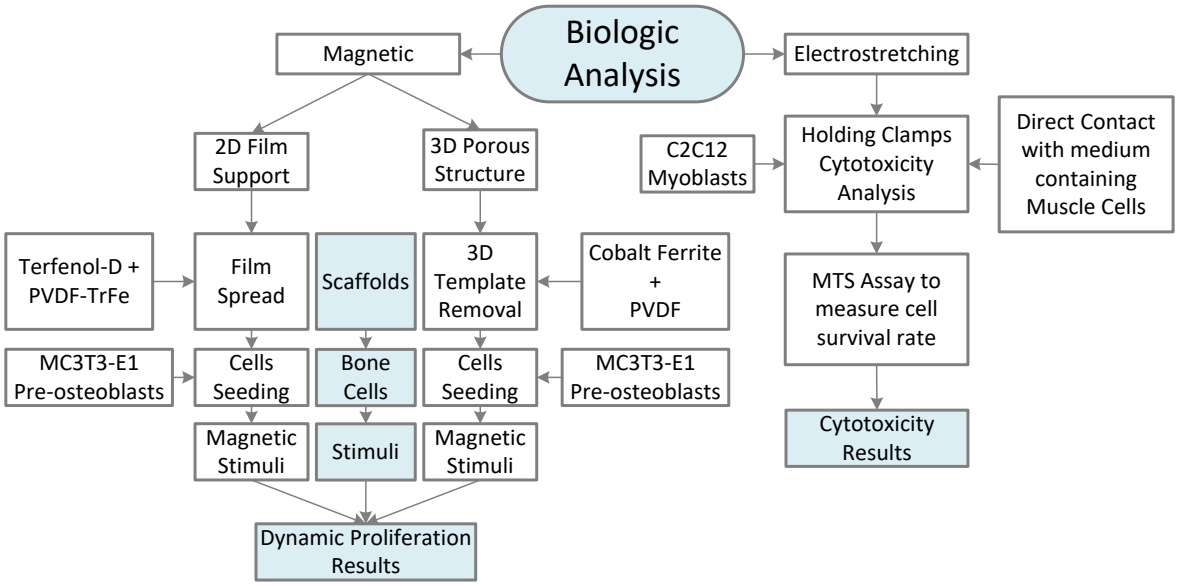

Figure 5.3 – Flowchart of the biological test analysis.

5.3.1 Magnetic Module Culture Results

As previously mentioned, incidence of bone disorders is steadily increasing and can be directly related with higher life expectancy, resulting in an higher number of elder population. Thus, TE plays a key role in the treatment of bone conditions related to slow regeneration and fractures. The magnetic synergic bioreactor module with ME scaffolds offers a closer recreation of the bone tissue microenvironment providing biochemical, mechanical and electromechanical stimulation factors, which are essential variables for an approach in bone healing.

5.3.1.1 3D Porous Scaffolds

For this module validation, three-dimensional porous magneto-active scaffolds were constructed, providing a proper bone-mimicking morphology while responding to magnetic stimuli, by assembling a piezoelectric polymer with magnetostrictive nanoparticles. Thereby, acting as an active

material that enhance cell function improving osteoblasts adhesion and proliferation, PVDF and 35-55 nm cobalt ferrite nanoparticles (CFO) were assembled through solvent casting method as previously reported in literature [163, 173] (following the approach of Figure 3.14 with nylon template).

5.3.1.1.1 Scaffolds Construction

Nanocomposites were fabricated at concentrations of 10% PVDF, a suitable quantity for fabricating 3D scaffolds [163], and 10% of CFO nanoparticles for magnetostriction. Cytotoxicity and cell culture validation can be extensively analyzed in [174]. Summarizing, the CFO nanoparticles were dispersed in DMF for 4h in an ultrasound bath in order to avoid nanoparticle agglomeration, resulting in a good dispersed solution. Followed by the addition of PVDF and Teflon mechanical stirrer until complete polymer dissolution. Then, using one of the methods discussed in [163], 3D scaffolds were built using nylon templates with 60, 80 and 120 µm porosity were cut into circles to fit a glass petri dish (Figure 5.4). By immersing the scaffolds in formic acid, the nylon plates were chemically degraded and thus the interconnected porous PVDF based scaffold were obtained. Finally, the scaffolds were prepared for cell culture, first by washing in a PBS solution and air-dried, as previously mentioned, to remove any trace of formic acid.

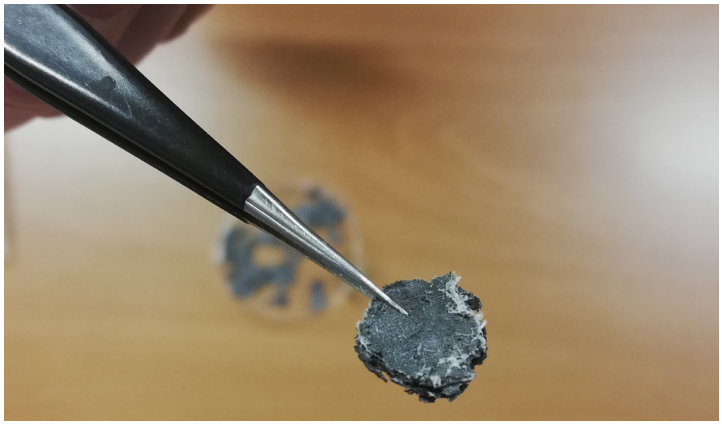

Figure 5.4 - 3D ME porous scaffold (PVDF/CFO) with visible traces of undissolved nylon template.

5.3.1.1.2 Cells Seeding

MC3T3-E1 pre-osteoblast cells were used for the cellular tests, although CFO nanoparticles are considered toxic for mammalian cells due to possible nanoparticle leaching from the material, the

indirect cytotoxicity evaluation was performed, which is based on the previously mention ISO 10993-5 standard test. Scaffolds with a diameter of 0.8 cm were sterilized by UV for 1 h each side and placed in a 24-well tissue culture polystyrene plate for 24 h and 7 days at 37 °C in a 95% humidified air containing 5% CO_2, followed by toxicity analysis through the MTT assay method resulting in a cell viability higher than 70% (Figure 5.5). Since the quantity of the nanoparticles was the same in the different developed scaffolds, the one with 80 µm porous diameter were tested for biocompatibility.

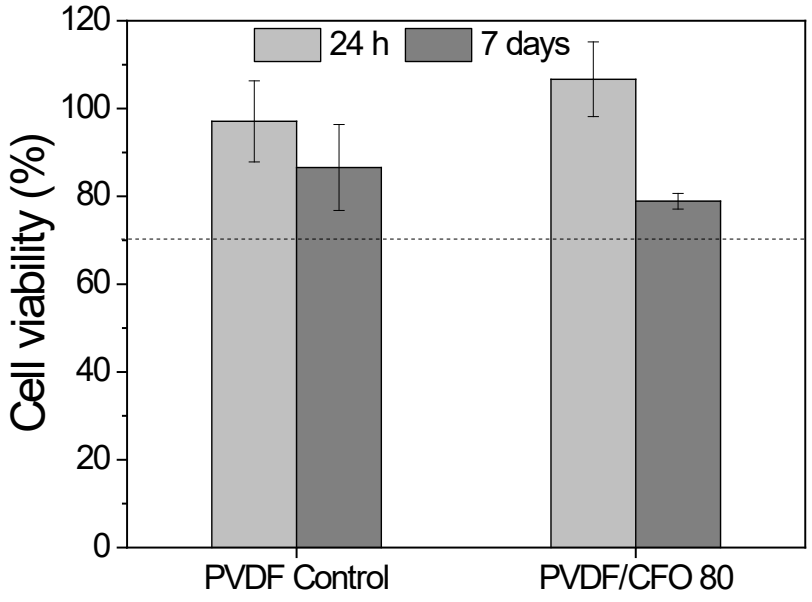

Figure 5.5 - Biocompatibility assessment through the leaching tests for determination of the toxicity of CFO NPs on the cells, by placing in contact the scaffolds with DMEM for 24 h and 7 days and measuring it with MTT assay [174].

Regarding cell culture assays under dynamic and static modes using the bioreactor, the different 3D scaffolds with a diameter of 0.8 cm were previously sterilized both sides using UV light and placed in the bottom of each well of a 24-well tissue culture polystyrene plate, whereas the MC3T3-E1 pre-osteoblast cells were seeded on each sample. Cells were seeded on the surface of the material for 30 min to enhance cell adhesion by adding $40x10^4$ cells.mL^{-1} (35 µL of Dulbecco® modified eagles minimal essential medium (DMEM) containing 15000 cells).

5.3.1.1.3 Stimuli

Two culture plates at these conditions were prepared and incubated for 24 h, after which one plate was kept stimuli-free at static conditions and the other was transferred to the magnetic bioreactor system and applying dynamic conditions such as an alternated magnetic field for up to 72 h. The

dynamic stimuli provided by the magnetic bioreactor was achieved through the following procedure: an active time of 16 h under magnetic stimuli, which is divided in intervals of 5 min active stimuli and 25 min of resting followed by a period of complete inactivity of 8 h (Figure 5.6).

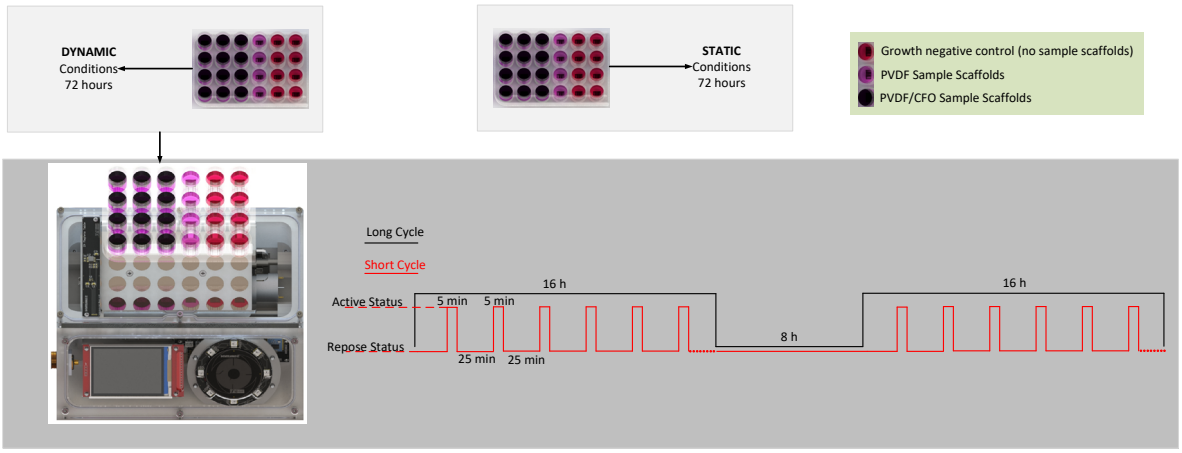

Figure 5.6 - Stimuli schedule timing programmed in the bioreactor for pre-osteoblast tissue culture assays using either static or dynamic conditions.

As previously mentioned in chapter 3, those conditions were selected in order to resemble the human body daily mechanical conditions divided by 16 h of activity and 8 h of sleep. Those short bursts of stimuli for a duration of 5 min were performed by displacing the magnetic table 25 mm at a frequency of 0.3 Hz, resulting in a magnetic field variation of up to 230 G within the culture wells. For every studied condition, three samples were assayed, and growing cells viability was determined through the MTS assay. MTS assay is a coloring method, which allow for determining cell viability of living cells similar to MTT assay. In this assay, the samples were transferred to a new 48-well plate and further incubated with a MTS solution (in a 1:5 ratio) at 37 °C and 5% CO_2. After 2 h, in order to measure cell density, 100 µL of each well were transferred to a 96-well plate and the optical density of each well was measured at 490 nm using a spectrophotometric plate reader (Biotech Synergy HT).

5.3.1.1.4 Results

The cell morphology on the top of the scaffolds was analyzed by scanning electron microscopy (SEM) using previous conditions after dehydration and fixation of the samples (Figure 5.8). For this assay, three main variables were considered: i) at static conditions, i.e. without magnetic stimulus and bearing in mind the single effect of the different morphologies related to pore size differences, ii) at dynamic conditions considering magnetic stimuli effect, and iii) the relative effect between the material morphologies and magnetic stimuli. In static conditions, larger pore sizes such as 80 and 120 µm

seems to enhance osteoblast proliferation when compared with 60 µm PVDF/CFO scaffolds (Figure 5.7).

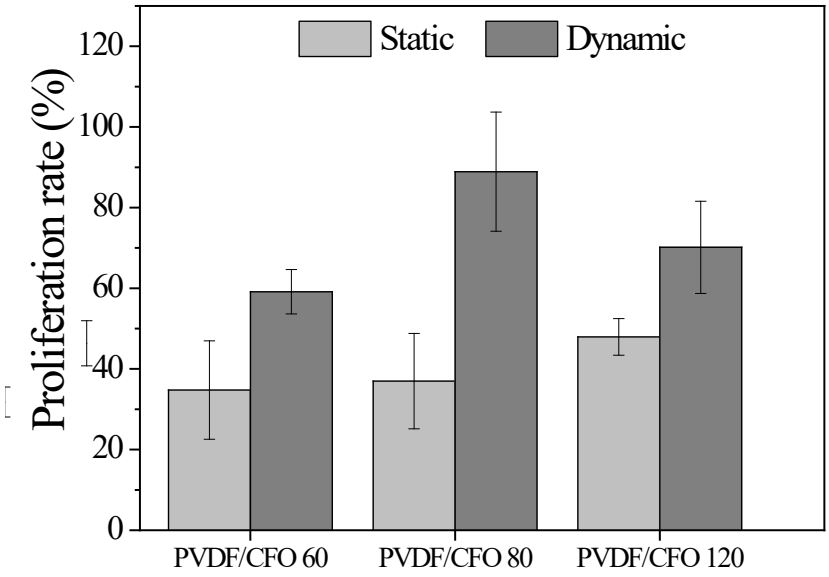

Figure 5.7 - Proliferation rate determined using MTS assay on the cells seeded on the top of the material after 4 days with and without magnetic stimuli. The proliferation rate was calculated regarding the cells growing on the material after 24 h adhesion, just before putting in contact with the bioreactor/magnetic stimuli [174].

It can be explained by the higher hydrophilicity of these materials, which improve cell adhesion and proliferation rate. Hydrophilic materials have proven to be efficient regarding nutrient transport for the cells, such as been observed in [175, 176] thus favoring proliferation and cell adhesion in the scaffold interior. However, this slight increase on proliferation rate (Figure 5.7) were not statistically significant. Nevertheless, the application of magnetic stimuli brings an unequivocal increase of proliferation rate in all samples, indicating a clear response of the scaffolds to the magnetic field, thus demonstrating that the bioreactor provides a suitable microenvironment to the pre-osteoblast cells (Figure 5.7). On all tested magneto-responsive materials, statistically significant differences of proliferation rate were observed on the growing cells. SEM images were taken at the interior and at material surface after four incubation days with and without magnetic stimuli in order to visualize the cell morphology that grow on each type of material (Figure 5.8). Thereby evaluating the tendency shown in the MTS assays presented in Figure 5.7.

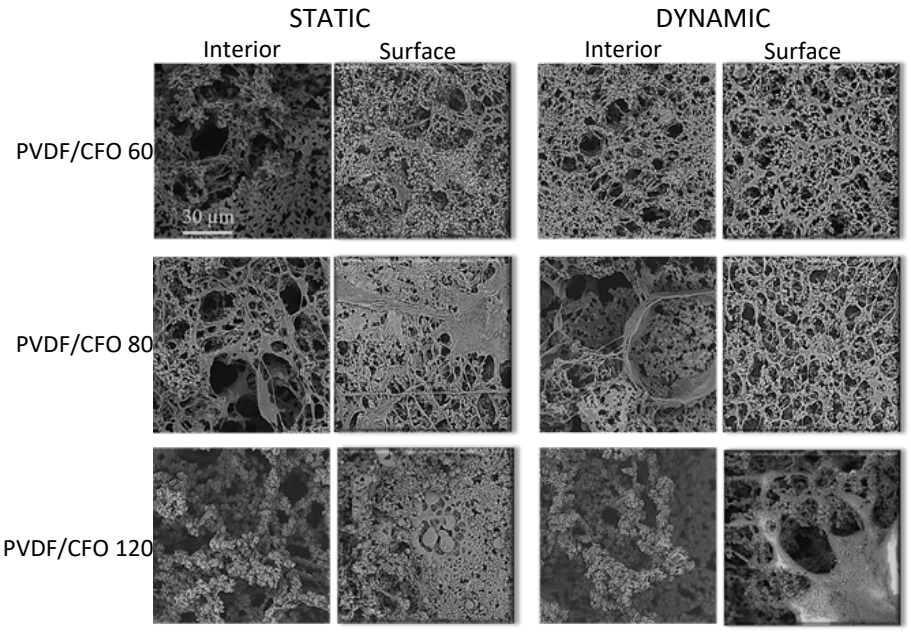

Figure 5.8 - SEM images of the surface of scaffold after culture with pre-osteoblast cells for 4 days at static and dynamic conditions, analysed at the surface and on the interior of the material. Cells within the interior of the scaffolds can be clearly observed for the samples with 80 µm pore size [174].

Regarding the effect of scaffold morphology at static conditions, it can be observed that contrary to what occurs on PVDF/CFO 80 and 120 scaffolds, on PVDF/CFO 60 the cells grow scattered on the material, while in the larger pore versions the cells colonize the materials (Figure 5.8). The results observed can be related with material morphology, where PVDF/CFO 60 present a morphology with less and smaller pore interconnections when compared with the other magneto-responsive scaffolds withstanding larger porosity. The larger pore scaffolds resemble more closely the pores found in bone (between 100 to 200 µm [177]), thus those structures are more suitable for a bone-mimicking platform which enhances cell seeding and proliferation [178]. Magnetic stimuli application has a shaping effect on cell morphology, whereas without the stimuli, cells elongate and become wider enough to cover the pores. With magnetic stimuli application, cells grow around the pores with a fair probability of being guided by the magneto-mechanical and electromagnetic stimuli, which drives them to build a well-organized spider web-like network around the pores. One effect that cannot be found in static conditions is the cell circle-shaped format interestingly developed in the interior of the PVDF/CFO 80 µm scaffold, whereas in the 120 µm template, the cells grow mainly at the surface of the material forming solid cell clusters. Static conditions exhibit the same type of clusters however, as many cells are rounded, it is an indication of cellular death and that magnetic stimulus is key for an efficient proliferation on 3D magneto-active scaffolds. This experiment is important because it provides

information about how to overcome the drawbacks of limited diffusion of metabolites, oxygen and growth factors to and out of 3D scaffolds as it has been reported in [178]. Finally, the only scaffold where cells were actually found at its interior was in the PVDF/CFO 80, relating morphology and magnetic stimuli as two key variables in order to obtain an efficient proliferation through the scaffold structure.

5.3.1.2 ME Film Scaffolds

Another cell culture was performed using the same cells type and stimuli signature but for a shorter period of 48 h instead of 72 h, but the scaffold was replaced by a ME film instead of a 3D structure with different scaffold components. Thus, magneto-active films were produced, in order to respond to magnetic stimuli, by assembling a piezoelectric polymer with magnetostrictive nanoparticles. Thereby, acting as an active material that enhance cell function improving osteoblasts adhesion and proliferation PVDF and Terfenol-D with approximately 1 μm were assembled through solvent casting method as previously reported in literature.

5.3.1.2.1 Scaffolds Construction

Therefore, nanocomposites were fabricated at concentrations of 10% PVDF and 30% of Terfenol-D nanoparticles for magnetostriction. Following an approach as in Figure 3.12, thus the Terfenol-D particles were dispersed in DMF for 2 h in an ultrasound bath in order to avoid nanoparticle agglomeration, resulting in a good dispersed solution. Followed by the addition of PVDF and Teflon mechanical stirrer until complete polymer dissolution. Then, the solution was spread in a clean glass substrate and place inside an oven at 210 °C for 10 min. After that, in order to achieve the polymer crystallization, the films were cooling down to room temperature. MC3T3-E1 pre-osteoblast cells were used for the cell proliferation assay non-poled films were used to study the effect of the mechanical stimuli in the cell proliferation and poled films to study the influence of the electromechanical stimulus. The ME films with a diameter of 1.3 cm were sterilized by UV for 1 h each side and placed in a 24-well tissue culture polystyrene plate.

5.3.1.2.2 Cells Seeding

A density of $3x10^4$ cells.mL^{-1} were seeded on each well and incubated for 24 h. After this incubation time, one plate was used for the static cell culture (without any stimulation) and the other transferred onto the bioreactor for 48 h at 37 °C in a 95% humidified air containing 5% CO_2. Then, the MTS assay was used in order to determine the cell viability. For every studied condition, three samples

were assayed, and growing cells viability was determined through a MTS assay. For this assay, three main variables were considered: i) at static conditions, i.e. without magnetic stimulus and bearing in mind the single effect of the different morphologies related to pore size differences, ii) at dynamic conditions considering magnetic stimuli effect, and iii) the relative effect between the material surface charge and magnetic stimuli.

5.3.1.2.3 Results

The application of magnetic stimuli brings an unequivocal increase of proliferation rate in all samples, indicating a clear response of the ME films to the magnetic field, thus demonstrating that the bioreactor provides a suitable microenvironment to the pre-osteoblast cells especially in positively charge Terfenol-D/PVDF film (Figure 5.9). On all tested magneto-responsive materials, statistically significant differences of proliferation rate were observed on the growing cells.

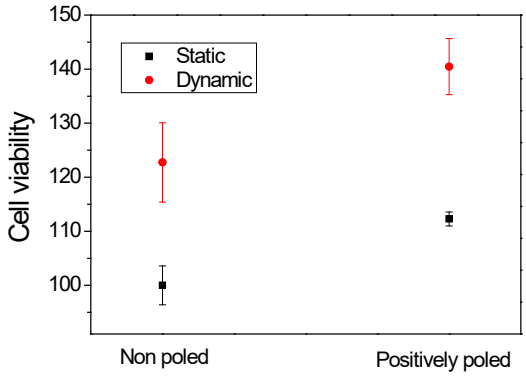

Figure 5.9 - Cell viability after 48 h of cell culture on Terfenol-D/PVDF films with and without magnetic stimuli. The cell viability was calculated regarding the cells growing on the non-poled ME film at static conditions. The non-poled scaffolds only provide magnetostriction vibration at the frequency of the magnetic field due to the lack of piezoelectric response from the PVDF layer, whereas the poled scaffolds present both mechanical and electrical response, which are applied in cell sites.

5.4 Electrostretching System Components Validation

In order to explore the use of the developed system components for stretching culture TE applications, the cytotoxicity of the components was evaluated. Although, the system main components and materials were selected to be biocompatible or at least covered by biocompatible materials such as PLA, stainless steel and gold, also all the electromechanic components inside the waterproof shell built with nylon and acrylic. Therefore, the metabolic activity of C2C12 myoblasts were evaluated through MTS assays when in contact with several system components individually in order to analyze each component and spot any possible individual contamination. The analyzed components were the PLA 3D printed clamp construct supports, stainless steel components such as screws, wires and contact holding plate, gold screw connectors and neodymium magnets plated with nickel schematized in Figure 4.9.

5.4.1 Clamps Components Cytotoxicity Analysis

Regarding those components, each one passed the MTT assays except for the gold screw connectors, which were just plated, and attaching them against the screws made small fissures, which ended up exposing the bio-incompatible inner metal and contaminating the medium and killing the grown cells. In addition, even though the permanent magnets were in the interior of the PLA construction around it, the nickel-plated components also contaminated the medium and killing the growing cells, thus revealing themselves unfit for the required task. Those issues were solved by removing the gold connectors and tie the thin stainless steel conductors directly to a dedicated contact stainless steel screw, whereas gold plated neodymium magnets removed any signs of contamination in the following trials, replacing the nickel-plated permanent magnets.

5.4.1.1 Results

Thus, LIVE/DEAD assays were performed to evaluate the effect of bioreactor components in the cell survival rate by measuring their cytotoxicity through a kit employed to probe cell viability. Propidium iodide is contained in the staining solution for staining dead cells (red color) and cell-permeable green fluorescent dye for staining living cells (green color). After the incubation time of 72 h, each sample received 30 µL of the staining solution, enabling an incubation time of 20 min at 37 °C. Later using a fluorescence microscope (Olympus BX51) the samples were observed (Figure 5.10).

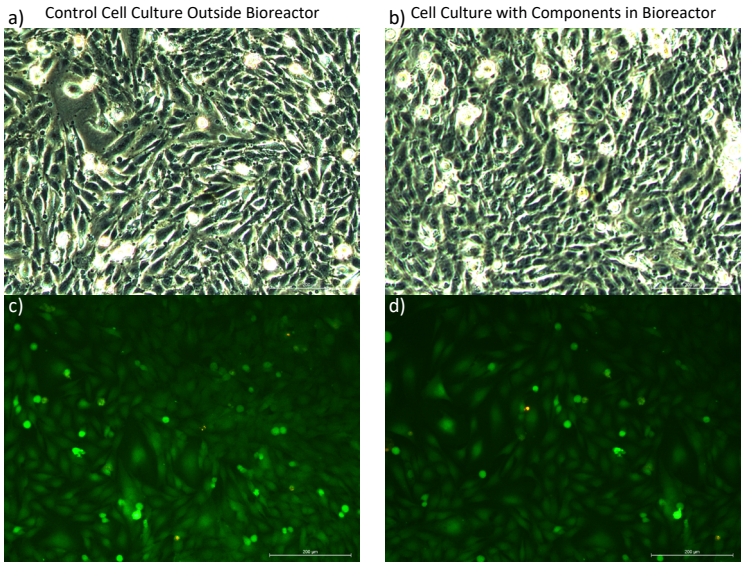

Figure 5.10 - Cell imaging on optical microscope a), b), and live and dead verification c), d) according to control cell culture and culture on bioreactor with its electro-stretching components.

Therefore, the cell viability results were compared with the control and, within a range of three replicates of the bioreactor components, the cell viability results are higher than 90% as it can be observed in the graph bar of Figure 5.11, and can be considered non-cytotoxic as it follows the ISO standard 10993-5 of higher cell viability greater than 70%. Furthermore, the use of DMSO for cellular dead viability proved to be successful providing a negative control of system biocompatibility and confirming that the results were not flawed by cell abnormal resistances due to possible mutations.

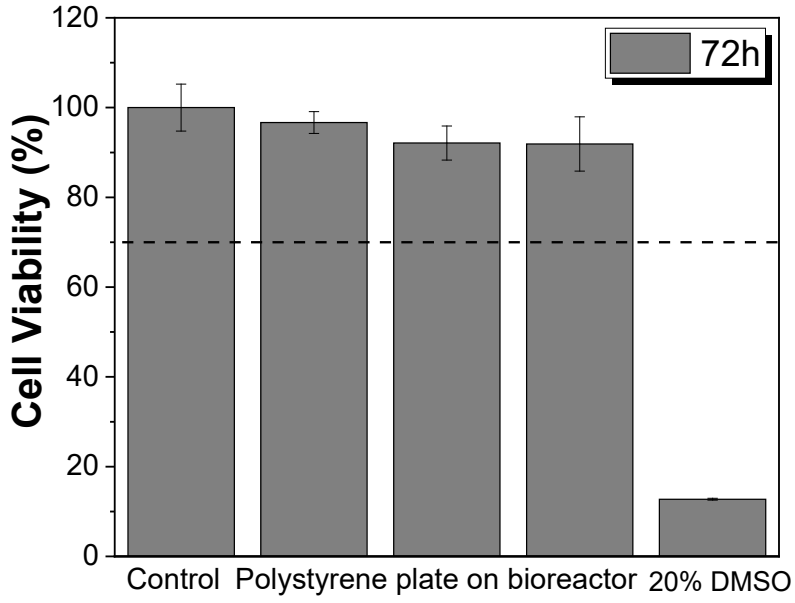

Figure 5.11 - Cell viability rate count, using control culture as reference and comparing with three more samples and negative control using DMSO.

Thereby, the electro-stretching bioreactor module allows to be used for TE cultures in future developments with this device. This component is meant to be used with fibrous scaffolds such as PVDF electrospun fibbers containing conductive fillers such as carbon nanotubes or graphene in order to provide the conductive properties the scaffold requires to apply electrical impulses to the seeded cell sites. However, film casted scaffolds filled with conductive nanoparticles can work as well for electro-stretching stimuli producing other types of tissues, which can be employed as skin grafts.

5.5 Summary

There is an ever-increasing search for more efficient strategies for many types of TE applications. Therefore, this fact is becoming a driving force in the R&D efforts to develop a new class of materials, smart materials that respond to stimuli, which triggers cellular response by an external stimulus. Thereby, the need for these materials and microenvironment stimulating devices (bioreactors) that produces such stimuli are key elements for the next developments in TE applications. During this chapter the maximum values, repeatability and precision of electromechanical components were tested, in order to set the optimal operating conditions for the bioreactor, according to each type of culture. The system offers good platform positioning conditions up to a speed of 8 mm/s, keeping the average error margin below 5%, whereas DC currents offer good stability with low variation with a maximum error rate of 3.85%. The current results can be improved with precision and more complex mechanics, in order to attenuate backlash a deliver better braking and positioning, however it only present higher error margin in the speeds over 8 mm/s, which are not so interesting for cell cultures and for what is expected of a biomimetic system. The controlled current approach controls the provided stimuli by adapting the available source voltage to the culture components electrical resistance, thus offering good cell culture protection from overcurrent peaks. However, closed loop solutions should be implemented in the future with extra low voltage leakage and superior noise attenuation system, such as a local faraday cage, the system offers good perspectives to be used for electrical stimuli TE applications.

Regarding the scaffolds and biologic experiments, they demonstrate the suitability of bioinspired magneto-responsive 3D scaffolds, as well as ME film scaffolds, for adhesion and proliferation of pre-osteoblasts, availing itself from the mechanical and electrical microenvironment conceived in the material. Although, both scaffold topology presented increased cell proliferation, the bone-like structure of the 3D porous scaffolds present the better results, beyond cell proliferation, the morphology and geometry of cell network. Thus, the macro porous structures were built for the TE experiment with three variations of porous sizes, in a process driven by PVDF crystallization in the β-phase in the presence of CFO nanoparticles. Thus, it was possible to obtain a similar morphology to the trabecular bone, possessing interconnected pores at the surface. The scaffolds containing bigger and higher amount of interconnected pores displayed hydrophilic properties, bearing as well, an

enhanced proliferation and penetration of cells within the scaffolds. The magneto-active scaffolds and respective actuation from the magnetic field were triggered by the magnetostrictive particles, inducing simultaneously a nucleation of the electroactive β-phase of the polymer and ME coupling. The β-phase content is directly related to the pore sizes, as the bigger pores present higher β-phase content, which can be associated with an effective interaction between the nanoparticle negative charges and the polymer. The better cell proliferation at static conditions (control) were found with PVDF/CFO 80 and 120, enlightening the scaffold morphology role for this purpose. Magnetic stimuli further increased cell viability on the scaffold structures, inducing solid spider web-like network of cells, which also grew inwards the PVDF/CFO 80 scaffolds. It was possible to conclude that the magnetic module of this bioreactor was able to provide an important contribute to build the proper microenvironment, whereas any material with the proper microenvironment to provide the morphology, physical environment of the tissue, mechanical and electrical cues to cells can be used synergistically with the system, outputting a complex chain of interactions.

The electro-stretching module was validated for future assays, mostly related to the invading culture components, which are required to hold the scaffolds for stretching while, simultaneously, provide the electrical contact for electrical stimuli on those same scaffolds. For the purpose, C2C12 myoblast cells were tested in contact with the materials passing the MTS assay with a cell viability over 90%, resulting in a non-cytotoxic evaluation. Thus, a biocompatible solution was achieved for all critical components of the bioreactor.

6 Conclusions

The main objective of this Ph.D. thesis was the design and fabrication of a magnetically actuated modular bioreactor suitable for biological experiments, in particular in the areas of bone and muscle TE, among others, where magnetically driven mechanical and/or electrical stimuli can be taken as advantage. TE field and operating principles for bone and muscle TE cultures were analyzed and taken into consideration before the design and development of this modular bioreactor. Thus, the required mechanisms were designed and constructed accordingly to the designed operating principles, achieving electromechanical viability through biocompatible materials, conventional mechanics and digital electronics comprehending potential for further integrability with other electronic modules that support digital communication. Tissue cultures can be performed using this system as it has been demonstrated through the toxicity tests employed in order to proof the validity of the system.

The final modular system relies in a central structure with the corresponding modular electronics, enabling to enclose different types of motor-based mechanical apparatus and operate with them. It also holds an user interface panel composed by a LCD display and side touch panel with lighting for system menu navigation behind clear acrylic, whereas, the main support includes the main processing PCB with master microprocessor, sensors connections and motor actuator connection. From the modular point of view, it was possible to achieve a modular structure to fit with the developed subsystems, both mechanically and electrically.

Those subsystems are required in the long-term research because TE support different strategies and challenges for bioengineering applications, allowing many research variations and features, demanding varying mechanisms for different stimuli mimicking cell microenvironment. Thereby, modular components, which can work in cooperation while giving room for newer devices and assemblies to be added in the long term, may be key for the next new generation of laboratory research bioreactors.

In the present work, two mechanical variations were designed and built, including a magnetic table displacement and a remote magnetic stretching mechanism that attracts magnetic clamps, which hold the scaffolds. The magnetic table offers high flexibility, enabling the possibility to exchange support for smaller permanent magnets and varying number of magnets, as well as fitting a conventional size culture plate. The stretching mechanism, works in the perpendicular axis to the previous module, and adds and decreases the distance between two lines of permanent magnets, enabling the magnetic clamps to vary their distance and thus stretch the scaffolds. Furthermore, an external electrical module, which receives commands from the master microprocessor and applies direct contact to the scaffolds clamps was designed, built and electrically tested. This system is to be used with the stretching mechanism for muscular cell cultures, as it has been shown to be beneficial in the literature. However, it may be used for other types of cells and culture conditions, as it has its own microprocessor, which enables it to produce many types of electrical signals that may prove to be useful for other biological experiments.

Regarding cell cultures, the results for the reported conditions with ME scaffolds and MC3T3-E1 pre-osteoblast cells, demonstrated the importance of ME stimuli for cellular proliferation by comparison with static conditions, which just relies in the scaffolds, medium and oxygen/carbon dioxide exchange. It was possible also, to analyze the influence that porosity plays in the cellular proliferation and colonization of the structure, resulting in a closer bone-like structure than the smaller ones. The fact that the proliferation rate more than doubled with a dynamic culture in one of the scaffolds types, and had at least 20% increase in the worst condition, bring solid prospects about the bioreactor viability for further research. Furthermore, the electro-stretching mechanism also displayed biocompatible clamps, enabling electro-stretching cell cultures.

Finally, as this project encompassed many fields of research and development, it had many steps and engineering decisions, according to the application purpose, user and biologic requirements, while needing to comply with the market supply standards of the conventional culture plates. As final remarks, it is possible concluded that: an operational system, which is able to provide controlled and scheduled stimuli in a biocompatible environment such as an incubator was achieved; smart scaffolds which provide the support and respond to magnetic stimuli bridging it to the cellular sites and shaping the magnetic field into other types of stimuli were achieved; and cellular proliferation response to dynamic cultures was significantly increased resulting in a beneficial development of the tissues being cultured.

6.1 Future Work

Even though many challenges have been successfully overcome, there is still components that lack improvement and may be enhanced in the future, although the majority are software related requiring several minor tweaks to increase precision and remote software support. Minor mechanical improvements should also be addressed. In terms of software, further development waits ahead as it has room for a better user interface regarding more features and improved touch response as well as an android app to communicate system variable readings and get remote commands. Additionally, firmware functionalities regarding variable settings for mechanics and higher flexibility in the number of time layers and respective interaction between them. Furthermore, the system lacks stimuli simulation according to start position, by using the hall sensor to read the magnetic field intensity variation, according to a reference position, during a complete cycle and drawing the respective magnetic curve. The mechanical components are already quite solid for the requirements however, the lack of system paws to absorb mechanical vibrations and noise emissions has been observed, and thus it is a small but important improvement, which will make the system more stable. Other mechanical issues rely in the stretching mechanism clamps, which are yet not user-friendly due its difficulty to get in place when every clamp is loose from each other and may tear the scaffold, thus a replacement system is required, based in a more complex robust stainless steel construction with sliding clamps with a biocompatible bearing platform.

Furthermore, as it has been explored throughout this document, especially at the second chapter, multi-stimuli synergies are usually benefic for ECM expansion and better grasp the in-vivo environment, which is being targeted to achieve as every biomimetic system such as a bioreactor. Thus, using a system such as the one developed during this thesis and by coupling it with more systems and platforms through simple setup components it is possible to create something like a magneto-perfusion bioreactor to use with 3D porous ME scaffolds to take better advantage of the perfusion. By adding detachable leakage proof chambers with channels for medium injection and ejection in different medium circuits it is possible to create the necessary accommodation for the scaffolds, while providing

medium free of cross contamination using multiple channels with multiple peristaltic pump heads. Thereby through controlled magnetic field and medium flow, it is possible to achieve a magneto-perfusion mechanism assembly, suitable for ME 3D porous scaffolds. Finally, it would be interesting to increase the range of experiences with the bioreactor with different cell types and stimuli conditions, in order access other evaluations and possibilities with this modular system.

As future perspectives, in the event of this device concept prove itself key in the development of cellular tissues or simulation of cellular conditions *in-vitro*, both mechanical concept and scaffold construction are easily expandable for higher yields. Furthermore, flexible to engineer new ways and methods of use, by adding external peripherals such as perfusion, hermetic compression chamber for magneto-compression or even a scheduled stirring container at the top of the bioreactor platform with magnetic stimuli from the bottom, among other possibilities. The use of magneto-active nanoparticles in the respective scaffold constructions triggers, this way, a growing interest to study the benefits of a magnetic field in many types of cellular cultures. Thus, the synergies between scaffolds and respective stimuli will play a leading role in the next generations of cellular growing bio-electromechanical devices.

Bibliography

1. Luo, Y., et al., *Three-Dimensional Scaffolds*, in *Principles of Tissue Engineering*. **2007**, Elsevier, 3ª edição: Amsterdam. p. p. 359–73.
2. Vacanti, C.A., *The history of tissue engineering.* Journal of cellular and molecular medicine, **2006**. 10(3): p. 569-576.
3. Howard, D., et al., *Tissue engineering: strategies, stem cells and scaffolds.* Journal of anatomy, **2008**. 213(1): p. 66-72.
4. Place, E.S., et al., *Synthetic polymer scaffolds for tissue engineering.* Chemical Society Reviews, **2009**. 38(4): p. 1139-1151.
5. Oragui, E., M. Nannaparaju, and W.S. Khan, *Suppl 2: The Role of Bioreactors in Tissue Engineering for Musculoskeletal Applications.* The open orthopaedics journal, **2011**. 5: p. 267.
6. Chung, S. and M.W. King, *Design concepts and strategies for tissue engineering scaffolds.* Biotechnology and applied biochemistry, **2011**. 58(6): p. 423-438.
7. Lutolf, M. and J. Hubbell, *Synthetic biomaterials as instructive extracellular microenvironments for morphogenesis in tissue engineering.* Nature biotechnology, **2005**. 23(1): p. 47.
8. Einhorn, T.A. and L.C. Gerstenfeld, *Fracture healing: mechanisms and interventions.* Nature Reviews Rheumatology, **2015**. 11(1): p. 45.
9. Quinlan, E., et al., *Development of collagen–hydroxyapatite scaffolds incorporating PLGA and alginate microparticles for the controlled delivery of rhBMP-2 for bone tissue engineering.* Journal of Controlled Release, **2015**. 198: p. 71-79.
10. Bacakova, L., et al., *Modulation of cell adhesion, proliferation and differentiation on materials designed for body implants.* Biotechnology advances, **2011**. 29(6): p. 739-767.
11. O'brien, F.J., *Biomaterials & scaffolds for tissue engineering.* Materials today, **2011**. 14(3): p. 88-95.
12. Tambe, D.T., et al., *Collective cell guidance by cooperative intercellular forces.* Nature Materials, **2011**. 10: p. 469.
13. Alsberg, E., et al., *Engineering growing tissues.* Proceedings of the National Academy of Sciences, **2002**. 99(19): p. 12025.
14. Abbott, A., *Biology's new dimension.* Nature, **2003**. 424(6951): p. 870-872.
15. Ribeiro, C., et al., *In vivo demonstration of the suitability of piezoelectric stimuli for bone reparation.* Materials Letters, **2017**. 209: p. 118-121.
16. Clarke, B., *Normal bone anatomy and physiology.* Clinical journal of the American Society of Nephrology : CJASN, **2008**. 3 Suppl 3(Suppl 3): p. S131-S139.
17. Ribeiro, C., et al., *Piezoelectric polymers as biomaterials for tissue engineering applications.* Colloids and Surfaces B: Biointerfaces, **2015**. 136: p. 46-55.
18. Ribeiro, C., et al., *Piezoelectric poly(vinylidene fluoride) microstructure and poling state in active tissue engineering.* Engineering in Life Sciences, **2015**. 15(4): p. 351-356.
19. Ribeiro, S., et al., *Electroactive biomaterial surface engineering effects on muscle cells differentiation.* Materials Science and Engineering C, **2018**. 92: p. 868-874.
20. Trumbull, A., G. Subramanian, and E. Yildirim-Ayan, *Mechanoresponsive musculoskeletal tissue differentiation of adipose-derived stem cells.* BioMedical Engineering Online, **2016**. 15(1).

21. Bukoreshtliev, N.V., K. Haase, and A.E. Pelling, *Mechanical cues in cellular signalling and communication.* Cell and Tissue Research, **2013**. 352(1): p. 77-94.
22. Tian, L., M.P. Prabhakaran, and S. Ramakrishna, *Strategies for regeneration of components of nervous system: scaffolds, cells and biomolecules.* Regenerative biomaterials, **2015**. 2(1): p. 31-45.
23. Simitzi, C., A. Ranella, and E. Stratakis, *Controlling the morphology and outgrowth of nerve and neuroglial cells: The effect of surface topography.* Acta Biomaterialia, **2017**. 51: p. 21-52.
24. Lee, Y.S. and T.L. Arinzeh, *The influence of piezoelectric scaffolds on neural differentiation of human neural stem/progenitor cells.* Tissue Engineering - Part A, **2012**. 18(19-20): p. 2063-2072.
25. Gaspar, D.A., V. Gomide, and F.J. Monteiro, *The role of perfusion bioreactors in bone tissue engineering.* Biomatter, **2012**. 2(4): p. 167-175.
26. Ahmed, S., et al., *New generation of bioreactors that advance extracellular matrix modelling and tissue engineering.* Biotechnology letters, **2018**: p. 1-25.
27. Zhao, J., et al., *Bioreactors for tissue engineering: An update.* Biochemical engineering journal, **2016**. 109: p. 268-281.
28. Selden, C. and B. Fuller, *Role of bioreactor technology in tissue engineering for clinical use and therapeutic target design.* Bioengineering, **2018**. 5(2): p. 32.
29. Pina, S., J.M. Oliveira, and R.L. Reis, *Natural-based nanocomposites for bone tissue engineering and regenerative medicine: A review.* Advanced Materials, **2015**. 27(7): p. 1143-1169.
30. Venkatesan, J., et al., *Alginate composites for bone tissue engineering: a review.* International journal of biological macromolecules, **2015**. 72: p. 269-281.
31. Simske, S.J., R.A. Ayers, and T. Bateman. *Porous materials for bone engineering*. in *Materials Science Forum*. **1997**. Trans Tech Publ.
32. Gomes, M.E., et al., *A new approach based on injection moulding to produce biodegradable starch-based polymeric scaffolds: morphology, mechanical and degradation behaviour.* Biomaterials, **2001**. 22(9): p. 883-889.
33. Pham, Q.P., U. Sharma, and A.G. Mikos, *Electrospinning of polymeric nanofibers for tissue engineering applications: a review.* Tissue engineering, **2006**. 12(5): p. 1197-1211.
34. Fukada, E. and I. Yasuda, *On the piezoelectric effect of bone.* Journal of the physical society of Japan, **1957**. 12(10): p. 1158-1162.
35. Guduru, R. and S. Khizroev, *Magnetic field-controlled release of paclitaxel drug from functionalized magnetoelectric nanoparticles.* Particle & Particle Systems Characterization, **2014**. 31(5): p. 605-611.
36. Lodi, M.B., A. Fanti, and S. Casu. *Analysis of superparamagnetic scaffolds: For bone tissue engineering in static magnetic and dynamic fields*. in *2016 Loughborough Antennas & Propagation Conference (LAPC)*. **2016**. IEEE.
37. Evans, D., et al., *Magnetic switching of ferroelectric domains at room temperature in multiferroic PZTFT.* Nature communications, **2013**. 4: p. 1534.
38. Gonçalves, R., et al., *Development of magnetoelectric $CoFe_2O_4$/poly (vinylidene fluoride) microspheres.* Rsc Advances, **2015**. 5(45): p. 35852-35857.
39. Li, Y., et al., *Magnetoelectric quasi-(0-3) nanocomposite heterostructures.* Nature communications, **2015**. 6: p. 6680.
40. Martins, P. and S. Lanceros-Méndez, *Polymer-based magnetoelectric materials.* Advanced Functional Materials, **2013**. 23(27): p. 3371-3385.

41. Mistry, A.S. and A.G. Mikos, *Tissue engineering strategies for bone regeneration*, in *Regenerative medicine II*. **2005**, Springer. p. 1-22.
42. Lee, E.A., et al., *Application of magnetic nanoparticle for controlled tissue assembly and tissue engineering.* Archives of pharmacal research, **2014**. 37(1): p. 120-128.
43. Xia, Y., et al., *Novel magnetic calcium phosphate-stem cell construct with magnetic field enhances osteogenic differentiation and bone tissue engineering.* Materials Science and Engineering: C, **2019**. 98: p. 30-41.
44. Yamamoto, Y., et al., *Hollow fiber bioreactor perfusion culture system for magnetic force-based skeletal muscle tissue engineering.* Journal of chemical engineering of Japan, **2012**. 45(5): p. 348-354.
45. El Haj, A.J.H. and J.P. Dobson, *Culturing tissue using magnetically generated mechanical stresses*. **2009**, Keele University, United Kingdom: United States.
46. Hernández-Hernández, H., et al., *Neurite outgrowth on chromaffin cells applying extremely low frequency magnetic fields by permanent magnets.* Archives of medical research, **2009**. 40(7): p. 545-550.
47. Freed, L.E., et al., *Advanced tools for tissue engineering: scaffolds, bioreactors, and signaling.* Tissue engineering, **2006**. 12(12): p. 3285-3305.
48. Ramos, G.A. and J.M. Hare, *Cardiac cell-based therapy: cell types and mechanisms of actions.* Cell transplantation, **2007**. 16(9): p. 951-961.
49. Fernandes, S., et al., *Autologous myoblast transplantation after myocardial infarction increases the inducibility of ventricular arrhythmias.* Cardiovascular research, **2006**. 69(2): p. 348-358.
50. Fouts, K., et al., *Electrophysiological consequence of skeletal myoblast transplantation in normal and infarcted canine myocardium.* Heart Rhythm, **2006**. 3(4): p. 452-461.
51. Kondoh, H., et al., *Longer preservation of cardiac performance by sheet-shaped myoblast implantation in dilated cardiomyopathic hamsters.* Cardiovascular research, **2006**. 69(2): p. 466-475.
52. Sbrana, F., et al., *Role for stress fiber contraction in surface tension development and stretch-activated channel regulation in C2C12 myoblasts.* American Journal of Physiology-Cell Physiology, **2008**. 295(1): p. C160-C172.
53. Siepe, M., et al., *Construction of skeletal myoblast-based polyurethane scaffolds for myocardial repair.* Artificial organs, **2007**. 31(6): p. 425-433.
54. Formigli, L., et al., *Cytoskeleton/stretch-activated ion channel interaction regulates myogenic differentiation of skeletal myoblasts.* Journal of cellular physiology, **2007**. 211(2): p. 296-306.
55. Woo, J.S., P.D. Allen, and E.H. Lee, *TRPC3-interacting triadic proteins in skeletal muscle.* Biochemical Journal, **2008**. 411(2): p. 399-405.
56. Huang, Y.-C., et al., *Rapid formation of functional muscle in vitro using fibrin gels.* Journal of Applied Physiology, **2005**. 98(2): p. 706-713.
57. Powell, C.A., et al., *Mechanical stimulation improves tissue-engineered human skeletal muscle.* American Journal of Physiology-Cell Physiology, **2002**. 283(5): p. C1557-C1565.
58. Rhim, C., et al., *Morphology and ultrastructure of differentiating three-dimensional mammalian skeletal muscle in a collagen gel.* Muscle & Nerve: Official Journal of the American Association of Electrodiagnostic Medicine, **2007**. 36(1): p. 71-80.
59. Huang, N.F., et al., *Myotube assembly on nanofibrous and micropatterned polymers.* Nano letters, **2006**. 6(3): p. 537-542.

60. Lam, M.T., et al., *The effect of continuous wavy micropatterns on silicone substrates on the alignment of skeletal muscle myoblasts and myotubes.* Biomaterials, **2006**. 27(24): p. 4340-4347.
61. Neumann, T., S.D. Hauschka, and J.E. Sanders, *Tissue engineering of skeletal muscle using polymer fiber arrays.* Tissue engineering, **2003**. 9(5): p. 995-1003.
62. Birla, R.K., Y. Huang, and R. Dennis, *Development of a novel bioreactor for the mechanical loading of tissue-engineered heart muscle.* Tissue engineering, **2007**. 13(9): p. 2239-2248.
63. Silvani, G., et al. *Cyclic mechanical cells stimulation of myoblasts in skeletal muscle tissue engineering: a preliminary study*. in *World Congress on Medical Physics and Biomedical Engineering, September 7-12, 2009, Munich, Germany*. **2009**. Springer.
64. Scott, J.B., et al., *Achieving acetylcholine receptor clustering in tissue-engineered skeletal muscle constructs in vitro through a materials-directed agrin delivery approach.* Frontiers in pharmacology, **2017**. 7: p. 508.
65. Saber, S., et al., *Flexor tendon tissue engineering: bioreactor cyclic strain increases construct strength.* Tissue Engineering Part A, **2010**. 16(6): p. 2085-2090.
66. Liu, C., et al., *Influence of perfusion and compression on the proliferation and differentiation of bone mesenchymal stromal cells seeded on polyurethane scaffolds.* Biomaterials, **2012**. 33(4): p. 1052-1064.
67. Bilgen, B., et al., *Design of a biaxial mechanical loading bioreactor for tissue engineering.* Journal of visualized experiments: JoVE, **2013**(74).
68. Correia, V., et al., *Design and validation of a biomechanical bioreactor for cartilage tissue culture.* Biomechanics and modeling in mechanobiology, **2016**. 15(2): p. 471-478.
69. Huang, C.Y.C., et al., *Effects of cyclic compressive loading on chondrogenesis of rabbit bone-marrow derived mesenchymal stem cells.* Stem cells, **2004**. 22(3): p. 313-323.
70. Hammerick, K.E., M.T. Longaker, and F.B. Prinz, *In vitro effects of direct current electric fields on adipose-derived stromal cells.* Biochemical and biophysical research communications, **2010**. 397(1): p. 12-17.
71. Balint, R., N.J. Cassidy, and S.H. Cartmell, *Electrical stimulation: a novel tool for tissue engineering.* Tissue Engineering Part B: Reviews, **2012**. 19(1): p. 48-57.
72. Serena, E., et al., *Electrical stimulation of human embryonic stem cells: cardiac differentiation and the generation of reactive oxygen species.* Experimental cell research, **2009**. 315(20): p. 3611-3619.
73. Chan, Y.-C., et al., *Electrical stimulation promotes maturation of cardiomyocytes derived from human embryonic stem cells.* Journal of cardiovascular translational research, **2013**. 6(6): p. 989-999.
74. Liao, I.-C., et al., *Effect of electromechanical stimulation on the maturation of myotubes on aligned electrospun fibers.* Cellular and molecular bioengineering, **2008**. 1(2-3): p. 133-145.
75. Pisani, G., et al., *An electro-mechanical bioreactor providing physiological cardiac stimuli*, in *Summer Workshop on Mechanics in Biology*. **2013**: Berlin.
76. Llucià-Valldeperas, A., et al., *Electromechanical conditioning of adult progenitor cells improves recovery of cardiac function after myocardial infarction.* Stem cells translational medicine, **2017**. 6(3): p. 970-981.
77. Rauh, J., et al., *Bioreactor systems for bone tissue engineering.* Tissue Engineering Part B: Reviews, **2011**. 17(4): p. 263-280.
78. Carvalho, L.S., et al., *Production Processes for Monoclonal Antibodies*, in *Fermentation Processes*. **2017**, IntechOpen.
79. Mygind, T., et al., *Mesenchymal stem cell ingrowth and differentiation on coralline hydroxyapatite scaffolds.* Biomaterials, **2007**. 28(6): p. 1036-1047.

80. Yoon, H.H., et al., *Enhanced cartilage formation via three-dimensional cell engineering of human adipose-derived stem cells.* Tissue Engineering Part A, **2012**. 18(19-20): p. 1949-1956.
81. Plunkett, N. and F.J. O'Brien, *Bioreactors in tissue engineering.* Technology and Health Care, **2011**. 19(1): p. 55-69.
82. Vunjak-Novakovic, G., et al., *Effects of mixing on the composition and morphology of tissue-engineered cartilage.* AIChE Journal, **1996**. 42(3): p. 850-860.
83. Bayley, R., et al., *The productivity limit of manufacturing blood cell therapy in scalable stirred bioreactors.* Journal of tissue engineering and regenerative medicine, **2018**. 12(1): p. e368-e378.
84. Rodrigues, C.A., et al., *Stem cell cultivation in bioreactors.* Biotechnology advances, **2011**. 29(6): p. 815-829.
85. Sart, S. and S.N. Agathos, *Large-scale expansion and differentiation of mesenchymal stem cells in microcarrier-based stirred bioreactors*, in *Bioreactors in Stem Cell Biology*. **2015**, Springer. p. 87-102.
86. del Carmen Oliver-Salvador, M., et al., *Shear rate and microturbulence effects on the synthesis of proteases by Jacaratia mexicana cells cultured in a bubble column, airlift, and stirred tank bioreactors.* Biotechnology and bioprocess engineering, **2013**. 18(4): p. 808-818.
87. Asenjo, J.A., *Bioreactor system design*. **1994**: CRC Press.
88. Eibl, R. and D. Eibl, *Design and use of the wave bioreactor for plant cell culture*, in *Plan tissue culture engineering*. **2008**, Springer. p. 203-227.
89. Esperança, M., et al., *Gas hold-up and oxygen mass transfer in three pneumatic bioreactors operating with sugarcane bagasse suspensions.* Bioprocess and biosystems engineering, **2014**. 37(5): p. 805-812.
90. Schwarz, R.P., T.J. Goodwin, and D.A. Wolf, *Cell culture for three-dimensional modeling in rotating-wall vessels: an application of simulated microgravity.* Methods in Cell Science, **1992**. 14(2): p. 51-57.
91. Martin, I., D. Wendt, and M. Heberer, *The role of bioreactors in tissue engineering.* TRENDS in Biotechnology, **2004**. 22(2): p. 80-86.
92. Akmal, M., et al., *The culture of articular chondrocytes in hydrogel constructs within a bioreactor enhances cell proliferation and matrix synthesis.* The Journal of bone and joint surgery. British volume, **2006**. 88(4): p. 544-553.
93. Takebe, T., et al. *Human elastic cartilage engineering from cartilage progenitor cells using rotating wall vessel bioreactor*. in *Transplantation proceedings*. **2012**. Elsevier.
94. Yu, X., et al., *Bioreactor-based bone tissue engineering: the influence of dynamic flow on osteoblast phenotypic expression and matrix mineralization.* Proceedings of the National Academy of Sciences, **2004**. 101(31): p. 11203-11208.
95. Singh, V., *Disposable bioreactor for cell culture using wave-induced agitation.* Cytotechnology, **1999**. 30(1-3): p. 149-158.
96. Åkerström, H., *Expansion of adherent cells for cell therapy*, in *Biology Education Centre, GE Healthcare Department of Cell Technologies*. **2009**, Uppsala University. p. 31.
97. Timmins, N., et al., *Closed system isolation and scalable expansion of human placental mesenchymal stem cells.* Biotechnology and bioengineering, **2012**. 109(7): p. 1817-1826.
98. Thomasi, S.S., M.O. Cerri, and A.C. Badino, *Average shear rate in three pneumatic bioreactors.* Bioprocess and biosystems engineering, **2010**. 33(8): p. 979-988.
99. Birru, B., N.K. Mekala, and S.R. Parcha, *Mechanistic role of perfusion culture on bone regeneration.* Journal of biosciences, **2019**. 44(1): p. 23.
100. Carrier, R.L., et al., *Perfusion improves tissue architecture of engineered cardiac muscle.* Tissue engineering, **2002**. 8(2): p. 175-188.

101. Grayson, W.L., et al., *Effects of initial seeding density and fluid perfusion rate on formation of tissue-engineered bone.* Tissue Engineering Part A, **2008**. 14(11): p. 1809-1820.
102. Santoro, R., et al., *Bioreactor based engineering of large-scale human cartilage grafts for joint resurfacing.* Biomaterials, **2010**. 31(34): p. 8946-8952.
103. Shahin, K. and P.M. Doran, *Strategies for enhancing the accumulation and retention of extracellular matrix in tissue-engineered cartilage cultured in bioreactors.* PloS one, **2011**. 6(8): p. e23119.
104. Lee, P.-Y., et al., *Fibroblast-seeded collagen gels in response to dynamic equibiaxial mechanical stimuli: A biomechanical study.* Journal of biomechanics, **2018**. 78: p. 134-142.
105. Huang, C., et al., *Effects of cyclic compressive loading on chondrogenesis of rabbit bone-marrow derived mesenchymal stem cells.* Stem cells, **2004**. 22(3): p. 313-323.
106. Feng, Z., et al., *An electro-tensile bioreactor for 3-D culturing of cardiomyocytes.* IEEE engineering in medicine and biology magazine, **2005**. 24(4): p. 73-79.
107. Darling, E.M. and K.A. Athanasiou, *Articular cartilage bioreactors and bioprocesses.* Tissue engineering, **2003**. 9(1): p. 9-26.
108. Ribeiro, C., et al., *Proving the suitability of magnetoelectric stimuli for tissue engineering applications.* Colloids and Surfaces B: Biointerfaces, **2016**. 140: p. 430-436.
109. Visiongain. *Global Bioreactors market set to grow to $1.6bn by 2024*. **2019** [cited 2019 4 September]; Available from: https://www.visiongain.com/global-bioreactors-market-set-to-grow-to-1-6bn-by-2024-says-new-visiongain-report-2/.
110. ReportLinker. *Top 50 Bioreactor Manufacturers 2019*. **2019** [cited 2019 3 September]; Available from: https://www.reportlinker.com/p05781245/Top-50-Bioreactor-Manufacturers.html?utm_source=PRN.
111. centrs, J.B. *All Bioreactor Manufacturers*. **2019** [cited 2019 3 September]; Available from: http://bioreactors.net/all-bioreactor-manufacturers/.
112. Flexcell. *FX-6000T™ Tension System*. **2018** [cited 2018 12 June]; Available from: https://www.flexcellint.com/product/fx6000t.
113. Flexcell. *Compression System*. **2018** [cited 2018 12 June]; Available from: https://www.flexcellint.com/category/compression.
114. Flexcell. *Streamer*. **2018** [cited 2018 12 June]; Available from: https://www.flexcellint.com/product/streamer.
115. Medical, E. *TC-3F bioreactor*. **2018** [cited 2018 20 June]; Available from: http://ebersmedical.com/tissue-engineering/bioreactors/load-culture/tc-3f-bioreactor.
116. Instruments, T. *BioDynamic 5200*. **2018** [cited 2018 14 May]; Available from: https://www.tainstruments.com/5200-products/.
117. Multimix, S. *Bioreactors*. **2018** [cited 2018 22 July]; Available from: https://www.satake.co.jp/en/product/cultivate/.
118. Cellscale. *Mechanical test systems*. **2018** [cited 2018 28 July]; Available from: https://cellscale.com/.
119. Shangkai, C., et al., *Transplantation of allogeneic chondrocytes cultured in fibroin sponge and stirring chamber to promote cartilage regeneration.* Tissue engineering, **2007**. 13(3): p. 483-492.
120. Liu, L., et al., *Novel strategy to engineer trachea cartilage graft with marrow mesenchymal stem cell macroaggregate and hydrolyzable scaffold.* Artificial organs, **2010**. 34(5): p. 426-433.
121. Vunjak-Novakovic, G., et al., *Dynamic cell seeding of polymer scaffolds for cartilage tissue engineering.* Biotechnology progress, **1998**. 14(2): p. 193-202.

122. García Cruz, D.M., M. Salmerón-Sánchez, and J.L. Gómez-Ribelles, *Stirred flow bioreactor modulates chondrocyte growth and extracellular matrix biosynthesis in chitosan scaffolds.* Journal of Biomedical Materials Research Part A, **2012**. 100(9): p. 2330-2341.
123. Song, K.-d., et al., *Three-dimensional expansion: in suspension culture of SD rat's osteoblasts in a rotating wall vessel bioreactor.* Biomedical and Environmental Sciences, **2007**. 20(2): p. 91.
124. Lei, X.-h., et al., *NASA-approved rotary bioreactor enhances proliferation of human epidermal stem cells and supports formation of 3D epidermis-like structure.* PloS one, **2011**. 6(11): p. e26603.
125. Wendt, D., et al., *Oscillating perfusion of cell suspensions through three-dimensional scaffolds enhances cell seeding efficiency and uniformity.* Biotechnology and bioengineering, **2003**. 84(2): p. 205-214.
126. Mizuno, S., F. Allemann, and J. Glowacki, *Effects of medium perfusion on matrix production by bovine chondrocytes in three-dimensional collagen sponges.* Journal of Biomedical Materials Research: An Official Journal of The Society for Biomaterials, The Japanese Society for Biomaterials, and The Australian Society for Biomaterials and the Korean Society for Biomaterials, **2001**. 56(3): p. 368-375.
127. Song, L., et al., *Successful development of small diameter tissue-engineering vascular vessels by our novel integrally designed pulsatile perfusion-based bioreactor.* PloS one, **2012**. 7(8): p. e42569.
128. Aleksieva, G., et al., *Use of a special bioreactor for the cultivation of a new flexible polyurethane scaffold for aortic valve tissue engineering.* Biomedical engineering online, **2012**. 11(1): p. 92.
129. Candiani, G., et al., *Chondrocyte response to high regimens of cyclic hydrostatic pressure in 3-dimensional engineered constructs.* The International journal of artificial organs, **2008**. 31(6): p. 490-499.
130. Correia, C., et al., *Dynamic culturing of cartilage tissue: the significance of hydrostatic pressure.* Tissue Engineering Part A, **2012**. 18(19-20): p. 1979-1991.
131. Lammi, M.J., et al., *Expression of reduced amounts of structurally altered aggrecan in articular cartilage chondrocytes exposed to high hydrostatic pressure.* Biochemical Journal, **1994**. 304(3): p. 723-730.
132. Parkkinen, J., et al., *Effects of cyclic hydrostatic pressure on proteoglycan synthesis in cultured chondrocytes and articular cartilage explants.* Archives of biochemistry and biophysics, **1993**. 300(1): p. 458-465.
133. Toyoda, T., et al., *Hydrostatic pressure modulates proteoglycan metabolism in chondrocytes seeded in agarose.* Arthritis & Rheumatism, **2003**. 48(10): p. 2865-2872.
134. Mauck, R.L., et al., *Functional tissue engineering of articular cartilage through dynamic loading of chondrocyte-seeded agarose gels.* Journal of biomechanical engineering, **2000**. 122(3): p. 252-260.
135. Wang, P.Y., et al., *Dynamic compression modulates chondrocyte proliferation and matrix biosynthesis in chitosan/gelatin scaffolds.* Journal of Biomedical Materials Research Part B: Applied Biomaterials, **2009**. 91(1): p. 143-152.
136. Wang, P.-Y. and W.-B. Tsai, *Modulation of the proliferation and matrix synthesis of chondrocytes by dynamic compression on genipin-crosslinked chitosan/collagen scaffolds.* Journal of Biomaterials Science, Polymer Edition, **2013**. 24(5): p. 507-519.
137. Altman, G., et al., *Cell differentiation by mechanical stress.* The FASEB Journal, **2002**. 16(2): p. 270-272.

138. Ladd, M.R., et al., *Bioreactor maintained living skin matrix.* Tissue Engineering Part a, **2008**. 15(4): p. 861-868.
139. Hülsmann, J., et al., *The impact of left ventricular stretching in model cultivations with neonatal cardiomyocytes in a whole-heart bioreactor.* Biotechnology and bioengineering, **2017**. 114(5): p. 1107-1117.
140. Hülsmann, J., et al., *A novel customizable modular bioreactor system for whole-heart cultivation under controlled 3D biomechanical stimulation.* Journal of Artificial Organs, **2013**. 16(3): p. 294-304.
141. Hu, J.-J., et al., *Development of fibroblast-seeded collagen gels under planar biaxial mechanical constraints: a biomechanical study.* Biomechanics and modeling in mechanobiology, **2013**. 12(5): p. 849-868.
142. Zhuang, H., et al., *Electrical stimulation induces the level of TGF-β1 mRNA in osteoblastic cells by a mechanism involving calcium/calmodulin pathway.* Biochemical and biophysical research communications, **1997**. 237(2): p. 225-229.
143. Brighton, C.T., et al., *In vitro bone-cell response to a capacitively coupled electrical field. The role of field strength, pulse pattern, and duty cycle.* Clinical orthopaedics and related research, **1992**(285): p. 255-262.
144. Tandon, N., et al. *Portable bioreactor for perfusion and electrical stimulation of engineered cardiac tissue*. in *2013 35th Annual International Conference of the IEEE Engineering in Medicine and Biology Society (EMBC)*. **2013**. IEEE.
145. Ghasemi-Mobarakeh, L., et al., *Electrical stimulation of nerve cells using conductive nanofibrous scaffolds for nerve tissue engineering.* Tissue Engineering Part A, **2009**. 15(11): p. 3605-3619.
146. Stewart, E., et al., *Electrical stimulation using conductive polymer polypyrrole promotes differentiation of human neural stem cells: a biocompatible platform for translational neural tissue engineering.* Tissue Engineering Part C: Methods, **2014**. 21(4): p. 385-393.
147. Wang, B., et al., *Myocardial scaffold-based cardiac tissue engineering: application of coordinated mechanical and electrical stimulations.* Langmuir, **2013**. 29(35): p. 11109-11117.
148. Schmidt, J.B. and R.T. Tranquillo, *Cyclic stretch and perfusion bioreactor for conditioning large diameter engineered tissue tubes.* Annals of biomedical engineering, **2016**. 44(5): p. 1785-1797.
149. Hansmann, J., et al., *Bioreactors in tissue engineering—principles, applications and commercial constraints.* Biotechnology journal, **2013**. 8(3): p. 298-307.
150. Viens, M., G. Chauvette, and E. Langelier, *A roadmap for the design of bioreactors in mechanobiological research and engineering of load-bearing tissues.* Journal of Medical Devices, **2011**. 5(4): p. 041006.
151. Lei, Y. and Z. Ferdous, *Design considerations and challenges for mechanical stretch bioreactors in tissue engineering.* Biotechnology progress, **2016**. 32(3): p. 543-553.
152. Martins, P., A. Lopes, and S. Lanceros-Mendez, *Electroactive phases of poly (vinylidene fluoride): determination, processing and applications.* Progress in polymer science, **2014**. 39(4): p. 683-706.
153. Zhai, J., et al., *Magnetoelectric laminate composites: an overview.* Journal of the American Ceramic Society, **2008**. 91(2): p. 351-358.
154. Silva, M., et al., *Optimization of the magnetoelectric response of poly (vinylidene fluoride)/epoxy/vitrovac laminates.* ACS applied materials & interfaces, **2013**. 5(21): p. 10912-10919.

155. Jin, J., et al., *Multiferroic polymer composites with greatly enhanced magnetoelectric effect under a low magnetic bias.* Advanced Materials, **2011**. 23(33): p. 3853-3858.
156. Guru, B.S. and H.R. Hiziroglu, *Electromagnetic field theory fundamentals*. **2009**: Cambridge university press.
157. Camacho, J. and V. Sosa, *Alternative method to calculate the magnetic field of permanent magnets with azimuthal symmetry.* Revista mexicana de física E, **2013**. 59(1): p. 8-17.
158. Supermagnete. *Physical Magnet Data*. **2013** [cited 2018 10 March]; Available from: https://www.supermagnete.de/eng/physical-magnet-data.
159. Martins, P., et al., *Optimizing piezoelectric and magnetoelectric responses on $CoFe_2O_4$/P (VDF-TrFE) nanocomposites.* Journal of Physics D: Applied Physics, **2011**. 44(49): p. 495303.
160. Ribeiro, S., et al., *Multifunctional Platform Based on Electroactive Polymers and Silica Nanoparticles for Tissue Engineering Applications.* Nanomaterials, **2018**. 8(11): p. 933.
161. Martins, P., et al., *Effect of poling state and morphology of piezoelectric poly (vinylidene fluoride) membranes for skeletal muscle tissue engineering.* Rsc Advances, **2013**. 3(39): p. 17938-17944.
162. Ribeiro, C., et al., *Influence of processing conditions on polymorphism and nanofiber morphology of electroactive poly (vinylidene fluoride) electrospun membranes.* Soft Materials, **2010**. 8(3): p. 274-287.
163. Correia, D.M., et al., *Strategies for the development of three dimensional scaffolds from piezoelectric poly (vinylidene fluoride).* Materials & Design, **2016**. 92: p. 674-681.
164. Community, W. *Data Acquisition*. **2019** [cited 2019 3 October]; Available from: https://en.wikipedia.org/wiki/Data_acquisition.
165. Alves, B.M.P., *E-book para controlo digital: teoria, matemática, modelos e simulações*. **2011**.
166. X-Engineer. *On-off control system*. **2019** [cited 2019 5 May]; Available from: https://x-engineer.org/graduate-engineering/signals-systems/control-systems/on-off-control-system/.
167. Ogunnaike, B.A. and W.H. Ray, *Process dynamics, modeling, and control*. Vol. 1. **1994**: Oxford University Press New York.
168. Instruments, N. *PID Theory Explained*. **2011** [cited 2017 5 February]; Available from: https://www.ni.com/en-ie/innovations/white-papers/06/pid-theory-explained.html.
169. Instruments, T. *Datasheet - DRV8872 3.6-A Brushed DC Motor Driver With Fault Reporting (PWM Control)*. **2016** [cited 2017 29 November]; Available from: http://www.ti.com/lit/ds/symlink/drv8872.pdf.
170. Instruments, T. *Datasheet - LMT85 1.8-V, SC70/TO-92/TO-92S, Analog Temperature Sensors*. **2017** [cited 2017 10 December]; Available from: http://www.ti.com/lit/ds/symlink/lmt85.pdf.
171. Analog Devices, I., *Versatile High Precision Programmable Current Sources Using DACs, Op Amps, and MOSFET Transistors*. **2010**, Analog Devices, Inc.: Application Note. p. 3.
172. Zumbahlen, H., *Staying Well Grounded.* Analog Dialogue, **2012**. 46(2): p. 17.
173. Ribeiro, C., et al., *Electroactive poly (vinylidene fluoride)-based structures for advanced applications.* Nature protocols, **2018**. 13(4): p. 681.
174. Fernandes, M., et al., *Bioinspired three-dimensional magneto-active scaffolds for bone tissue engineering.* ACS applied materials & interfaces, **2019**.
175. Webb, K., V. Hlady, and P.A. Tresco, *Relative importance of surface wettability and charged functional groups on NIH 3T3 fibroblast attachment, spreading, and cytoskeletal organization.* Journal of Biomedical Materials Research: An Official Journal of The Society for Biomaterials, The Japanese Society for Biomaterials, and the Australian Society for Biomaterials, **1998**. 41(3): p. 422-430.

176. Chang, H.-I. and Y. Wang, *Cell responses to surface and architecture of tissue engineering scaffolds*, in *Regenerative medicine and tissue engineering-cells and biomaterials*. **2011**, InTechOpen.
177. Doktor, T., et al., *Pore size distribution of human trabecular bone: Comparison of intrusion measurements with image analysis.* Engineering Mechanics, **2011**.
178. McHale, M.K., N.M. Bergmann, and J.L. West, *Histogenesis in Three-Dimensional Scaffolds*, in *Principles of Regenerative Medicine*. **2019**, Elsevier. p. 661-674.